Dissertation zur Erlangung des Doktorgrades der Fakultät für Chemie und Pharmazie der Ludwig-Maximilians-Universität München

---

The role of nuclear actin in distinctive DNA double strand break repair pathways - actin as a novel target for combination chemotherapy

---

Lisa Sabrina Pfitzer

aus

Stuttgart, Deutschland

2018

Erklärung

Diese Dissertation wurde im Sinne von §7 der Promotionsordnung vom 28. November 2011 von Herrn Prof. Stefan Zahler von der Fakultät für Chemie und Pharmazie betreut.

Eidesstattliche Versicherung

Diese Disseration wurde eigenständig und ohne unerlaubte Hilfe erarbeitet.

München, 10. Juli 2018

.....

Lisa Pfitzer

Dissertation eingereicht am:	24.05.2018
1. Gutachter:	Prof. Dr. Stefan Zahler
2. Gutachterin:	Prof. Dr. Angelika M. Vollmar
Mündliche Prüfung am:	05.07.2018

Meinen Eltern

Contents

List of Figures

List of Tables

1 Summary

Classical chemotherapy is often accompanied by severe adverse effects and new combination therapy options to circumvent this problem are still needed. Actin binding substances have shown promising results in different experimental setups but have not made it into the clinics yet. The proposed role of actin in DNA damage repair, however, makes actin binders potential combination partners with DNA damage inducing chemotherapeutics like doxorubicin. In this study, actin binding substances, such as the actin polymerizer jasplakinolide and the depolymerizer latrunculin B (LB), were applied to investigate the mechanisms of the proposed role of actin in nuclear DNA double strand break (DSB) repair pathways and to assess whether the application of actin binders is feasible for combination cancer therapy.

DSB induction by doxorubicin treatment led to a reduction of a mobile nuclear actin fraction and to an increase in polymerized actin in the nucleus, suggesting that the polymerization state of nuclear actin plays a crucial role in DNA damage signalling. DSB repair strongly depended on the maintenance of the actin equilibrium and actin manipulation inhibited DSB repair by influencing specific signalling cascades in distinctive DSB repair pathways. During homology directed repair (HDR) and single strand annealing (SSA), actin binders affected the recruitment of replication protein A (RPA) to the site of DNA damage, a process that is essential for the induction of both pathways. RPA was bound to nuclear actin under control conditions and released after damage induction, indicating that actin is directly involved in the recruitment of this repair factor. Furthermore, during non-homologous end joining (NHEJ), actin binders reduced activating phosphorylation of DNA-PK. Functionally, synergistic effects of low dose combination therapy of Doxo and LB on proliferation in different cancer cell lines could be demonstrated *in vitro*, and these effects could be linked to an increased DNA damage level in tumor cells *in vivo*.

In summary, these findings imply a direct involvement of actin in nuclear DNA damage repair mechanisms and propose a possible application of actin binding substances for combination therapy with DNA damage inducing agents.

2 Introduction

2.1 The role of DNA damage induction and repair in cancer therapy

2.1.1 Cancer incidence and general treatment strategies

Cancer is a multifactorial malignant disease and is one of the leading causes for death worldwide with lung, liver, colorectal and breast cancer among the most frequent cancer types [1–3]. The generation of malignant tumors happens during a multistep process in which healthy cells acquire distinctive capabilities that help them become tumorigenic. These capabilities that are required for tumorigenesis were termed hallmarks of cancer. They include, among others, the increase in cell proliferation due to the enabling of replicative immortality and the escape from cell death induction and growth suppression, as well as the activation of angiogenesis, invasion and metastasis [4, 5]. Targeting the above mentioned hallmarks is considered a promising strategy for tumor therapy. Classical chemotherapeutics, like the DNA damage inducing agent doxorubicin or the cytoskeleton targeting paclitaxel, mainly address the first two mentioned characteristics, namely increased cell proliferation and evasion of cell death. Doxorubicin causes cell cycle arrest and cell death by inducing high levels of DNA damage, whereas paclitaxel attacks the microtubule system. As highly proliferative cells, such as cancer cells, strongly depend on functional DNA replication and cytoskeleton functions, both agents can successfully be used for cancer therapy [6, 7]. However, high proliferation rates are not exclusive to cancer cells and neither the DNA nor the cytoskeleton represent tumor tissue specific targets. Treatment with these chemotherapeutics leads therefore to severe side effects [7, 8]. To reduce unwanted side effects during cancer therapy, more selective agents were designed. To give one example, the development of kinase inhibitors was based on the idea to inhibit signalling pathways that are hyperactivated in cancer due to tumor specific mutations [9]. Veramufenib for instance specifically inhibits mutated BRAF in melanoma and showed very promising results in clinical trials. However, resistance developed after only a few months, probably because of the very high specificity of this approach [10]. In general, initially efficient monotherapies often fail after a prolonged time period due to the development of resistances [11]. In order to evolve towards a malignant status, cancer cells have to acquire modifications in more than one of the above mentioned processes [5]. Targeting not only one but several of those hallmarks by combination therapy represents a strategy to on the one hand increase the efficacy of the administered drugs and thereby reduce side effects and on the other hand prevent rapid development of treatment resistances.

As the number of cancer patients is still expected to grow [3] and the above mentioned problems that arise during cancer therapy are often still not solved, the need to develop new strategies remains. The formulation of new combination therapies offers a promising approach.

2.1.2 Induction of DNA damage by the chemotherapeutic doxorubicin

Doxorubicin (Doxo), also called adriamycin, belongs to the class of anthracyclines and was first isolated as a metabolite of Streptamyces peucetius var. caesiues [12] (see Fig. 1).

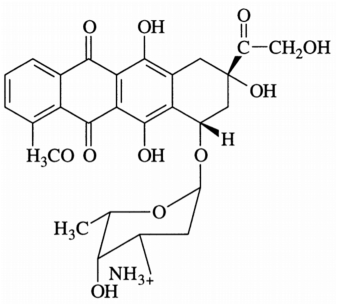

Figure 1: **Chemical structure of doxorubicin [13].**

Doxo binds to DNA and topoisomerase 2 (top2) isoenzymes. The formation of top2-doxo complexes at the DNA induces DNA double strand breaks (DSBs) and thereby inhibits DNA replication and promotes cell cycle arrest and apoptosis [6, 14–16]. Additionally, Doxo is involved in the generation of reactive oxygen species (ROS) and thus increases oxidative stress in cells [8]. It is nowadays widely used in the clinics for chemotherapeutic cancer treatment, such as breast, lung and ovary carcinomas [17]. However, due to its short half-life in the blood circulation and its extensive non-selective tissue distribution, treatment with Doxo is accompanied with severe side effects. Even though Doxo proved to be highly efficient in cancer therapy, it leads to both acute and delayed cardiotoxicity as cardiomyocytes are especially sensitive to Doxo induced oxidative stress. As a consequence, cancer patients that underwent anthracycline chemotherapy carry the risk for early cardiovascular morbidity [18–20].

Although Doxo shows dose-limitations due to its organ toxicity, it is still considered to be one of the most potent chemotherapeutics. It is therefore a promising candidate for combination therapy to make use of its anti-tumoral potential and even further increase its efficacy while reducing unwanted secondary effects. A rather new idea is to exploit dysregulated DNA damage repair signalling for cancer therapy. The FDA approval of the first DNA repair inhibitor olaparib [21] showed that DNA repair inhibition is indeed feasible for cancer therapy. The addition of DNA repair factor inhibitors to DNA damage inducing chemotherapeutics, however, represents a so far uninvestigated approach. Further extensive research is therefore needed to evaluate in detail if the inhibition of a potential tumor suppressive process such as DNA damage repair can be used for cancer therapy in combination with DNA damage inducing agents.

2.1.3 DNA double strand break repair pathways

The DNA damage response (DDR) describes the collectivity of all processes that are directly involved in the repair of damaged DNA and also includes all associated pathways that are activated. After sensing of damages DNA, cell cycle arrest ensures that the cell gets enough time to repair the damage, whereas cell death is induced if the extent of DNA damage is too high to be repaired in time. Depending on the type of damage, different repair pathways are triggered [22, 23]. In this work, mainly the double strand break of the DNA and its associated repair pathways will be explained in detail, since it is inflicted by treatment of cells with chemotherapeutics such as doxorubicin and represents the most deleterious type of damage.

Double strand breaks are sensed by MRN complex, which is composed of the three members Mre11, Rad50 and Nbs1. MRN is involved in early DNA repair processes by its recruitment to the site of damage followed by the phosphorylation and activation of its numerous substrates (see Fig. 2). The activation of MRN not only starts signalling pathways directly necessary for DNA repair but also regulates associated processes such as cell cycle checkpoint activation. MRN is therefore considered to be one of the key players of DSB repair in the cell (reviewed in [24, 25]). One important substrate of the MRN complex is ATM which is activated upon DSB induction and plays a fundamental role in DSB repair [24, 26]. The ATM-Chk2 pathway is not only involved in Rad51-dependent DNA repair, but also in Cdc25-dependent cell cycle arrest and p53-mediated apoptosis induction (see Fig. 2). ATM furthermore phosphorylates the histone H2AX at Ser139 [27], which leads to the recruitment of the nuclear protein MDC1, a multidomain scaffolding protein that is important for many functions of phosphorylated H2AX (yH2AX) during DSB repair [28, 29]. MDC1 amplifies the DSB response as it recruits MRN and retains ATM associated to MRN, resulting in its prolonged activation [30, 31]. Phosphorylation of H2AX is thus involved in early DSB signalling. Detection of yH2AX foci is often used as a biomarker for damaged DNA as phosphorylation of H2AX represents a very sensitive indicator of the presence of DSBs [32, 33].

Double strand breaks can be repaired by four different repair pathways and the choice depends primarily on the cell cycle state of the cell (see Fig. 3). Non-homologous end joining (NHEJ) describes the annealing of blunt DNA ends which occurs throughout the cell cycle, but dominantly in GO/G1 and G2, and functions independently of sequence homology. On the contrary, the other three pathways, homology-directed repair (HDR), single strand annealing (SSA) and alternative end joining (alt-EJ), are homology-based repair pathways and depend to different extents on DNA end resection, i.e. the processing of DNA adjacent to the DSB to generate ssDNA (reviewed in [34, 35]).

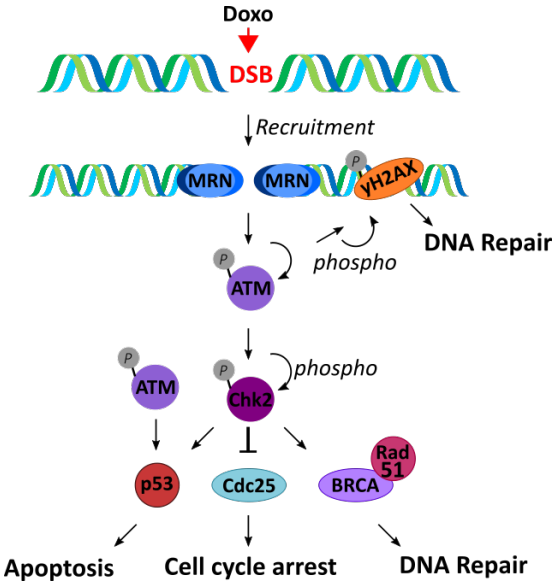

Figure 2: **The MRN-ATM-yH2AX pathway in double strand break (DSB) repair (simplified).** The MRN complex is formed upon DSB induction and is responsible for the activation of signalling pathways involved in DNA repair and induction of apoptosis and cell cycle arrest. MRN phosphorylates ATM which leads to the activation of its kinase activity. ATM phosphorylates e.g. Chk2, H2AX and p53.

During NHEJ, the Ku70/80 heterodimer (Ku) is the first protein complex that is recruited to free DNA ends that appear upon DSB induction. The resulting Ku-DNA complex forms the basis for the recruitment of nucleases, polymerase and ligases that are required for the joining of both adjacent DNA ends of the DSB [36, 37]. Binding of Ku to DNA presumably leads to conformational changes that allow additional binding of DNA-PKcs (catalytical subunit) [38, 39]. The DNA dependent protein kinase (DNA-PK) is thus formed by the binding of its catalytical subunit to DNA-bound Ku, resulting in its activation. Activated DNA-PK extensively phosphorylates itself but also many other targets involved in NHEJ [40, 41]. One important target of DNA-PK is the endonuclease Artemis. If two DNA ends are unsuitable for direct ligation, for example due to incompatible 3' or 5' overhangs, Artemis can be recruited in complex with DNA-PKcs and upon autophosphorylation of DNA-PK is activated by it and gains its endonuclease activity [42]. Endo- and exonuclease activities are needed for limited DNA end resection (<5 nucleotides) to ensure that the two DNA ends are compatible and Artemis seems to be the primary nuclease for that [43]. For example, Artemis removes the incompatible 3' and 5' DNA overhangs in order to create DNA ends that can be ligated later by the XRCC4-DNA ligase IV complex [37]. Ku catalyzes DNA ligation, i.e. the bridging between two DNA ends, as it promotes the binding of XRCC4-DNA ligase to the DNA ends [44–46]. Ku also interacts with polymerases μ and λ which promote ligation of DNA ends [37, 47]. The two subunits of the DNA-PK - Ku and DNA-PKcs - are thus key players in NHEJ signalling, since they regulate many involved factors.

As mentioned above, the other DSB repair pathways depend on DNA end resection, i.e. the nucleolytic degradation of DNA ends. End resection results in ssDNA sections which are required for recruitment of specific repair proteins involved in homology based repair pathways [48, 49].

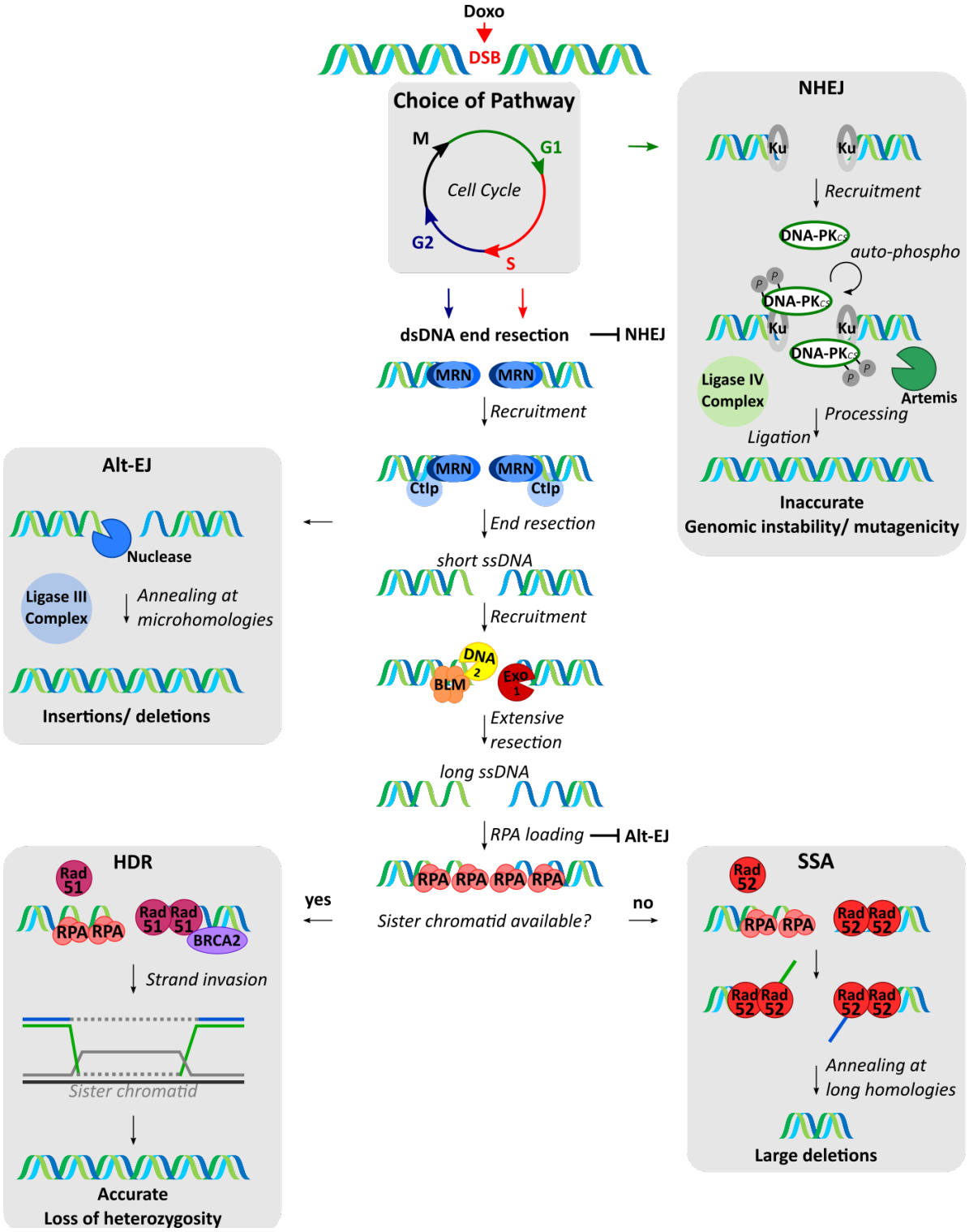

Figure 3: **Distinct pathways for DNA double strand break repair.** Dependent on the cell cycle state, DNA double strand breaks (DSB) will be repaired by non-homologous end joining (NHEJ), alternative end joining (Alt-EJ), homology derived repair (HDR) or single strand annealing (SSA).

The above mentioned MRN complex plays a crucial role in the induction of end resection, for example due to the exo- and endonuclease activities of Mre11 [50, 51]. Together with its interaction partner CtIP (C-terminal binding protein 1 (CtBP1) interacting protein) the MRN complex mediates the first step of end resection to generate short ssDNA sections [52]. The limited end resection by MRN and CtIP is sufficient for the activation of alt-EJ, which utilizes PARP-1 mediated annealing at short homologous DNA sequences (<10bp = microhomologies). Nucleases, polymerases as well as the DNA ligase III complex can be involved in alt-EJ, depending on how it is orchestrated [34].

In the second step of end resection, termed 'extensive resection', EXO1 (exonuclease 1) and DNA2 endonuclease/-BLM helicase are recruited to generate longer ssDNA tails [52] that are required for the binding of replication protein A (RPA). RPA is a heterotrimer composed of the RPA70 (=RPA-1), RPA32 (=RPA-2) and RPA14 (=RPA-3) subunits [53] and its binding to ssDNA is crucial for the initiation of both HDR and SSA. During HDR, which can only occur if a template, i.e. the sister chromatid, is available, BRCA2 mediates RPA replacement by Rad51 [54]. Coating of the ssDNA with Rad51 is required for strand invasion of the intact homologous region on the sister chromatid which serves as the template for accurate repair [55, 56]. The DNA strand is then extended by a DNA polymerase which leads to the creation of a D-loop. After D-loop creation, the error is repaired either by the formation of a Holliday junction or is completed via noncrossover products without Holliday junction formation (termed synthesis-dependent strand annealing pathway) [57].

The second RPA dependent pathways is SSA which is not based on sister chromatid exchange but uses homologous repeat sequences that flank the DSB. Rad52 binds to the ssDNA-RPA complex and together they facilitate both the alignment and the annealing of homologies around the break [55, 58, 59]. ERCC1 forms a complex with XPF that cleaves 3'ssDNA tails upon annealing, gaps are filled by DNA polymerases and the activation of DNA ligase completes SSA [60].

2.2 The actin cytoskeleton - a potential target?

2.2.1 Actin structure and function in cytoplasm and nucleus

The cytoskeleton of the cell is a dynamic polymer network which is comprised of three main components (reviewed in [61]): the microtubule system [62], intermediate filaments [63] and microfilaments (also known as the actin cytoskeleton) [64].

Actin, a 42 kDa structural protein, is highly conserved through all species and belongs to the most abundant proteins - almost all eukaryotic cells harbour genes for actin. Actin can be found in both muscle and non-muscle cells [65, 66] and in mammals in six different isoforms, α_{cardiac}-, α_{skeletal}-, α_{skeletal}-, β_{cyto}-, γ_{cyto}- and γ_{smooth}-actin (reviewed in [67]). In general the actin cytoskeleton is essential for the mechanical structure and motility of a cell and thus plays a role in many physiological functions [68]. The actin cytoskeleton is involved in the formation of cellular structures like lamellipodia, stress fibers and focal adhesions which are needed for cell movement and migration [69]. Additionally, actin is crucial for cell division and proliferation as the functional separation of two daughter cells during cytokinesis of mammalian cells depends on the contractile ring of actin filaments. Furthermore, eukaryotic cells transport organelles along the actin cytoskeleton making it also an important transport system in cells [68].

Actin exists in two states in the cell, monomeric G-actin and polymerized, filamental F-actin. F-actin is formed in a three steps process which includes a nucleation, an elongation and a steady state phase (Fig. 4). During the first phase, three to four G-actin monomers aggregate into unstable oligomers (nuclei). The addition of further actin monomers leads in the next phase to the rapid elongation of the nucleus into a filament. The F-actin filament will grow until a steady state is obtained in which an exchange of actin monomers is still observed, but without any change in the total mass of F-actin filaments (described in [70]). Actin filaments are asymetric, also termed polar, with a pointed (-) end where actin monomers can be dissociated (depolymerization of the actin filament), preferably when bound to ADP, and a barbed (+) end at which ATP-bound actin monomers can be added (polymerization of actin) [71]. Both poly- and depolymerization processes of actin are tightly controlled by on the one hand proteins that bind to monomeric G-actin and on the other hand proteins that bind to the barbed end of F-actin filaments (reviewed in [71, 72]). Up to now more than 100 actin binding proteins (ABPs) are known to be directly involved in the regulation of the dynamic process of actin polymerization [68]. To name only a few, gelsolin and ADF/cofilin are involved in the actin turnover by promoting actin filament disassembly [73, 74], whereas profilin and the Arp2/3 complex play a central role in filament assembly (reviewed in [71, 75, 76]). Arp2/3 complex e.g. is activated by WASP family proteins and catalyses nucleation of F-actin filaments with free barbed ends [71]. Polymerization of actin is therefore a very dynamic process depending on the needs of the cell.

For a long time actin function has mostly been associated with the cytoplasm, but since its discovery in the nucleus in 1969 [77], an increasing number of studies suggests important nuclear functions of actin. In contrast to cytoplasmic actin, nuclear actin is believed to exist mainly as monomers or oligomers under physiological conditions [78], but polymerization of nuclear actin

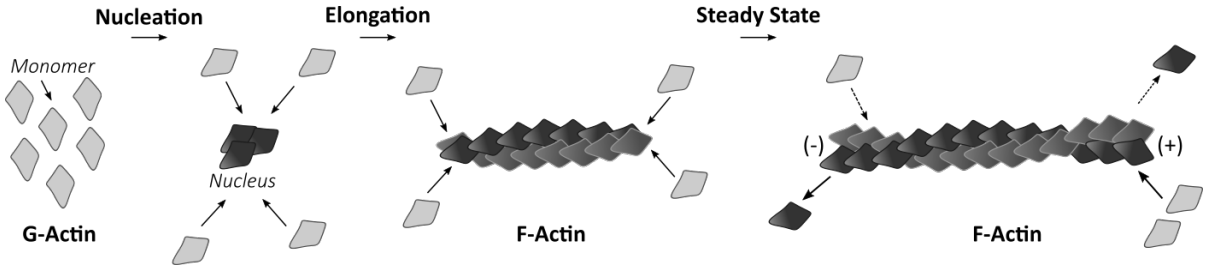

Figure 4: **States of actin in the cell.** Three actin monomers (G-actin) form a nucleus which is the basis for the formation of filamental F-actin during the elongation process until a tightly regulated steady state is obtained. In the cell F-actin is mainly polymerized at the barbed end (+) and depolymerized at the pointed end (-).

seems to occur as a stress response e.g upon heat shock or DNA damage induction [79, 80]. Polymerized actin in the nucleus was first described by McDonald et al. [81] and actin nucleators were found later on in the nucleus as well (reviewed in [82]), strengthening the assumption that actin filament assembly also happens in the nucleus. Moreover, different mechanisms of active actin transport from and to the nucleus have been described. In general, nucleocytoplasmic traffic of proteins occurs via nuclear pores, either by passive diffusion (<40kDa) or active transport receptors (>40kDa) [83]. Actin does not harbor a NLS sequence and cannot pass the nuclear pores by passive diffusion and is thereby considered to be dependent on one or more transport systems. ABPs, such as cofilin, harbor NLS motifs and might therefore play a role in the transport of actin from or to the nucleus. Cofilin and importin-9 were shown to be important for the import of actin to the nucleus [80, 84, 85], whereas exportin-6 was found to be responsible for the export of profilin-bound actin [86]. In addition, actin harbors two NES (nuclear export sequence) sequences which are necessary for the actin export via exportin-1 [87]. Actin is considered to be involved in different nuclear mechanisms. Actin is for example not only responsible for the mechanical integrity of the cytoplasm but also of the nucleus, as the nuclear matrix was found to mainly consist of actin [88]. Additionally, actin was proposed to function in chromatin remodeling and modifying mechanisms, as it is part of chromatin remodeling complexes during transcriptional activation and in histone acetyl transferase complexes (chromatin modifiers) (reviewed in [89, 90]). Along these lines, actin seems to be important for the regulation of RNA polymerase II-mediated transcription [91]. Several studies have been published that propose an involvement of nuclear actin in DNA damage repair signalling as well (see 2.2.4).

2.2.2 Targeting actin with actin binding substances

The state of actin can be manipulated by two distinct classes of actin binding substances (Fig. 5 and 6). Polymerizers, such as jasplakinolide, chondramides and miuraenamides promote polymerization (or aggregation) of actin and therefore increase the F-actin pool in the cell. On the contrary, depolymerizers, such as latrunculin B and chivosazole reduce the appearance of filamental actin and increase the G-actin pool.

Among the actin polymerizers, jasplakinolide (Jaspla) was first described in 1988 as an antifungal agent isolated from the soft-bodied sponge Jaspis species (Astrophorida, Jaspidae) [92]. Jaspla is a potent inducer of actin polymerization and binds with phalloidin competitively to

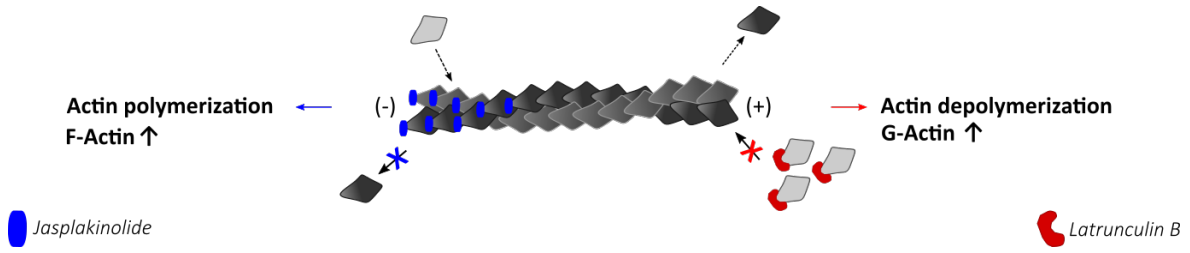

Figure 5: **Targeting of actin by actin binding substances.** The state of actin can be manipulated by two distinct classes of actin binding substances. Polymerizers promote actin polymerization and thereby increase the F-actin pool in the cell. Among the polymerizers, jasplakinolide binds to F-actin and impairs depolymerization of actin at the (-) end. Depolymerizers, on the contrary, decrease the F-actin pool by preventing polymerization of actin. For example, Latrunculin B binds to G-actin and impairs addition of actin monomers to an existing actin filament.

F-actin, resulting in stabilized filamental actin that is resistent to depolymerization *in vitro* [93]. Chondramides, first isolated from the myxobacterial strain Chondromyces crocatus, are structurally very close to Jaspla and act in a similar way as they also bind to the actin binding site of phalloidin [94, 95]. Like Jaspla, chondramides stabilize existing actin filaments and reduce the number of physiological actin stress fibers in the cell by unphysiological actin aggregation [95, 96]. Miuraenamides were first isolated from the myxobacterial strain SMH-27-4 as potential antibiotic agents [97] and miuraenamide A (Miu) was later identified as another actin binding and polymerizing substance [98]. Miu can now be obtained by full synthesis [99, 100].

As mentioned above, actin can also be manipulated in the opposite way, by preventing actin polymerization and thereby increasing the G-actin pool. Both toxins latrunculin A and B, purified from two Latrunculia magnifica species (marine sponges), were one of the first identified actin depolymerizers. Effects of latrunculins on microfilament organization were found to be pronounced, but reversable, and specific to actin (and not microtubules) [101]. Four years later it could be shown that the effect of latrunculin on the actin organization is caused by a direct binding of latrunculin to actin monomers which leads to an impairment of actin polymerization [102]. Total synthesis of latrunculin B (LB) has been possible for over 20 years [103] and it is still used for research as a classical actin depolymerizer. Chivosazoles are less known and characterized actin binding substances, isolated from the culture broth of the secondary metabolite-producing myxobacteria strain So ce56 (S. cellulosum) [104]. Chivosazole A and F show strong effects on the actin cytoskeleton of cells, comparable to latrunculins. *In vitro* it could be shown that chivosazoles not only inhibit actin polymerization but also cause depolymerization of already existing actin filaments [105]. Chivosazoles are not as widely used yet, but provide new tools for actin manipulation and investigation.

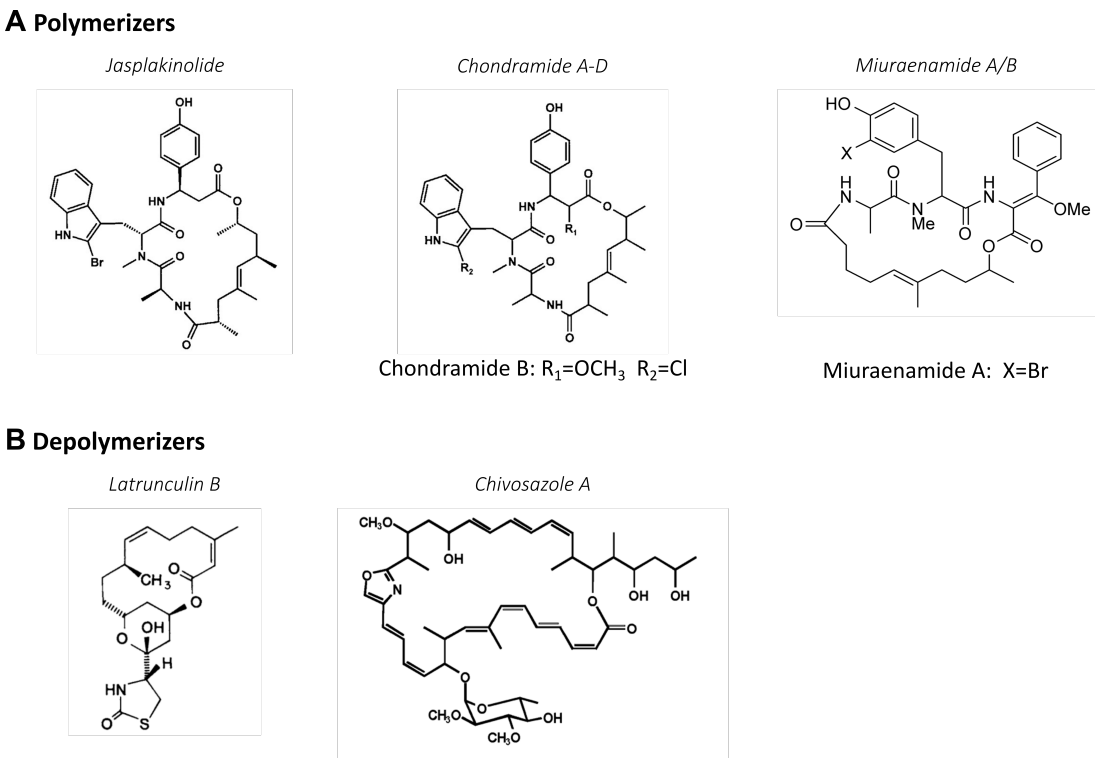

Figure 6: **Structures of actin binding substances. A Polymerizers.** Jasplakinolide [95], Chondramides [95], Miuraenamides [97]. **B Depolymerizers.** Latrunculin B [106], Chivosazole A [104].

2.2.3 The cytoskeleton as a chemotherapeutic target - potential application of actin binding substances

Actin is required for cellular functions like proliferation and migration, processes that are absolutely necessary for the development of malignant and metastatic cancers [5]. Actin represents thus a promising target for cancer therapy, a strategy which is not applied in the clinics yet, mainly due to feared severe side effects.

Nevertheless, targeting of actin has been suggested as a potential approach for cancer treatment by different groups, as actin manipulation exhibits anti-proliferative and anti-metastatic characteristics on tumor cells. Anti-tumor activities of Jaspla could be shown *in vitro* in three prostate carcinoma cell lines and *in vivo* in Lewis lung carcinoma and prostate carcinoma xenografts. Moreover, application of Jaspla showed additive effects when combined with radiotherapy in different experimental approaches [107, 108]. In our group, chondramide showed anti-metastatic potential in migration and invasion assays *in vitro* and inhibited metastasis to the lungs in a breast cancer model *in vivo*, which was linked to the inhibition of the cellular contractility [109]. Furthermore, chondramide induced caspase dependent apoptosis in breast cancer cell lines, whereas non-tumor breast epithelial cells were found to be less sensitive to chondramide treatment [110]. Although latrunculins and chivosazoles act the opposite way, they nevertheless have been reported to exhibit chemotherapeutic potential. In human gastric adenocarcinoma cells (MKN45, NUGC-4), latrunculin A treatment induced caspase dependent apoptosis *in vitro* and led to improved survival rates of mice bearing MKN45 or NUGC-4 tumors [111]. Additionally, latrunculin A was reported to enhance radiosensitivity in cancer cells in colony formation

assays and to impair yH2AX-formation upon radiation [112]. Furthermore, chivosazoles A and F both showed high anti-proliferative activity in human cancer cell lines [105].

Although actin binding substances showed anti-cancer characteristics in different experimental setups, until now, the application of actin binding substances as a potential cancer therapy approach has not been studied in detail and is still far from clinical use. The above mentioned actin binding substances are nevertheless promising candidates for further investigations and preclinical development.

2.2.4 Impact of actin reorganization on nuclear DNA damage signalling pathways

The presence of damaged DNA induces a great diversity of signalling pathways in the cell and actin dynamics seem to influence the response to DNA damage on multiple levels. Polymerization of actin has been reported to be induced by DNA strand breaks and to be required for DSB repair.

It has been suggested by several groups that nuclear actin may play a direct role in DNA damage (repair) signalling. One study showed that a reduction of the nuclear actin pool by knockdown of the nuclear actin import factor IPO9 led to an increase in the number of DSBs after treatment with methyl methanesulfonate (MMS). Knockdown of the export factor XPO6, and the consequent increase of the nuclear actin pool, did not show any significant effects on DBSs after treatment [79]. Thus, the availability of actin in the nucleus seems to be important for DNA damage repair processes. Furthermore, nuclear actin filament formation could be detected upon DNA damage induction by application of specific fluorescent probes that enable visualization of actin in the nucleus [79]. To conclude, not only the existence of sufficient nuclear actin but its polymerization was proposed to be required for efficient DSB repair [79, 113]. Actin binding substances have been applied by several groups in order to investigate the role of different actin states in DNA damage repair processes. Latrunculin treatment of cells prior to irradiation impaired DNA damage repair. The disruption of actin polymerization by latrunculin has been shown to interfere with the chromatin association of different DSB repair proteins (Ku80, Mre11, Nbs1, ATM, Chk2) upon DNA strand break in subcellular fractions [113]. Polymeric actin was found to be bound to Ku in a F-actin pulldown assay and polymerization of actin was therefore considered to be essential for DSB repair [113]. In pulldown assays of HeLa nuclear extracts, in addition to Ku, other DNA damage repair factors, like RPA-3 and DNA-PKcs, have been suggested as potential actin binding proteins. However, the proposed interactions have not been experimentally validated in this study [114]. If disruption of polymerized actin has an effect on the phosphorylation of the most commonly used DNA damage marker H2AX is not clear, as different groups published opposing results [112, 113]. Moreover, nuclear F-actin seems to participate in the binding of p53 to the nuclear matrix and p53 binding to F-actin was increased upon DNA damage induction [115].

In addition to direct functions of nuclear actin on DNA damage repair, indirect effects of actin on nuclear processes have been published. F-actin can directly bind to p53 [116] and inhibits its nuclear import by retaining it in the cytoplasm [117], which allows the cell to repair the damage

before cell cycle arrest or apoptosis are started. On the other hand, the G-actin binding protein JMY is released upon actin polymerization following DNA damage induction and can now enter the nucleus to enhance transcriptional activity by directly binding to p53 [118, 119].

The above mentioned examples show that the regulation of DNA damage induced mechanisms by reorganization of actin, both in the cytoplasm and in the nucleus, is very complex and has to be tightly regulated and is still far from being completely understood.

2.3 Aim of the study

Classical chemotherapeutics are potent agents against cancer, but due to their insufficient specificity, treatment is often accompanied by severe side effects. Combination therapy is a promising concept to make use of the anti-tumor characteristics of chemotherapy, while reducing substance concentrations and unwanted secondary effects. One approach is to combine DNA damage inducing agents with additional DNA repair inhibitors. Hovewer, most of the substances investigated for this purpose have not (yet) surpassed preclinical trials and novel combination therapy formulations are still needed. Actin binding compounds are still not used in the clinics, but represent a promising tool as malignant cells are often especially dependent on cytoskeletal functions. In addition, an involvement of actin in nuclear DNA damage processes has been suggested, but is not yet well understood. Nevertheless, a potential requirement of functional actin in DNA repair makes it a possible candidate for combination therapy with DNA damaging agents.

The aim of this study was on the one hand to uncover the underlying mechanisms behind the proposed involvement of actin in nuclear processes during DNA double strand repair and on the other hand evaluate the application of actin binding substances in combination with the chemotherapeutic doxorubicin as a novel strategy for cancer therapy.

3 Materials and Methods

3.1 Materials

3.1.1 Technical equipment

Table 1

Product	**Supplier**
BIO-RAD PowerPac Basic Electrophoresis Power Supply	Bio-Rad Laboratories, Munich, Germany
ChemiDoc^{TM}Touch Imaging System	Bio-Rad Laboratories, Munich, Germany
FACSCanto^{TM}II	BD Biosciences, Heidelberg, Germany
FACSCalibur^{TM}	BD Biosciences, Heidelberg, Germany
Heated Plate for 1 Chamber in Multi-Well Format	Ibidi, Martinsread
Heated Plate universal fit	Ibidi, Martinsread
Heracell^{TM}150, CO_2 incubator	Thermo Fisher Scientific, Germering, Germany
Herasafe^{TM}KS, biological safety cabinet	Thermo Fisher Scientific, Germering, Germany
HLC HBT 130, thermo block	Biometra, Goettingen, Germany
Leica TCS SP8 SMD	Leica Microsystem, Wetzlar, Germany
Mikro 22R, centrifuge	Hettich, Tuttlingen, Germany
NanoDrop 1000 Spectrophotometer	Peqlab, Wilmington, USA
Stage top chamber Bold Line	Okolab, Pozzuoli, Italy
Sunrise^{TM}Microplate Absorbance Reader	Tecan, Maennedorf, Austria
Vi-Cell^{TM}RX Cell Viability Analyzer	Beckman Coulter, Fullerton, USA
VXR Vibrax®, shaker	IKA®-Werke, Staufen, Germany

3.1.2 Consumables

Table 2

Product	**Supplier**
Cell culture flasks, plates	Sarstedt, Nuembrecht, Germany
Eppendorf Sace Lock Tubes	Eppendorf, Hamburg, Germany
FACS tubes	Sarstedt, Nuembrecht, Germany
Falcons	TPP, Trasadingen, Switzerland
Haake W19, water bath	Thermo Haake, Karlsruhe, Germany
Ibidi^{TM} μ-Slide 8 Well	Ibidi, Munich, Germany
Ibidi^{TM} μ-Slide 12 Well, removable chamber	Ibidi, Munich, Germany
Microscope glas slides and coverslips	Fisher Scientific GmbH, Schwerte, Germany
Nitrocellulose membran, Hybond-ECLTM	Amersham Bioscience, Freiburg, Germany

3.1.3 Substances

Chondramide B and Chivosazole were kindly provided by Prof. Dr. Rolf Müller, Helmholtz Centre for Infection Research, Saarland University, Saarbrücken, Germany. Jasplakinolide was purchased from R&D Systems, Bio-Techne GmbH, Wiesbaden, Germany. Latrunculin B was purchased from Sigma Aldrich, Taufkirchen, Germany. Miuraenamide A was kindly provided by Prof. Dr. Uli Kazmaier, Institute for Organic Chemistry, Saarland University, Saarbrücken, Germany. All actin binding substances were dissolved in DMSO and stored at -20°C. Doxorubicin hydrochloride was purchased from Sigma Aldrich, Taufkirchen, Germany, diluted in H_2O and stored at 4°C.

3.1.4 Chemicals and reagents

All chemicals not listed in this section were purchased from Sigma Aldrich, Taufkirchen, Germany.

Table 3

Product	**Supplier**
2,2,2-trichloroethanol	Sigma Aldrich, Taufkirchen, Germany
2,2'-azino-bis(3-ethylbenzothiazoline-6-sulfonic acid)	Sigma Aldrich, Taufkirchen, Germany
7-AAD (7-Aminoactinomycin D)	Fisher Scientific GmbH, Schwerte, Germany
Agarose, low gelling temperature	Sigma Aldrich, Taufkirchen, Germany
Universal-Agarose, peqGOLD	VWR Chemicals, Darmstadt, Germany
Amersham Hybond ECL nitrocellulose membrane	GE Healthcare Europe, Freiburg, Germany
Amersham HybondP 0.45 PVDF membrane	GE Healthcare Europe, Freiburg, Germany
Blotto (non-fat dry milk powder)	Carl Roth, Karlsruhe, Germany
Bovine Serum Albumin	Sigma Aldrich, Taufkirchen, Germany
Bradford reagent Roti®-Quant	Carl Roth, Karlsruhe, Germany
CellTiter-Blue®	Promega, Mannheim, Germany
Complete™ (protease inhibitor)	Roche diagnostics, Penzberg, Germany
Crystal violet	Carl Roth, Karlsruhe, Germany
Dulbecco's mofidifed Eagle's medium	PAN Biotech, Aidenbach, Germany
Dimethylsulfoxide	Sigma Aldrich, Taufkirchen, Germany
Ethylenediaminetetraacetic acid	Carl Roth, Karlsruhe, Germany
Fetal Calf Serum	PAA Laboratories, Pasching, Austria
Fluorsave™ Reagent	Millipore, Darmstadt, Germany
FuGENE® HD Transfection Reagent	Promega, Mannheim, Germany
GelRed™ Nucleic Acid Stain	Biotium, Fermont, USA
Glutamine	Sigma Aldrich, Taufkirchen, Germany
HiMark™ Pre-Stained Standard	Fisher Scientific GmbH, Schwerte, Germany
Hoechst 33342	Sigma Aldrich, Taufkirchen, Germany
Luminol	AppliChem, Darmstadt, Germany
McCoy's medium	PAA Laboratories, Pasching, Austria
Na_3VO_4	Sigma Aldrich, Taufkirchen, Germany
Page Ruler Prestained Protein Ladder	Germentas, St. Leon-Rot, Germany

Table 3: *continued from previous page*

Product	Supplier
Paraformaldehyde	Polysciences, Pennsylvania, USA
Penicillin/Streptomycin 100x	PAA Laboratories, Pasching, Austria
Phosphatase inhibitor	Roche diagnostics, Penzberg, Germany
Protein A/G PLUS-Agarose (sc-2003)	Santa Cruz Biotechnology, Inc., Heidelberg, Germany
Puromycin hydrochloride	Fisher Scientific GmbH, Schwerte, Germany
Pyronin Y	AppliChem, Darmstadt, Germany
Pyruvate	PAA Laboratories, Pasching, Austria
Rhodamine-phalloidin	Life technologies, Darmstadt, Germany
Rotiphorese® Gel 30 (37,5:1)	Carl Roth, Karlsruhe, Germany
RPMI 1640 medium	PAN Biotech, Aidenbach, Germany
Sodium dodecyl sulfate	Carl Roth, Karlsruhe, Germany
Tris hydrochloride	Sigma Aldrich, Taufkirchen, Germany
Triton X-100	Millipore, Darmstadt, Germany
Trypsin	PAN Biotech, Aidenbach, Germany
Tween 20	VWR, Darmstadt, Germany
Yo-Pro®-1 Iodide	Fisher Scientific GmbH, Schwerte, Germany

3.1.5 Mixtures and kits

Table 4

Product	Supplier
Duolink® PLA Protein Detection Technology	Sigma Aldrich, Taufkirchen, Germany
Liver Dissociation Kit, mouse (130-105-807)	Miltenyi Biotec GmbH, Bergisch Gladbach, Germany

3.1.6 General buffers and solutions

Buffers and solutions not mentioned here are specified in the respective method section.

PBS pH7.4 123.3mM NaCL, 10.4mM Na_2HPO_4, 3.2mM KH_2PO_4, H_2O.
PBS+Ca^{2+}/Mg^{2+} 136.9mM NaCl, 8.1mM Na_2HPO_4, 1.5mM KH_2PO_4, 2.7mM KCl, 0.5mM $MgCl_2$, 0.7mM $CaCl_2$, H_2O.
PBS-B 1mg/ml BSA, 0.01% sodium azide, PBS.
Trypsin/EDTA 0.05% Trypsin, 0.02% EDTA, PBS.

3.1.7 Software

Table 5

Product	Application	Supplier
Adobe Reader	PDF software	Adobe Systems Software
Bibtex	References	Open source
FlowJo	FACS analysis	Tree Star Inc.
GraphPad Prism	Data visualization, statistics	GraphPad Software, Inc.
ImageJ	Image analysis	Open source
Inkscape	Image editing	Open source
JabRef	References	Open source
Magellan™	Protein concentration	Tecan
Microsoft Office Package	Data analysis, text editing	Microsoft
Latex	Text editing program	Open-source

3.2 Methods

3.2.1 Cell culture

3.2.1.1 Cell lines

All cell lines used for this thesis are listed in (Tab. 6).

Table 6: **Cell lines**

Cell line	Cell type	Source
HeLa	cervival cancer (human)	DSMZ (Leibniz Institute, Braunschweig, Germany)
T24	urinary bladder carcinoma (human)	DSMZ (Leibniz Institute, Braunschweig, Germany)
4T1-luc	breast cancer (mouse)	Perkin Elmer (Rodgau, Germany)
U2OS (I-SceI)	bone osteosarcoma (human)	[120]

HeLa and T24 cells were cultured in DMEM, 4T1 cells in RPMI. U2OS I-SceI reporter cell lines were cultivated in McCoy's medium + 1μg/ml puromycin.

3.2.1.2 Standard cell culture conditions

Cells were cultured under standard conditions (37°C, 5% CO_2, 95% humidity) in medium + 10% FCS + 1% Pen/Strep (complete medium, CM), depending on the cell line. All used cell lines were cultured as adherent growing cells and had to be detached from the cell culture flask by incubation with TE. Prior to any experiment, both cell density and viability were determined with the ViCELL cell viability analyzer.

If not stated otherwise in all experiments for combination treatment of Doxo with any actin substance, cells were pre-treated with each respective actin substance for 90mins before the addition of Doxo. Maximum percentage of DMSO never exceeded 0.1%.

3.2.1.3 Thawing and cryopreservation of cells

For cryoconservation, cell pellets (5min, 1500rpm) were suspended in 1ml FCS + 10% DMSO and stored in liquid nitrogen. Cryopreserved cells were thawed at 37°C for a few minutes and then transferred to a tube with CM. After centrifugation (5min, 1500rpm), cell pellets were resuspendend in fresh CM and transferred to a cell culture flask.

3.2.1.4 Transient transfection of cells

For transient protein overexpression, cells were plated 24h prior to the transfection. FuGENE® HD transfection reagent (Promega) was applied according to the manufacturer's suggestion. Follow-up experiments were conducted 24h after addition of FuGENE® HD transfection reagent. In case cells were treated with any substance, medium was changed to CM to exclude any possible interference by the combination of reagents.

3.2.2 Cell viability and proliferation

3.2.2.1 Metabolic activity

Metabolic activity of HeLa and T24 cells was determined with the CellTiter-Blue assay (Promega) adjusted from the manufacturer's protocol. 5000 cells were seeded in 96-well plates in 100μl medium and incubated for 24h, followed by treatment with Doxo [25nM] alone or in combination with actin substances LB [500nM] or Jaspla [50nM], respectively. After 72h, 20μl of CellTiter-Blue reagent were added to each sample, incubated for 2-4h at 37°C and fluorescence signal measured at 530 nm with a microplate reader (SpectraFluor Plus, Tecan).

3.2.2.2 Colony formation assay

Clonogenic survival, after treatment with Doxo [250nM] and actin substances LB [1μM], Jaspla [100nM], was determined by colony formation assay. HeLa cells (1x10^5 cells/ well) or T24 (0.75x10^5 cells/ well) were seeded in 12-well plates and treated with Doxo alone or in combination with the respective actin substances for 2h. Cells were then washed with PBS, trypsinized, counted and 1500 cells seeded in one well (6-well plate) in 3ml medium (performed in duplicates). After 6 days, cells were washed with PBS, fixed in methanol (15 min) and cells stained with crystal violet solution (30 min). Excess crystal violet was afterwards removed by washing with H_2O. Images of the individual wells were taken and total growth area was determined using the ImageJ plugin ColonyArea.

Crystal violet solution 0.5% crystal violet, 20% methanol, H_2O.

3.2.3 Flow cytometry

Cells used in this work usually emitted fluorescence after they had been infected with plasmids that contained cassettes for GFP, or after staining with fluorophor-coupled secondary antibodies. All experiments were either conducted with BD FACSCanto II^{TM} (BD Biosciences) or FACScalibur (BD Biosciences).

As free Doxo shows fluorescence properties with an emission comparable to propidium iodide (emission maximum at 560-590nm), alternatives had to be applied for flow cytometry analysis of cell viability and cell cycle status of the cells (see 3.2.3.1 and 3.2.3.2. Doxorubicin fluorescence is quenched, however after binding to DNA and thereby did not cause any problems for the analysis of chromatin bound proteins (see 3.2.3.4).

3.2.3.1 YoPro exclusion assay

YoPro exclusion assay was performed to identify the proportion of apoptotic cells after treatment with Doxo alone or in combination with actin substances. Cells were treated for 48h, harvested in cold PBS-B and DNA stained with YoPro (YO-PRO^{TM}-1 Iodide (491/509), Thermo Fisher) with a final YoPro concentration of 1μM and flow cytometry analysis was performed immediately afterwards. In comparison to propidium iodide, not only dead but also apoptotic cells become permeant to the dye.

3.2.3.2 Cell cycle analyses

To analyze the impact of combination therapy on cell cycle arrest, 7-AAD (ThermoFisher) was applied, a fluorescent molecule and intercalating agent which binds like propidium iodide to double stranded nucleic acids and can therefore be used to quantitatively assess DNA content in cells by flow cytometry.

Cells were plated in 12 well plates ((1x10^5 cells/ well) and cultured in CM for 24h followed by treatment with Doxo and the respective actin substances. After 48h cells were harvested, spinned down (5min, 1500rpm), cell pellets washed with PBS and afterwards fixed with 250μM methanol at 4°C. Fixed cells were washed once more with PBS, resuspended in 250μl of PBS-B + 10μl/sample/7-AAD + 0.1mg/ ml RNAse A and incubated for 1h at 37°C. First in a FSC/SSC plot cell debris was excluded, then cell aggregates of two or more cells were removed and cell cycle phases were analyzed in histograms with cell count erected over fluorescence intensity. The percentage of cell death was calculated with a subG1 gate.

3.2.3.3 I-SceI-based reporter systems

Principle of the I-SceI-based reporter system. I-SceI-based reporter cell lines were used to study DNA damage repair capacity after actin substance treatment (principle presented in [120]). These reporter cell lines express GFP-expression cassettes that are interrupted by one or more recognition sites for the endonuclease I-SceI. Transient overexpression of I-SceI (pCBASceI, addgene plasmid nr.26477, [121]) leads to one or more cuts in the GFP cassette, and upon repair via the respective DNA repair pathway, the cell restores the correct GFP sequence, which can be measured by flow cytometry (percentage of GFP$^+$ cells). In this work, four reporter cell lines were used (see Tab. 7 and Fig. 7). In the DR-GFP cell line, the GFP cassette harbors one I-SceI recognition site and a 5' and 3' truncated iGFP that serves as a repair template which is required for homology directed repair (HDR). The construct used for the SA-GFP cell line harbors two GFP fragments (a 5' and a 3' truncated fragment), which share 266nt homology and are separated by 2.7kb. Here, the I-SceI recognition site is localized in the 3' fragment and

successful single strand annealing will lead to a GFP$^+$ product. The GFP expression cassette of the EJ2 cell line is separated from the promoter by the I-SceI recognition site which is followed by a sequence of several stop codons. The I-SceI site and the stop codon sequence are surrounded up- and downstream by an 8nt microhomology. Alternative end joining (alt-EJ) will lead to a deletion of the stop codons (35nt) and the restoration of a functional GFP. The cell line EJ5-GFP contains a GFP cassette that harbors two I-SceI recognition sites and is separated from the promotor by a puromycin resistance marker. Distal non-homologous end joining (NHEJ) leads to a deletion of the puromycin sequence and thereby restores the expression of a functional GFP.

Table 7: **U2OS I-sceI-based reporter cell lines**

Cell line	DNA DSB repair pathway
DR-GFP	Homology directed repair (HDR)
SA-GFP	Single strand annealing (SSA)
EJ2-GFP	Alternative end joining (alt-EJ)
EJ5-GFP	Non-homologous end joining (NHEJ)

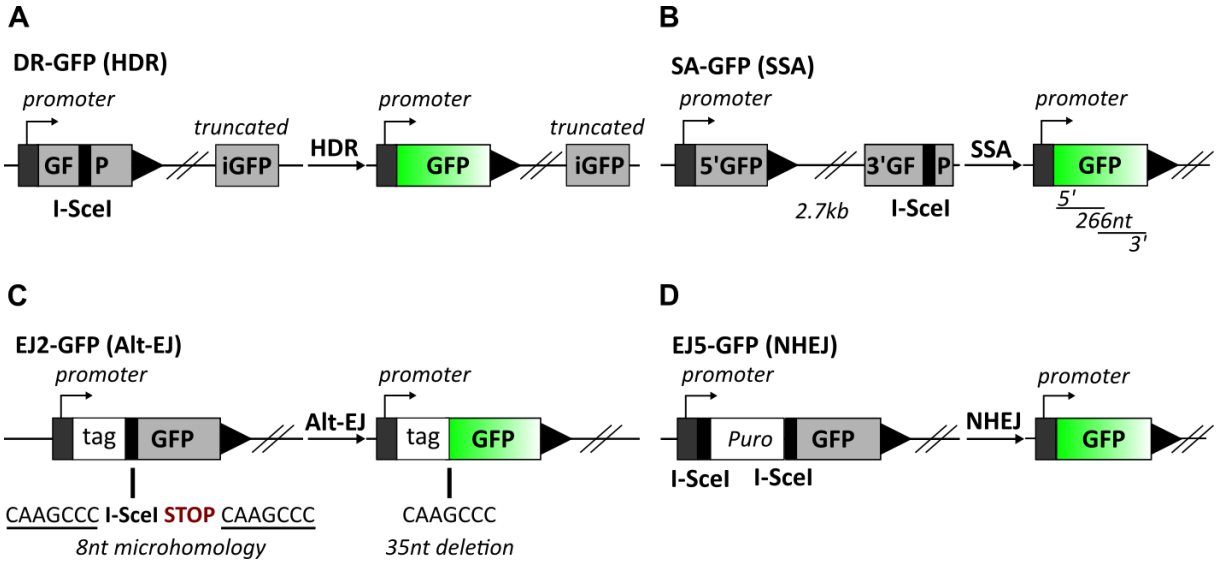

Figure 7: **Principle of the I-SceI-based reporter system. A DR-GFP.** The GFP cassette is interrupted by an I-SceI recognition site and 5' and 3' truncated iGFP can serve as a template during HDR. **B SA-GFP.** The construct harbors two GFP fragments (a 5' and a 3' truncated fragment) that are oriented in the same direction, share 266nt homology and are separated by 2.7kb. The 3' fragment harbors the I-SceI recognition site. **C EJ2-GFP.** The GFP is connected upstream to a tag and separated from it by the I-SceI recognition site and a sequence of several stop codons. Both are surrounded by an 8nt microhomology. Alt-EJ will lead to a deletion of the stop codons (35nt) and a GFP-positive product. **D EJ5-GFP.** The GFP cassette harbors two I-SceI recognition sites and is separated from the promotor by a puromycin resistance marker (puro). Distal NHEJ will delete the puro sequence and restore the expression of GFP.

Experimental setup. U2OS-I-SceI reporter cells were seeded (1x10^{5}cells/ well) and transfected on the fowolling day in duplicates with the above mentioned pCBASceI plasmid to transiently overexpress the I-SceI endonuclease. After 6h of incubation, medium was changed to normal CM and actin substances added, LB [500nM], Jaspla [50nM], ChB [75nM]. In case of the EJ5 cell line, medium without puromycin had to be applied, as successful repair deletes the

puromycin resistance. After 72h, cells were harvested in PBS-B and flow cytometry performed with viable cells. Cell debris and dead cells were excluded with a linear SSC-A/ FSC-A gate, cell doublets eliminated with a linear FCS-W/ FSC-A gate and the percentage of GFP^+ cells measured.

3.2.3.4 Chromatin association of DNA damage repair proteins

Recruitment of DNA damage repair factors to the site of damage can be measured by flow cytometry if the respective protein is directly or indirectly bound to chromatin after induction of DNA damage. This allows the analysis of larger cell populations compared to the standard foci formation immunocytochemistry protocol. The functionality of this approach was published in [122] and the assay performed accordingly. HeLa cells were seeded in 12 well plates ((1x10^5 cells/ well) 24h prior to the experiment. The next day, cells were treated with Doxo [250nm] for 2h alone or in combination with the respective actin substance and afterwards harvested in cold PBS. In the next crucial step, cells were resuspended in extraction buffer and incubated on ice for 5-10mins to extract unbound protein. Cells were then washed in PBS-B and fixed with 4% PFA in PBS for 15mins at room temperature and washed with cell washing buffer once. Primary antibodies (Tab. 8) were diluted in cell washing buffer and cells incubated for 1h at room temperature or at 4°C over night, washed once with cell washing buffer and incubated for 30mins at room temperature with the respective secondary antibody (Tab. 9), washed again and resuspended in PBS-B for FACS analysis. Prior to the actual FACS analysis, compensation was performed as 2 colors were measured with one laser (RPA-2: PE, yH2AX: 488). Compensation beads for unstained, PE and FITC channels were used (antibodies see Tab. 9) and compensation performed according to the manufacturer's (BD Biosciences) protocol. Cell debris was excluded with a linear SSC-A/ FSC-A gate, single cells isolated using a linear FCS-W/ FSC-A gate and positive cells defined by a third gate in a log 488/ PE histogram. In this work, chromatin association of RPA-2 and yH2AX upon DNA damage induction was analyzed.

Extraction buffer 0.2% Triton X-100, PBS.
PBS-B 1mg/ml BSA, PBS.
Washing buffer 1% FCS, 0.1% sodium acide, 0.1% saponine, PBS.

Table 8: **Primary antibodies for chromatin association assay**

Protein	Provider	Species	Dilution
Histone H2A.X phospho-Ser-130 (yH2AX)	Cell Signaling (2577)	Rabbit	1:200
RPA-2	Abcam (ab2175)	Mouse	1:500

Table 9: **Secondary antibodies for chromatin association assay**

Fluorophore	Provider	Species	Dilution
Alexa Fluor 488	Thermo Fisher (A11034)	Goat anti-rabbit	1:1000
PE	BD Biosciences (550083)	Rat Anti-mouse IgG1	1:1000
FITC isotype control	BD Biosciences (557721)	Mouse	20μl/sample
PE k isotype control	BD Biosciences (556029)	Mouse	20μl/sample

3.2.4 Microscopy

3.2.4.1 Alkaline comet assay

Cells were seeded 24h prior to the experiment in 12-well plates. After treatment of cells with Doxo [250nM] and the indicated actin substances for 2 hours, Doxo was removed and medium replaced with or without the respective actin substances for 4 hours (repair time). Doxo treatment without any repair time served as positive control. Approximately 1x10^4 cells were then seeded in agarose (0.7% in PBS, low gelling) at 37°C on pre-coated glas slides (0.8% in PBS, pre-coating performed twice), incubated on ice for 10mins and lysed at 4°C over night in comet lysis buffer. After lysis, electrophoresis was performed at 4°C at 35 V for 15 min with a current flow of approximately 250mA. After electrophoresis, glass slides were incubated in neutralization buffer for 10min, and then stained with 1x GelRed^{TM} (Thermo Fisher Scientific) in H_2O for 15min, followed by three washing steps in H_2O and fixation in 70% ethanol. Glass slides were sealed with FluorSave^{TM} (EMD Millipore) and images taken with a 20x or 40x objective. Images were analyzed with OpenComet (ImageJ) and tail moments calculated and normalized on Doxo repair samples or untreated controls.

Comet lysis buffer 0.1M EDTA-Na_2, 2.5M NaCl, 10mM Tris HCl, 1% Triton-X 100, NaOH (ad. pH=10), H_2O.
Comet electrophoresis buffer 1.5M NaCl, 5mM EDTA-Na_2, 0.5M NaOH, H_2O.
Comet neutralization buffer 0.4M Tris HCl, NaOH (ad. pH=7), H_2O.

3.2.4.2 General immunocytochemistry protocol

Between 1x and 2x10^4 cells per well were seeded and cultivated for at least 24h before starting any treatment. Cells were then washed with cold PBS, and fixed with 4% PFA for 15mins at room temperature, permeabilized with 0.2% Triton-X 100 for 10mins, blocked with 5% BSA in PBS for at least 30mins at room temperature and stained with the primary antibody over night at 4°C. The next day, cells were washed once with PBS, then incubated for at least 30mins in the secondary antibody, washed again and co-stained for actin and nuclei with rhodamine phalloidin (Thermo Fisher Scientific) and Hoechst (Thermo Fisher Scientific), respectively. Cells were then mounted with one drop of FluorSave^{TM} (EMD Millipore). Images were taken with a Leica SP8 microscope featuring a 63x objective and analyzed with ImageJ.

Table 10: **Antibodies and dyes for immunocytochemistry**

Type	Target	Provider	Species	Dilution
Primary	yH2AX	Cell Signaling (2577)	Rabbit	1:500
Primary	RPA-2	Abcam (ab2075)	Mouse	1:250
Primary	DNA-PK (T2609)	Abcam (ab18356)	Mouse	1:150
Secondary	anti-mouse	Invitrogen (A11001)	Goat	1:500
Secondary	anti-rabbit	Invitrogen (A11008)	Goat	1:500
Rhodamine/phalloidin	actin	Thermo Fisher Scientific	-	1:400
Hoechst 33342	DNA	Thermo Fisher Scientific	-	1:50

3.2.4.3 Chromatin texture

Cells were seeded in ibidi 8 well μ-slides and treated wih the respective substances. Cells were then fixed in 4% PFA for 10min, permeabilized in 0.05% Trion X-100 for 5min, washed twice with PBS and stained with Hoechst (2μg/ml) for 15min and mounted with Fluorsave^{TM}. Images were taken with a Leica TCS SP8 with a resolution of 4096x4096, image acquisition speed at 400hz and 6 line averages. Hypotonic treatment (media 35:65 water) and hypertonic treatment (320 mM sucrose in media) were applied for 10min before fixing of the cells as controls for chromatin relaxation or condensation respectively. Images were analyzed with the GLCM_Texture plugin (ImageJ).

3.2.4.4 Chromatin relaxation assay

U2OS pa-GFP H2B expressing cells were plated the day before the experiment. Prior to imaging, cells were pre-treated for 90 minutes with the indicated actin substances, followed by Hoechst treatment for 1h alone or in combination with the respective actin substance. DMSO treated cells served as control. Specific nuclear areas were photoactivated by the 405 nm laser to induce local DNA damage and followed up over time (36 cells each sample). For decondensation assay, chromatin relaxation was measured every 4 seconds for 120s. To evaluate recondensation, chromatin relaxation was measured for 990s after induction of DNA damage (mean value of 36 cells).

3.2.4.5 Nuclear run-on assay

Cells were treated with the indicated substances and 5mM 5-Fluorouracil (5-FU) (Sigma Aldrich) was added for the last 70min. Fixation and staining was performed as described in 3.2.4.2. Cells were stained with anti-BrdU antibody (B8434, Sigma Aldrich) as primary antibody and Alexa Fluor 488 (A11001, Invitrogen) as secondary antibody. Percentages of positive cells were calculated. Treatment with actinomycin D (7.5μg/ml, Sigma Aldrich) served as positive control for transcriptional inhibition.

3.2.4.6 Foci formation assay

1.5x10^4 cells per well were seeded in 8-well slides (Ibidi) and treated with Doxo [250nM] for 2h, with or without repair time, and in combination with different actin substances as indicated. Fixation and staining was performed as described in 3.2.4.2. The number of foci was either counted manually or with the FindFociGUI (ImageJ) plugin.

3.2.4.7 Duolink assay

To show a possible binding of actin to nuclear DNA damage repair factors on a single cell basis, a proximity ligation assay - Duolink® assay - was performed according to the providers' suggestions (Sigma Aldrich). Briefly, cells were seeded in 12-well (removable) microscopy slides (Ibidi) and treated the next day with Doxo [250nM] for 1h in combination with the actin substances or transfected with actin plasmids YFP NLS Beta-Actin (control plasmid, addgene plasmid 60613), YFP NLS Beta-Actin G13R (depolymerization mutant, addgene plasmid 60615), YFP

NLS Beta-Actin S14C (polymerization mutant, addgene plasmid 60614) 24h prior to the experiment. Cells were then fixed with 4% PFA for 15mins at room temperature, permeabilized with 0.2% Triton X-100 for 5min and blocked with 1% BSA in PBS for 20mins. Primary antibodies were added to the cells (see Tab. 11) and incubated for 1h at room temperature and, after one washing step, Duolink® assay was performed. For Doxo treated samples, Duolink® In Situ Detection Reagents Green were used, while for YFP transfected cells Duolink® In Situ Detection Reagents Red. Images were taken with the Leica SP8 microscope and analyzed with ImageJ. Numbers of positive events in nuclei were counted manually.

Table 11: **Duolink® antibodies**

Target	Provider	Species	Dilution
RPA-2	Abcam (ab2075)	Mouse	1:250
DNA-PKcs	Cell Signaling (12311)	Mouse	1:50
Actin	Sigma Aldrich (A2066)	Rabbit	1:100
Ku70	Abcam (ab92450)	Rabbit	1:200
Actin	Sigma Aldrich (AMAB91241)	Mouse	1:200

3.2.4.8 Life cell imaging

For life cell imaging of transfected cells a stage top cell chamber (Bold Line, Okolab) was installed on a Leica SP8 microscope to maintain the required culturing conditions (37°C, 5% CO_2, 95% humidity). To visualize actin in living cells, different plasmids were used (see Tab. 12).

Table 12: **Actin plasmids for life cell imaging**

Plasmid	Source
Actin-GFP	addgene (plasmid 21948)
Actin-mCherry	addgene (plasmid 54966)
Actin-Chromobody® (GFP)	ChromoTek GmbH, Planegg-Martinsried, Germany

3.2.4.9 Fluorescence correlation spectroscopy

FCS measurements were performed on a Leica TCS SP8 SMD microscope together with the Picoquant LSM Upgrade Kit. Cells were seeded in ibidi 8 well μ-slides with glass bottoms and transfected with Actin-GFP (addgene plasmid 21948) 24h prior to the FCS measurement. The effective volume (Veff) and structure parameter (κ) were measured prior to each independent experiment (see equation below) using 1nM ATTO488 dye solution (ATTO-TEC GmbH, Siegen, Germany). In every selected nucleus (five nuclei each round), three different points were measured for 45s per point at 4 different time points (0, 10, 30, 60min). Doxorubicin [250nM] was added after the zero-time point measurement. Control measurements without the addition of any compound were performed accordingly to verify that photobleaching does not influence the analysis. FCS curves were analyzed with the Picoquant SymPhoTime V 5.2.4.0 software and fitted with a single diffusing species and a triplet state.

$$G_{3D}(\tau) = \frac{1}{N} \cdot \left(1 + \frac{T}{1-T} e \frac{\tau}{\tau_t}\right) . \left(1 + \frac{4D \cdot \tau}{{\omega_r}^2}\right)^{-1} \cdot \left(1 + \frac{4D \cdot \tau}{{\omega_z}^2}\right)^{-\frac{1}{2}}$$

$$V_{Eff,3D} = \pi^{\frac{3}{2}} . {w_0}^2 . z_0 \quad ; \quad D_{3D} = \frac{{w_0}^2}{4\tau} \quad ; \quad < C > = \frac{<N>}{V_{Eff} . N_A}$$

3.2.5 Protein Biochemistry

3.2.5.1 Lysis of cells

Cells were harvested and washed with cold PBS and lysed with cell lysis buffer (dependent on the experiment) + protease inhibitor (1:25) + phosphatase inhibitor (1:10). Cell lysates were cleared by centrifugation (10min, 10000rpm, 4°C) and protein lysates stored at -20°C.

For determination of protein concentrations, the BCA™ Protein Assay Kit (Thermo Scientific) was used and the absorption of each sample measured with an ELISA reader (Tecan, Magellan).

3.2.5.2 Western blot

For standard western blot assay, cells were lysed with Milanese buffer. For separation of proteins SDS polyacrylamide electrophoresis was performed using polyacrylamide gels (8-12%; 10-well and 15-well) and sodium dodecyle sulfat (SDS) buffers. For denaturation 5x sample buffer was added to the protein sample to a final concentration of 1x and boiled for 5min at 95°C. Samples were then loaded unto polyacrylamide gels and electrophoresis was performed (20min at 200V followed by 45min at 100V). After electrophoresis proteins were transferred to nitrocellulosis or PVDF membranes by tank blotting at 100V for 100min or at 30V overnight depending on the size of the protein of interest at 4°C. Non-specific binding was blocked by incubation in blocking solution for 1h at room temperature and was then washed with TBS-T three times for 10min. The membrane was afterwards incubated in the primary antibody (in blocking solution) at 4°C overnight. The next day the membrane was washed with TBS-T three times for 10min and then incubated with a suitable secondary HRP-conjugated antibody for 1h at room temperature. The membranes were incubated with HRP Homemade ECL solution and analyzed by ChemiDoc Touch Imaging System (Bio-Rad). The band intensities of detected proteins were calculated by ImageLab (Bio-Rad) and normalized to the total protein amount (stainfree gel) or actin or tubulin as loading control.

Table 13: **Antibodies for western blot**

Target	Provider	Species	Dilution
RPA-2	Abcam (ab2075)	Mouse	1:1000
DNA-PK	Cell Signaling (12311)	Mouse	1:1000
Actin	Sigma Aldrich (A2066)	Rabbit	1:1000
Actin	MAB1501 (Millipore)	Mouse	1:1000
Ku70	Abcam (ab92450)	Rabbit	1:1000
yH2AX Ser139	Cell Signaling (2577S)	Rabbit	1:1000
p-Chk2 Thr68	Cell Signaling (2661)	Rabbit	1:1000
p-ATM Ser1918	Cell Signaling (5883)	Rabbit	1:1000
anti-mouse (HRP)	abcam (ab97240)	Goat	1:10000
anti-rabbit (HRP)	Dianova (111-035-144)	Goat	1:10000

Milanese lysis buffer 50mM Tris, HCl (pH8), 150mM NaCl, 1% NP40 0.5% sodium deoxycholate, 0.1% SDS, 300μM Na_2VO_3, 1mM NaF, 3mM ß-glyerophosphate, 10mM pyrophosphate, H_2O. Freshly added prior to experiment: 20mM H_2O_2, 200mM PMSF, protease inhibitor cocktail (Roche), phosphatase inhibitor cocktail (Roche).
5x sample buffer 3.13M Tris HCl (pH 6.8), 10% Glycerol , 20% SDS , 16% DTT, 5% Pyronin Y, H_2O. 1x SDS sample buffer diluted 1:5 in H_2O.
Separating gel 5ml 30% Rotiphorese®, 3.75ml 1.5M Tris HCl (pH8.8), 150μl SDS 10%, 6.1ml H_2O, 0.5% 2,2,2-trichloroethanol, 15μl TEMED, 75μl 10% APS.
Stacking gel 1.275ml 30% Rotiphorese®, 750μl 1.25M Tris HCl (pH6.8), 75μl 10% SDS, 5.25ml H_2O, 15μl TEMED, 75μl 10% APS.
5x Electrophoresis buffer 24.8mM Tris-base, 191.8mM Glycine, 3.5mM SDS, H_2O. For 1x buffer diluted in H_2O.
5x Tank buffer 25mM Tris-base, 192mM Glycine, H_2O. For 1x buffer diluted in H_2O + 20% methanol.
TBS-T (pH8.0) 24.8mM Tris HCl, 190mM NaCl, 0.2% Tween 20, H_2O.
Blocking solution PBS + 0.02% Tween20 + 5% non-fat dry milk/BSA.
HRP Homemade ECL 1.25mM Luminol, 0.2mM Cumaric acid, 0.1M Tris-base HCl (pH8.5), 0.009% H_2O_2, H_2O.

3.2.5.3 Co-immunoprecipitation

Cells were lysed with hypotonic buffer, cell suspension passed thrice through a syringe (25G needle) and nuclei isolated by centrifugation (10000rpm, 10min, 4°C). Nuclei were lysed with nuclei lysis buffer, suspension passed twice through a 30G needle, two sonification pulses were applied and suspension spinned down (10000rpm, 10min, 4°C). Cell residues were discarded. 20μl of the resulting protein sample were used for immunoblotting as an input control. The rest was incubated with 10μl of the respective pulldown antibody for 2h at 4°C (see Tab. 14). Protein samples of untreated cells incubated only with beads, or with beads + the respective IgG Control were used as negative controls. Agarose beads (Protein A/G PLUS-Agarose, Santa Cruz) were then added for one more hour followed by washing of beads twice with nuclei lysis buffer and twice with PBS + 150mM KCl + 2mM $MgCl_2$. Immunoprecipitates were collected by centrifugation at 2500rpm for 5min at 4°C. After the last washing step, beads were resuspended in 40μl 1x sample buffer and boiled at 95°C for 5min and immunoblotting performed for both

pulldown protein and the respective potential binding partner (as described in 3.2.5.2).

Hypotonic buffer 10mM HEPES (pH7.9), 1.5mM $MgCl_2$, 10mM KCL, 0.5mM DTT, 0.1% NP-40 (v/v), ad. H_2O.
Nuclei lysis buffer 20mM HEPES (pH7.9), 20% glycerol, 2mM $MgCl_2$, 150mM KCL, 0.2mM EDTA, 0.5mM PMFS, 0.5mM DTT, ad. H_2O.

Table 14: **Antibodies for Co-immunoprecipitation**

Target	Provider	Species
RPA-2	Abcam (ab2075)	Mouse
Actin	Sigma Aldrich (A2066)	Rabbit
Ku70	Abcam (ab92450)	Rabbit
Normal rabbit IgG (Control)	Cell Signaling (2729)	Rabbit
Normal mouse IgG (Control)	Santa Cruz (sc2025)	Mouse

3.2.6 In vivo tumor mouse model

BALB/cOlaHsd female mice were obtained from Envigo (Netherlands) at an age of 6 weeks and experiments started at the age of 8 weeks. All performed animal experiments were approved by the District Government of Upper Bavaria in accordance with the German Animal Welfare and Institutional guidelines.

A tumor mouse experiment was performed to show DNA damage repair inhibition *in vivo* (Fig. 8). 1x10^6 4T1-luc cells per mouse were diluted in 100μl PBS and injected subcutaneously. Tumors were grown for 7 to 10 days before the start of treatment. Mice were treated with 3mg/kg Doxorubicin i.v. (diluted in PBS) alone or in combination with 0.1mg/kg Latrunculin B, i.p. (5% DMSO + 10% solutol in PBS) for 24h. Mice were then sacrificed and tumors harvested, mechanically disrupted and incubated in enzyme mix (Miltenyi Biotech) for 45min at 37°C. Digested tissue was then filtered through cell strainers with a size of 40μm to obtain single cell suspensions. Cells were counted and seeded accordingly for alkaline comet assay (performed as described in 3.2.4.1).

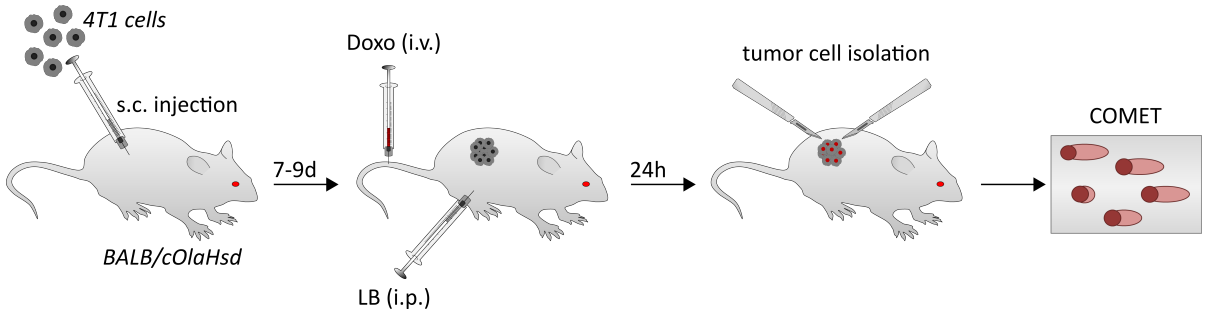

Figure 8: **Setup of xenograft mouse model.**

3.2.7 Statistics

Unless stated otherwise, all experiments were performed three times in independent experiments. Dependent on the assay, one-way ANOVA test with relevant post tests (Dunnetts Multiple Comparisons or Sidaks multiple comparisons test) or t-test (paired or unpaired) were used to assess the significance of difference between treatment groups as indicated in each respective experiment. P-values <0.05 were considered significant.

Potential synergism of combination treatment was assessed by calculation of Bliss value with normalized values (NV). All bliss values >1 were considered synergistic.

$$Bliss\ value = \frac{NV\ (combination)}{(NV\ substance\ 1 + NV\ substance\ 2) - (NV\ substance\ 1 * NV\ substance\ 2)}$$

The statistical analysis was conducted with GraphPad Prism 7.

4 Results

4.1 Actin and its role in nuclear DNA damage repair processes

Actin reorganization has been suggested to be induced during DNA damage response (DDR), although its direct role in nuclear DNA damage repair signalling processes has not been investigated yet to a greater extent. Nuclear actin has been described to be polymerized upon DNA damage induction and is therefore assumed to be required for the functioning of DNA repair [79]. However, only very few studies have been published so far that show a direct link of actin to DNA damage repair factors. There is hence still the need for further investigations to obtain a better understanding of nuclear actin regulation during DNA damage repair signalling and to answer the question whether nuclear actin is indeed involved in DNA DSB repair and if yes, how.

To study DNA damage response, DNA DSBs were introduced by doxorubicin treatment. Actin manipulation was achieved by either overexpression of actin mutant plasmids or treatment with actin binding compounds. Low doses of actin binders were applied to analyze specific effects of actin manipulation on DNA damage responses and to avoid unwanted cytotoxic effects. Mostly, classical actin binding substances, namely latrunculin B (actin depolymerizer) and jasplakinolide (actin polymerizer) were applied.

4.1.1 Actin binders influence cytoplasmic and nuclear actin.

Effects of low dose treatment with actin binders on actin morphology, both in the cytoplasm and in the nucleus, were examined.

In the cytoplasm, low dose treatment with the actin depolymerizer LB resulted in a fast disruption of the actin cytoskeleton structure after only 30 minutes, which led to shrinkage of cells and loss of cell-cell contacts. Those strong morphological changes were found to remain stable for at least three hours. Cytoplasmic actin filaments started to form again six hours after application of LB and after 24 hours, the structure of the actin cytoskeleton in the cytoplasm was completely recovered (Fig. 9).

Treatment with the polymerizer Jaspla caused formation of actin aggregates in the cytoplasm that started to be visible 90 minutes after substance application and were stable for up to 24 hours. Cell-cell contacts were not completely lost by Jaspla treatment (Fig. 9).

HeLa cells transfected with an actin-GFP plasmid revealed differential changes in nuclear actin levels upon application of actin binders. LB treatment resulted in elevated nuclear fluorescence signals, i.e. in a rather fast accumulation of actin in the nucleus (Fig. 10A). On the contrary,

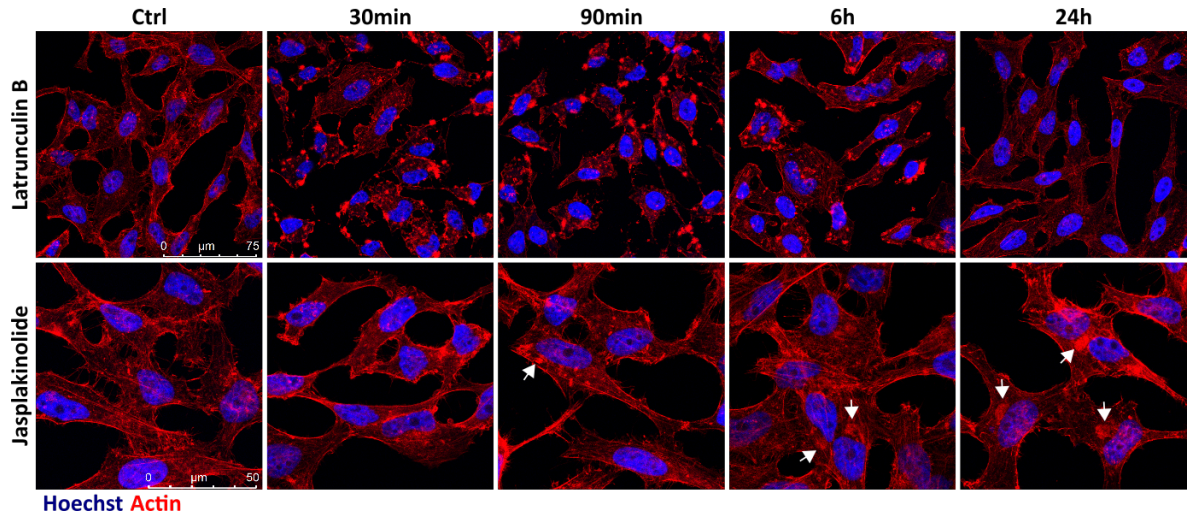

Figure 9: **Effects of actin binders on cytoplasmic actin.** HeLa cells were treated with latrunculin B [500nm] or jasplakinolide [100nM]. Cells were fixed at the indicated time points, permeabilized and stained for F-actin (rhodamine-phalloidin, red) and DNA (Hoechst, blue). White arrows mark jasplakinolide induced actin aggregates.

Jaspla slightly diminished nuclear actin levels (Fig. 10A). Independent of the character of actin manipulation, an increased polymerization of nuclear actin was triggered upon overexpression of the nuclear actin-Chromobody® plasmid (ChromoTek) in combination with either LB or Jaspla treatment (Fig. 10B).

Thus, in addition to the obvious effects of actin binders on cytoskeletal actin, influences on nuclear actin were detected as well. Interestingly, changes in protein levels of nuclear actin were found to be dependent on the class of the actin binding compound, whereas alterations in the polymerization state of nuclear actin were not.

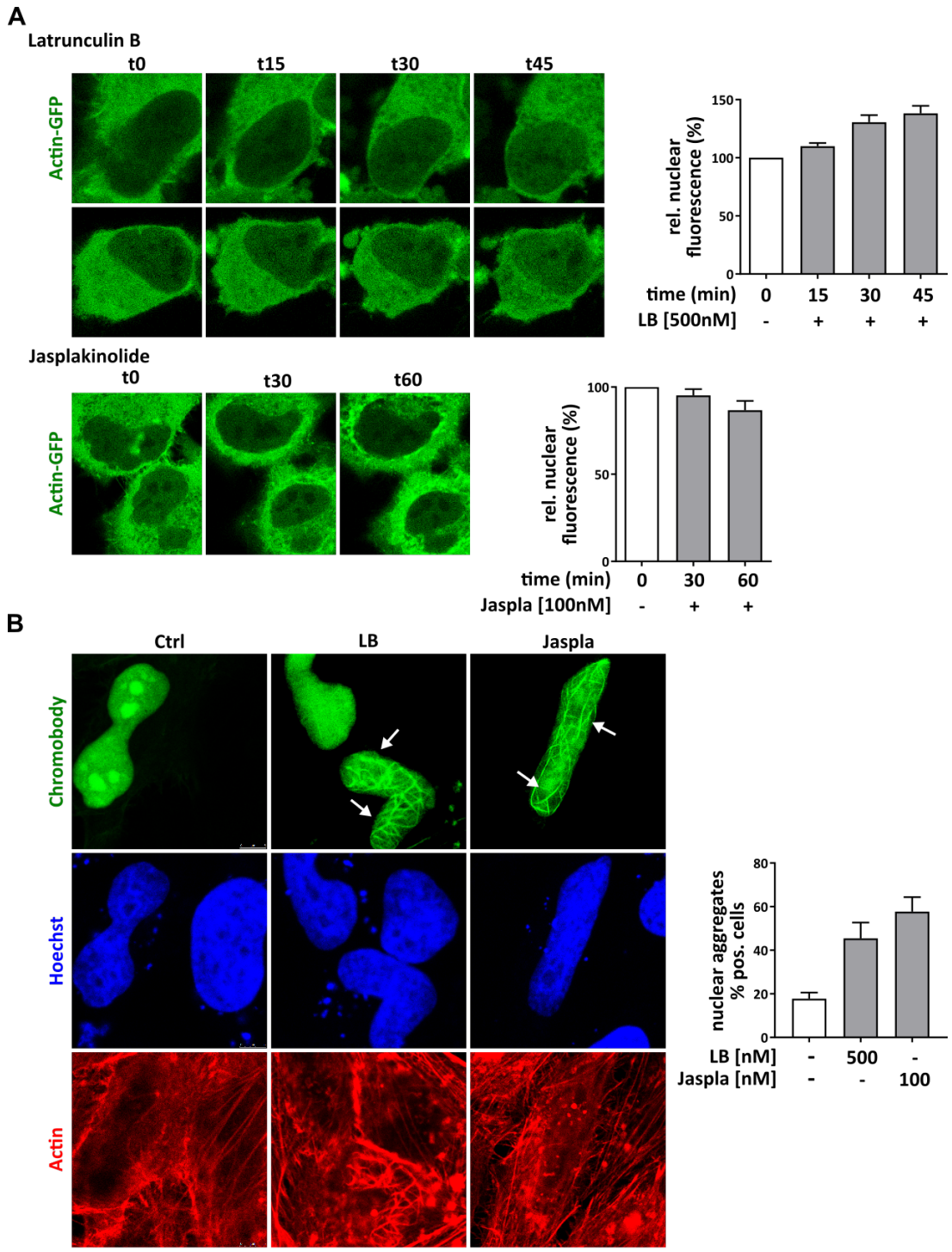

Figure 10: **Effects of actin binders on nuclear actin. A Nuclear actin levels.** HeLa cells were transfected with actin-GFP and life cell imaging was performed. Fluorescence intensities in the nucleus were measured at the indicated time points after addition of the actin binding substances. Mean values of two ROIs each of at least 15 cells (three independent rounds) are depicted. **B Nuclear actin polymerization.** HeLa cells were transfected with nuclear actin-Chromobody® plasmid, treated with the indicated actin substances for 2h, then fixed, permeabilized and stained with rhodamine-phalloidin and Hoechst. The number of cells positive for nuclear actin aggregates was counted. Exemplary nuclear actin filaments are highlighted by white arrows. Mean values of at least three independent experiments (+/- SEM) with at least 20 cells per experiment are shown.

4.1.2 Manipulation of the actin equilibrium inhibits DNA double strand break repair.

Single cell electrophoresis (comet assay) was performed in order to analyze whether actin is involved in the repair of Doxo induced DSBs. Actin was manipulated either by treatment of cells with actin binders (Fig. 11A) or by overexpression of mutant actin plasmids (Fig. 11B).

The repair of double strand breaks induced by Doxo treatment was inhibited independently of the type of actin manipulation (Fig. 11). Both a decrease of polymerized actin due to actin depolymerizers (LB or chivosazole A) or transfection with G13R-NLS-YFP (actin polymerization mutant) and the increase of polymerized actin by treatment with actin polymerizers (Jaspla, ChB or miuraenamide A) or over expression of S14C-NLS-YFP (actin depolymerization mutant) led to impaired DNA damage repair. Pre-treatment with actin binding substances prior to addition of Doxo achieved stronger effects on the repair capacity. On the contrary, no increased DNA damage was detected with actin manipulation alone. Elevated levels of DSBs are therefore unlikely to derive from accumulation of DNA damage, but are rather caused by defects in DNA damage repair due to additional actin manipulation.

Thus, a tight control of the actin equilibrium in the cytoplasm and/or the nucleus seems to be required for functional repair of Doxo induced DNA DSBs.

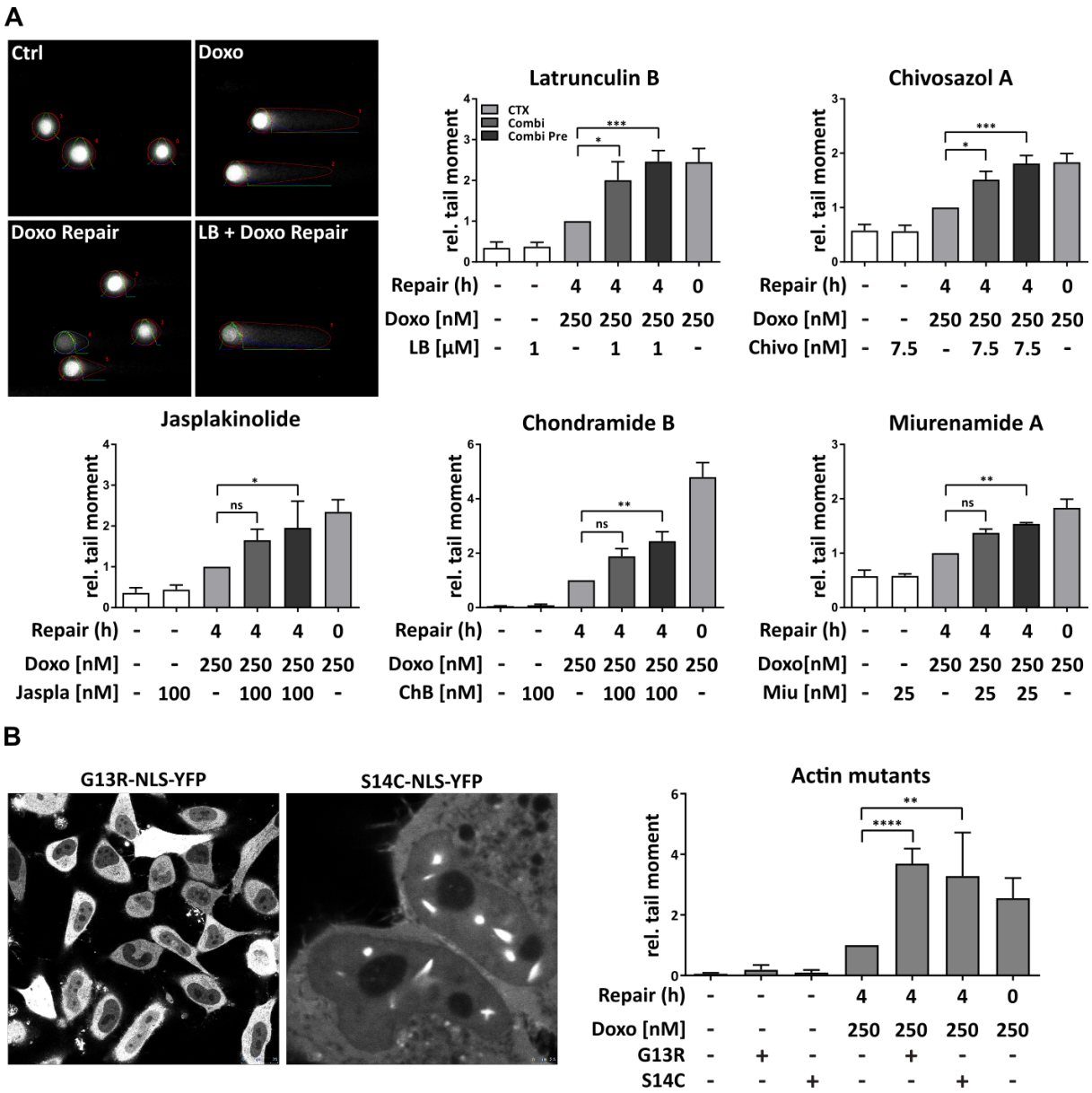

Figure 11: **Actin manipulation inhibits DNA damage repair. A Actin binding compounds.** HeLa cells were treated with 250nM Doxo for 2h with or without addition of the indicated actin substances (pre = pretreatment with actin substance for 90mins). Doxo was then removed and cells incubated in DMEM (Doxo Repair) or DMEM + the respective actin substance. Doxo treatment alone without repair time served as positive control. Images were analyzed with OpenComet (ImageJ, output examples shown on the left) and tail moments calculated. Relative tail moments are shown (normalized on Doxo repair samples). *Comet assays with chivosazol A and miurenamide A performed by Anja Arner.* **B Actin mutants.** Cells were transfected with G13R-NLS-YFP or S14C-NLS-YFP, 24h prior to the induction of DNA damage with Doxo and comet assay performed as described in A. Untransfected cells were used as a negative control.
Mean values (+/- SEM) of at least three independent experiments are shown (one-way ANOVA, *p<0.05, **p<0.01, ***p<0.005,****p<0.0001, ns not significant).

4.1.3 Doxorubicin induced DNA damage affects nuclear actin states.

The formation of nuclear actin filaments upon DNA damage induction has been suggested to be required for DNA damage repair [79, 113]. Nevertheless, the influence of DNA DSB signalling on nuclear actin organization and vice versa is still not well understood.

Actin polymerization upon DNA damage induction in HeLa cells transfected with the nuclear actin probe nuclear actin-Chromobody® could be confirmed. The number of cells with nuclear GFP-positive actin aggregates was strongly increased upon Doxo treatment (Fig. 12A). Additional co-transfection experiments were performed to exclude the possibility that the observed effect is only caused by a shift of actin to the nucleus due to the overexpression of an actin binding antibody that is fused to a NLS (i.e. the nuclear actin-Chromobody®). Co-transfection of mCherry-actin (without a NLS) and the nuclear actin-Chromobody® did not lead to increased mCherry-actin levels in the nucleus (Fig. 12B). In order to analyze if DNA damage leads to nuclear import or export of actin, cells were transfected with actin-GFP, and fluorescence intensity ratios of nucleus to cytoplasm measured before and 1h after addition of Doxo. No significant changes in the ratio of actin levels could be observed (Fig. 12C), which implies that actin reorganization in the nucleus is not caused by import from or export to the cytoplasm. With this experimental setup, no nuclear actin aggregates could be observed. Although chromobody overexpression did not significantly alter nuclear actin levels, it cannot be excluded that it artificially stabilizes established actin structures, leading to disproportionate effects (reviewed in [123]). To circumvent this problem and strengthen the finding that actin is reorganized in the nucleus upon DSB induction, FCS measurements were performed (Fig. 12D). Upon DNA damage induction by Doxo treatment, concentrations of free nuclear actin (actin-GFP) were significantly decreased in a time dependent manner (Fig. 12D2), whereas diffusion coefficients remained at a similar value (Fig. 12D3). A decrease of free actin in the nucleus could be explained by an export of actin to the cytoplasm (which was not observed in (Fig. 12C)) or by an increase in the immobile (not measurable) actin fraction due to actin polymerization or recruitment.

Hence, induction of DSBs indeed seems to alter the state of actin in the nucleus shifting the equilibrium to a more polymerized/immobile actin fraction. This observation rises the question which role the recruitment and/or polymerization of actin plays in DNA damage induced signalling.

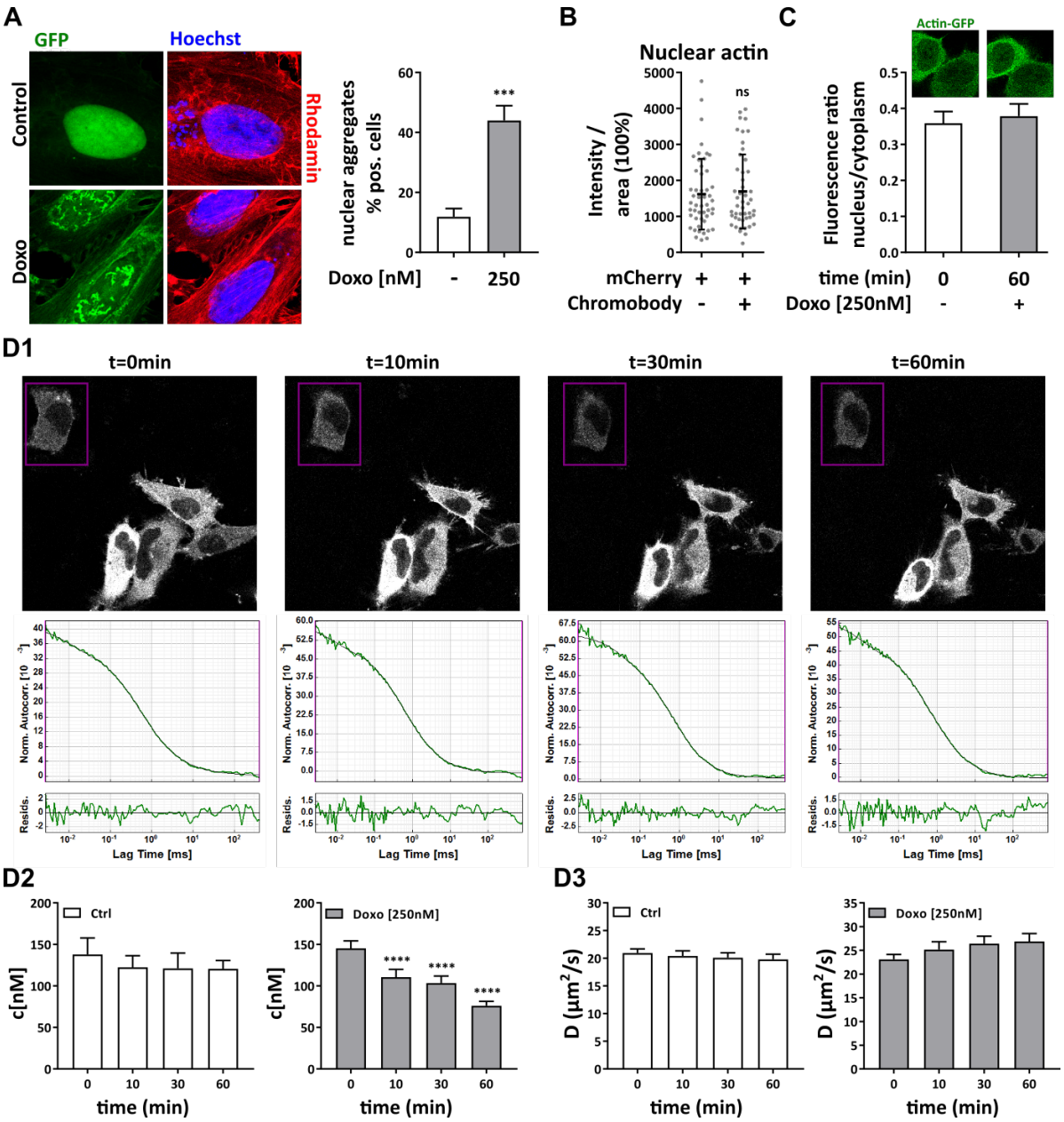

Figure 12: **Influences of Doxo induced DNA damage on nuclear actin. A Nuclear actin polymerization.** After transfection with Chromobody®, HeLa cells were treated with Doxo and cells positive for nuclear actin aggregation counted. Mean values (+/- SEM) are shown (unpaired t test, two-tailed, ***p<0.005). **B Influence of nuclear actin-Chromobody® on nuclear actin level.** Cells were transfected with mCherry-actin alone or in combination with Chromobody® and fluorescence intensity of nuclear mCherry expression was measured. Single values of three independent experiments are depicted (unpaired t test, two-tailed, ns not significant). **C Nuclear actin level.** Cells overexpressing actin-GFP were treated with Doxo, and fluorescence intensities measured before and 1h after addition of Doxo (mean values of two ROI per cell). Graph shows ratio of measured intensities of nucleus to cytoplasm. Up to 20 cells in three independent rounds were analyzed. **D FCS.** Cells overexpressing actin-GFP were treated with Doxo and single points FCS measurement of nuclear actin was performed at the indicated time points. **D1.** Example pictures of one round are shown and corresponding fitting curves of one cell (indicated by purple rectangle) depicted. Nuclear concentrations of actin **D2** and diffusion coefficients **D3** were determined in three independent experiments (at least 30 cells). Untreated cells served as control (10 cells). Graphs show mean values +/- SEM. **** p<0.0001, paired t test, two-tailed. *Analysis of FCS measurement performed by Themistoklis Zisis.*

4.1.4 Actin binding substances do not affect chromatin structure and overall transcriptional activity at low concentrations.

Chromatin reorganization plays a role in DSB repair, it is e.g. important for repair factor recruitment. The nuclear matrix is mainly composed of actin [88]. The local reorganization of the chromatin structure might therefore depend on the state of actin. As a consequence, actin manipulation could alter DSB induced chromatin changes, resulting in impeded DNA damage repair.

Doxorubicin has been described to induce chromatin compaction (measured in isolated chromatin) [124], although the role of this process has not been specified yet. Global condensation and relaxation can be measured by analysis of chromatin texture upon staining of DNA with Hoechst in fixed cells. An increase in contrast and a decrease of correlation compared to the control indicates chromatin compaction (e.g. after hypertonic treatment), whereas the decrease in contrast and increase of correlation indicates relaxation (hypotonic treatment). Single treatment with LB and Jaspla did not lead to changes in global chromatin texture (Fig. 13). The minor global chromatin compaction upon Doxo treatment was not impaired in combination with Jaspla and only slightly altered in combination with LB (Fig. 13).

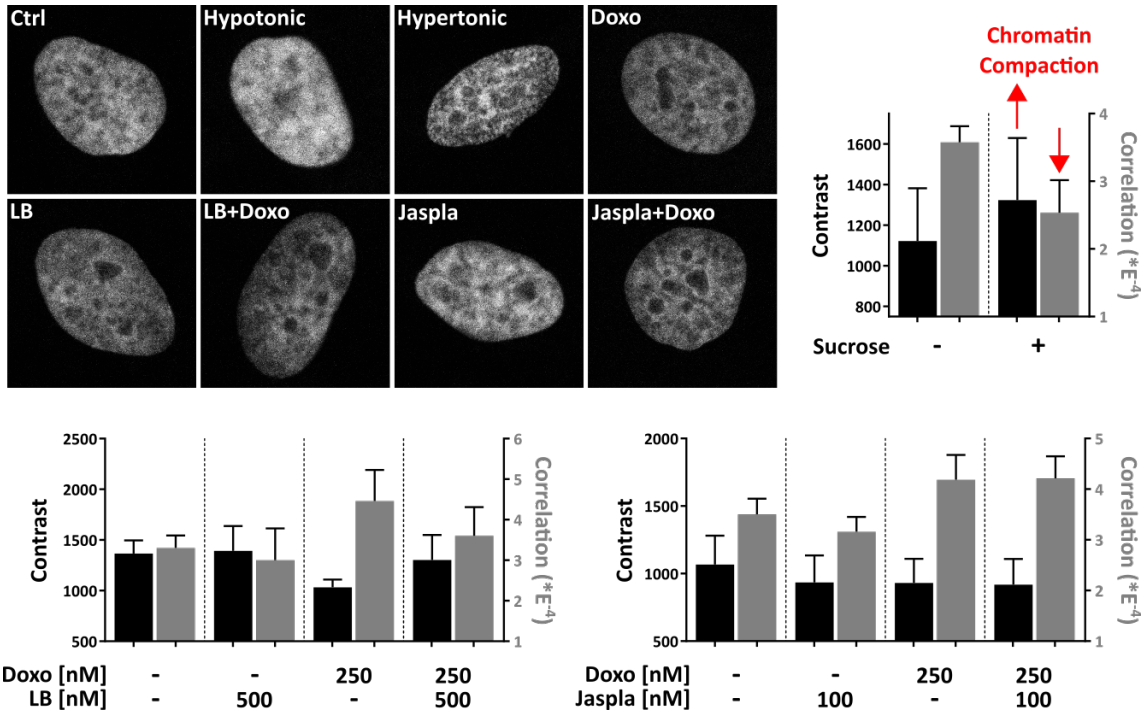

Figure 13: **Low dose treatment with actin binders does not change global chromatin texture.** After treatment, cells were fixed and permeabilized and stained for Hoechst. Hypotonic treatment (media 35:65 water) and hypertonic treatment (320mM sucrose in media) were applied as positive controls for chromatin relaxation or condensation, respectively. Images were taken with a Leica TCS SP8 with a resolution of 4096x4096 and analyzed with the GLCM_Texture plugin (ImageJ).

Local chromatin relaxation occurs upon DSB formation and is required for efficient DNA repair as only relaxed chromatin allows recruitment of specific DNA damage repair proteins to the site of damage [125, 126]. To analyze whether changes in chromatin structure by administration of actin binding substances impairs local DNA damage mediated chromatin decondensation,

chromatin relaxation was measured with or without precedent actin binder treatment in U2OS pa-GFP H2B expressing cells (Fig. 14). None of the applied actin binders impeded chromatin decondensation during the first 120 seconds after local UV-induced DNA damage (Fig. 14A). Following the DSB induced relaxation, chromatin structures are usually quickly re-established [126]. Chromatin recondensation was still functioning in the presence of Jaspla and was not delayed (Fig. 14B).

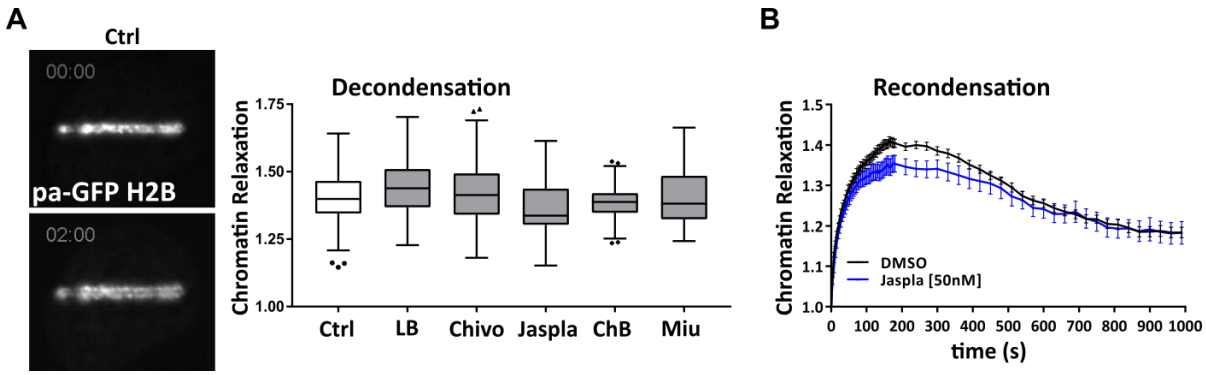

Figure 14: **Chromatin relaxation upon DNA damage induction.** U2OS pa-GFP H2B expressing cells were plated the day before. Prior to imaging, cells were pre-treated for 90 minutes with the indicated actin substances, followed by Hoechst treatment for 1h alone or in combination with the respective actin substance. Specific nuclear areas were photoactivated by the 405 nm laser to induce local DNA damage and followed up over time. **A Decondensation.** Cells were treated with the indicated actin substances (LB [1M], Chivo [7nM], Jaspla [100nM], ChB [75nM], Miu [25nM]) and chromatin decondensation was measured every 4 seconds for 120s (36 cells each sample, n=2-3). DMSO treated cells served as control (one exemplary image of control cells 0min and 2min after induction of damage is shown on the left). **B Recondensation.** Chromatin relaxation of Jaspla treated cells was measured for 990s after induction of DNA damage (mean value of 36 cells). DMSO treated cells served as control.
Chromatin relaxation assays performed by Rebecca Smith at the department of Physiological Chemistry, LMU, Munich.

Global chromatin compaction by Doxo treatment and local chromatin relaxation upon UV-induced damage was not impeded by the addition of actin binders at low concentrations. Inhibition of DNA damage repair is thus most likely not caused by general obstruction of repair factor recruitment due to decreased chromatin relaxation at the site of damage.

Inhibition of transcription and the resulting reduction of repair factor protein levels could be another general mechanism responsible for repair inhibition by actin binding compunds. To measure overall transcriptional activity, nuclear run-on assay was performed. With this assay, incorporation of 5-FU, which happens when transcription is ongoing, can be visualized by immunocytochemistry. Short term low dose treatment with both actin binders LB and Jaspla did not decrease transcriptional activity (Fig. 15). It is therefore unlikely that DNA damage repair is inhibited due to general inhibition of transcription of proteins involved in DDR upon low dose treatment with actin binding substances.

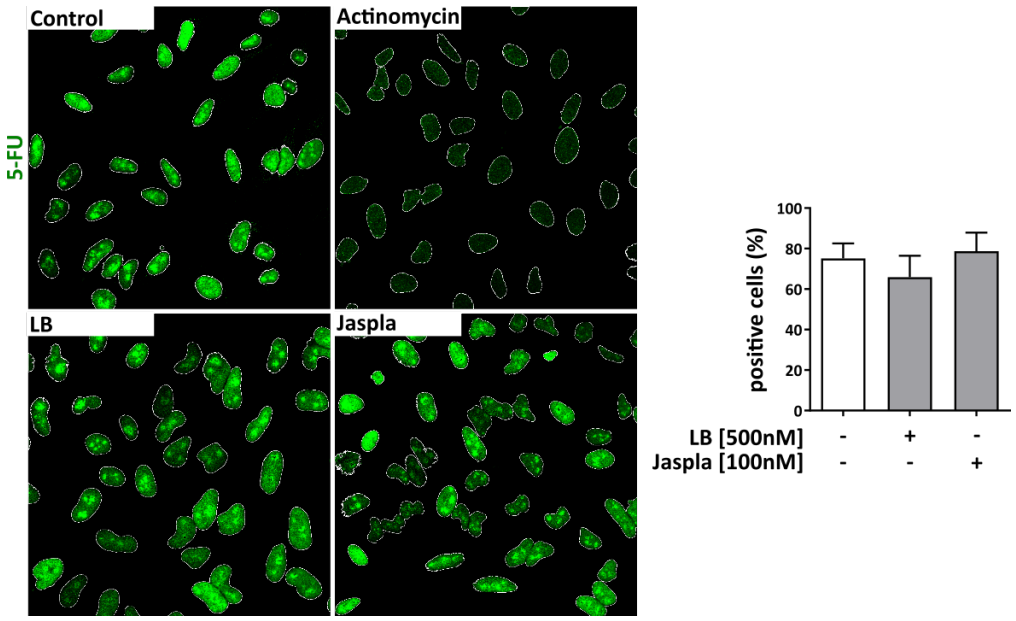

Figure 15: **Low dose treatment with actin binders does not inhibit overall transcriptional activity.** HeLa cells were treated with LB or Jaspla for 2h. Treatment with actinomycin (7.5μg/ml) served as positive, DMSO treatment as negative control. 5-FU was added, cells fixed, permeabilized and stained for incorporated nucleotid analogons (anti-BrdU antibody). Percentages of positive cells were calculated (mean values +/- SEM). At least 150 cells were analyzed for each condition in three independent experiments.

4.1.5 Actin manipulation does not inhibit activation of the ATM-Chk2 pathway and phosphorylation of histone H2AX.

The detection of DNA DSB by MRN leads to activation of numerous signalling cascades. MRN phosphorylates and thereby activates for instance ATM which subsequently activates Chk2. The ATM-Chk2 pathway is involved in many DNA damage induced processes, such as DNA repair, cell cycle arrest or apoptosis induction [24, 26]. The activation of the ATM-Chk2 pathway can be evaluated through phosphorylation levels of both members at Ser1981 and Thr68, respectively, as these represent activating phosphorylation sites. To test if the inhibition of DNA damage repair by different actin binders is caused by a reduced activation of the ATM-Chk2 pathway, initiation of phosphorylation at both activating sites upon DNA damage induction was measured by western blot (Fig. 16). However, no reduction in phosphorylation by addition of LB, Jaspla or ChB could be observed. Phosphorylation of ATM was even significantly increased when treated with LB or Jaspla. Actin binders alone did not induce phosphorylation of ATM or Chk2.

MRN also phosphorylates histone H2AX adjacent to the break which functions as a scaffold for many proteins involved in DNA damage repair [28, 29]. Foci formation by phosphorylation of surrounding H2AX can be visualized by immunocytochemistry. After DNA damage induction with Doxo, a strong increase in cells positive for yH2AX could be detected, which was not significantly impeded by additional application of the actin binding substances LB or Jaspla (Fig. 17A). Combination treatment with LB only led to a small decrease in cells positive for yH2AX foci formation. Flow cytometry analysis was performed to measure chromatin association of yH2AX (Fig. 17 B) and western blot to determine phosphorylation of H2AX (Fig. 17C). The

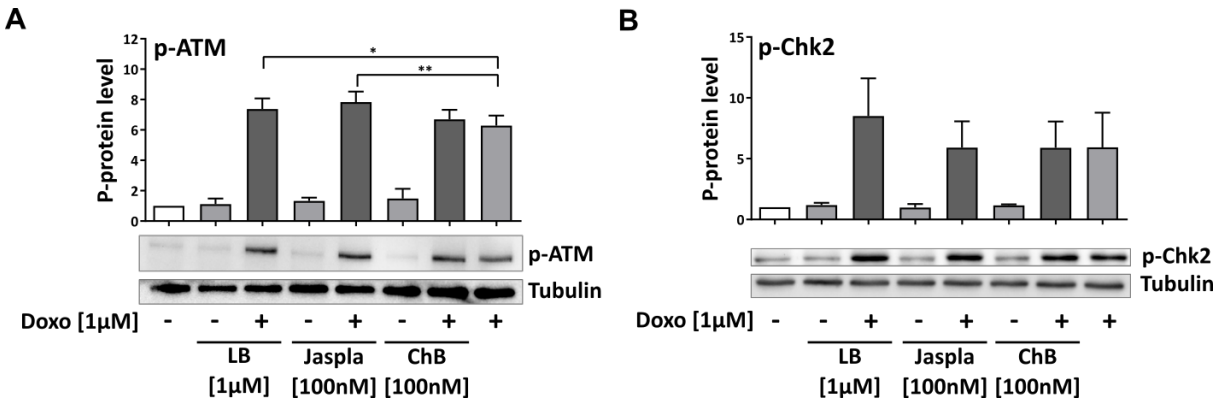

Figure 16: **Phosphorylation of ATM and Chk2 upon Doxo induced DNA damage.** HeLa cells were treated with Doxo alone or in combination with the indicated substances for 1h. Cells were harvested and lysed and immunoblotting performed. Tubulin served as loading control. Values were calculated with ImageLab, normalized on untreated control (n=3, values +/- SEM). One blot out of three independent experiments is depicted as an example. **A ATM.** Phosphorylation at Ser1981. One-way ANOVA, Dunetts multiple comparisons test * $p<0.05$, ** $p<0.01$. **B Chk2.** Phosphorylation at Thr68.

slight reduction of yH2AX foci numbers upon LB combination treatment (as shown in Fig. 17A) could not be confirmed with these methods.

In summary, actin binders did not impair phosphorylation of ATM, Chk2 and histone H2AX. An inhibition of early phosphorylation events was therefore not considered to be the cause of decreased DNA DSB repair by actin manipulation.

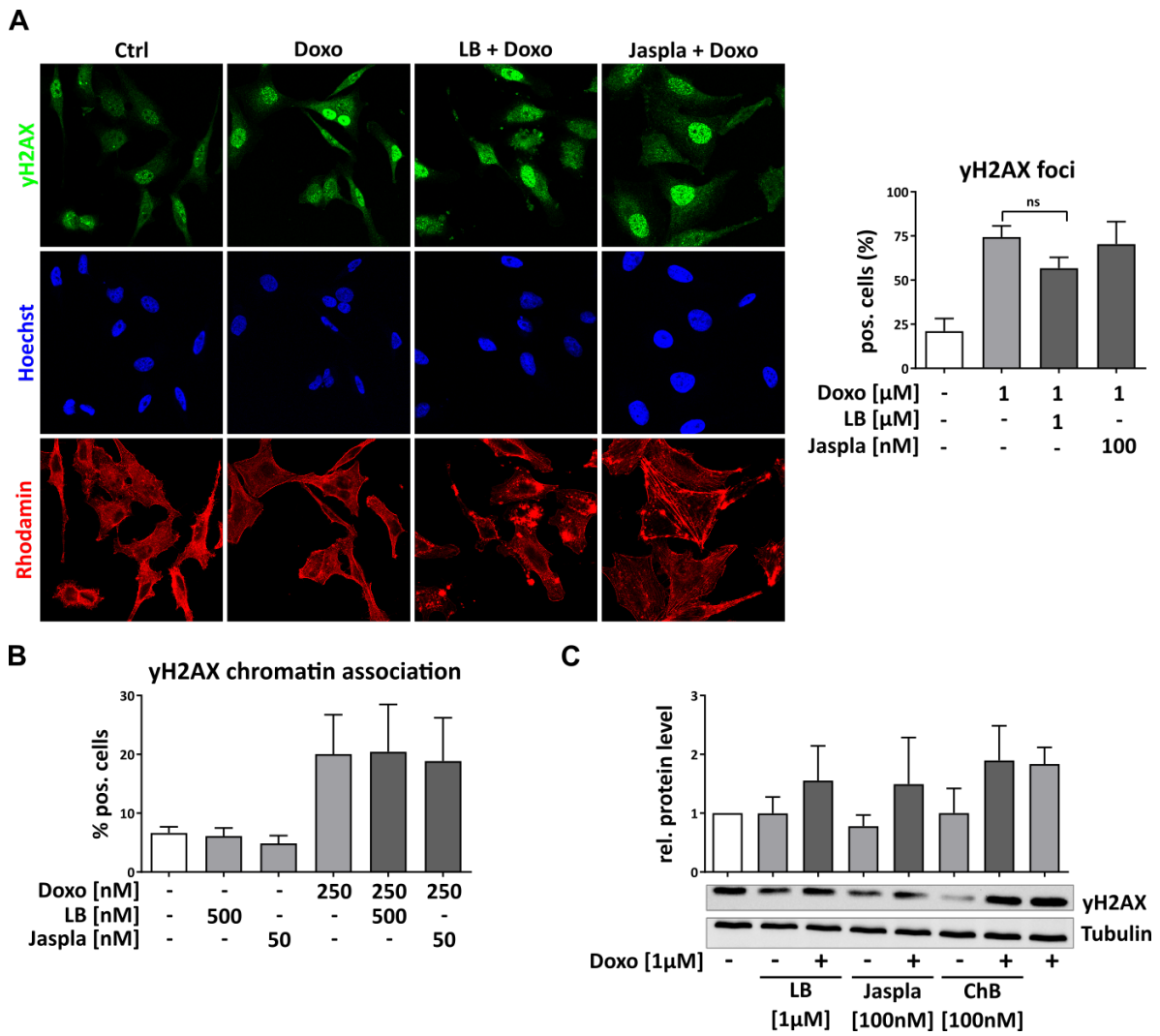

Figure 17: **Actin binders do not decrease phosphorylation of histone H2AX upon Doxo induced DNA damage. A γH2AX foci formation.** Cells were treated with Doxo alone or in combination with the depicted actin substances for 2h, cells fixed and stained for γH2AX, nuclei (Hoechst) and the cytoskeleton (rhodamine). Examples are shown on the left. Cells with more than 5 foci were defined as positive and the percentage of positive cells calculated. Graph on the right shows mean values (+/- SEM) of three independent experiments (unpaired t test, ns not significant). **B γH2AX chromatin association.** HeLa cells were treated with the indicated substances for 2h. Unbound protein was excluded by washing with extraction buffer, cells fixed with 4% PFA and stained for γH2AX and flow cytometry performed (n=3). **C γH2AX protein level.** HeLa cells were treated with Doxo and the indicated actin binders for 1h. Cells were harvested, lysed and immunoblotting performed. Tubulin served as loading control. Values were calculated with ImageLab, normalized on control (untreated). One exemplary blot out of three experiments is shown.

4.1.6 Actin binders inhibit distinctive DSB repair pathways.

Distinctive repair pathways are activated upon DSB induction. The choice between non-homologous end joining (NHEJ), alternative end joining (alt-EJ), homology directed repair (HDR) and single strand annealing (SSA), primarily depends on the cell cycle state of the cell. To study DNA damage repair capacity in detail, I-SceI-based reporter cell lines that can distinguish between all four DSB repair pathways have been developed (published in [120] and described in detail in 3.2.3.3). Transient overexpression of the endonuclease I-SceI leads to cuts in specific GFP cassettes that are interrupted by one or more I-SceI recognition site(s). The repair of I-SceI induced breaks results in a rescue of GFP expression. GFP-positive cells can then be measured by flow cytometry.

Treatment with actin binders after induction of DSB by transient I-SceI expression led to differential responses (Fig. 18). Both actin polymerizers Jaspla and ChB inhibited NHEJ, whereas LB did not reduce NHEJ capacity (Fig. 18A). Alternative end joining was not influenced by any of the applied actin binding substances (Fig. 18B). On the contrary, the impairment of both pathways HDR (Fig. 18C) and SSA (Fig. 18D) did not depend on the type of actin manipulation and was significant for both LB and Jaspla.

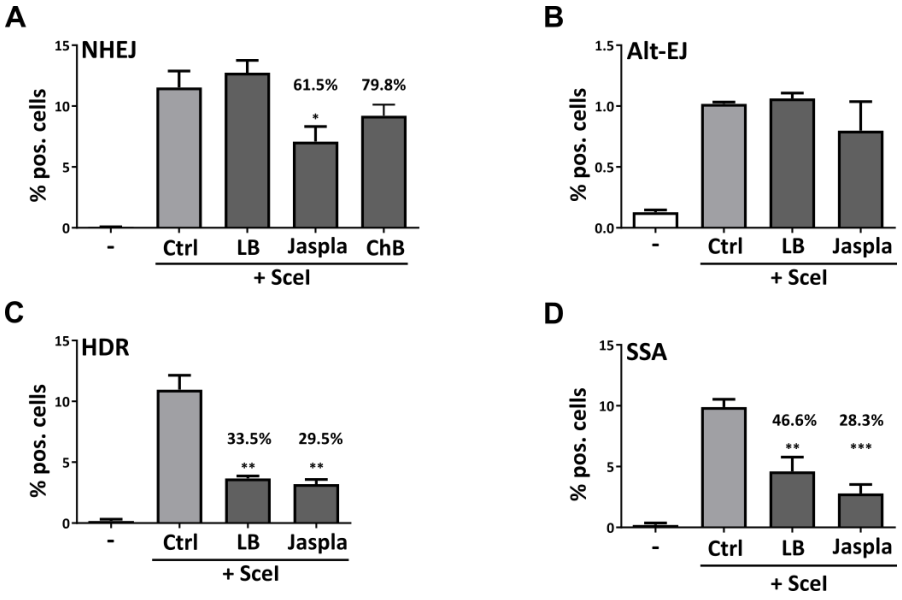

Figure 18: **Effects of actin manipulation on distinctive DSB repair pathways.** U2OS cells expressing one of each respective reporter system were transfected with pcBASE (overexpression of I-SceI) and then cultivated with or without the indicated actin substances (LB [500nM], Jaspla [50nM], ChB [75nM]) for 72h. Percentages of GFP-positive cells were measured by flow cytometry. Experiment performed in duplicates. Mean values of three independent experiments are shown (+/- SEM), unpaired t test, one-tailed, * $p<0.05$, ** $p<0.01$, *** $p<0.005$. **A NHEJ.** Non-homologous end joining. **B Alt-EJ.** Alternative end joining. **C HDR.** Homology directed repair. **D SSA.** Single strand annealing.

In summary, actin binding substances inhibit specific pathways that play a role in the repair of Doxo induced DSBs.

4.1.7 Ku70 binds to nuclear actin and actin binders decrease activation of DNA-PK.

DSB repair by non-homologous end joining was inhibited by increased actin polymerization due to Jaspla and ChB treatment (as shown in Fig. 18A). One of the key events for NHEJ initiation is the activation of DNA-PK, which is induced by the recruitment of DNA-PKcs (catalytical subunit) to DNA-bound Ku70/80. Its kinase activity is further elevated by numerous auto-phosphorylation events [40, 41]. Activation of DNA-PK can therefore be correlated with increased phosphorylation of specific sites.

Doxo induced autophosphorylation of DNA-PK (pDNA-PK) at T2609 was decreased after treatment with Jaspla or ChB, as displayed by a reduction of pDNA-PK foci in the nucleus. Inhibition of DNA-PK autophosphorylation by ChB was significant after a short term treatment of two hours (Fig. 19A). The slight effects of Jaspla on phosphorylation after two hours were further increased after four additional hours of repair time (Fig. 19A+B). LB treatment showed only weak effects on DNA-PK autophosphorylation (Fig. 19A).

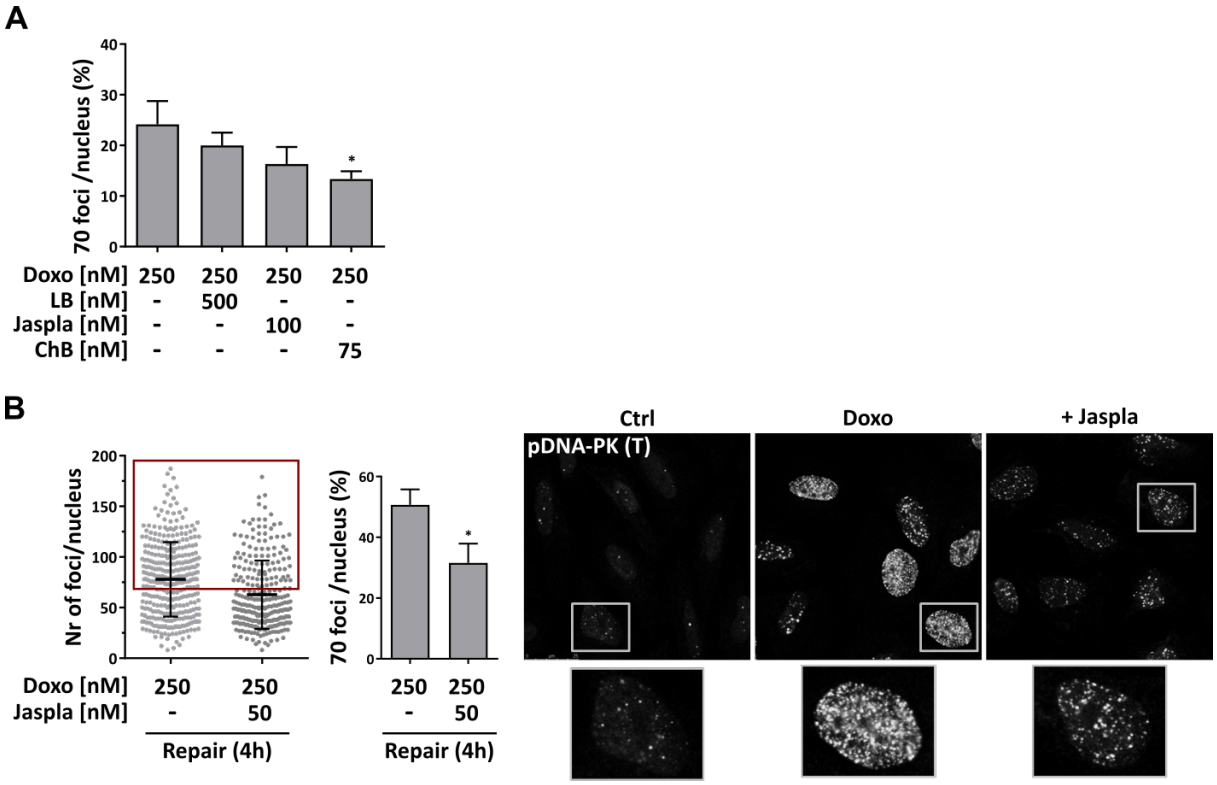

Figure 19: **Autophosphorylation of DNA-PK (T2609).** HeLa cells were treated with Doxorubicin with or without additional actin substance treatment for 2h. For measurements without repair time, cells were then fixed, permeablized and immunocytochemistry performed. For measurements with repair time, Doxorubicin was removed after 2h and cells incubated in DMEM +/- Jaspla (4h repair time) followed by fixation and permeabilization. Foci were visualized by antibody staining against pDNA-PK (T2609). Foci were counted with FiJi Plugin FindFOCI GUI. Cells with at least 70 foci per nucleus were determined as strong positive cells and percentages calculated. At least 100 nuclei were analyzed for each sample (n=3, unpaired t test, one-tailed, * $p<0.05$). **A** No repair time. **B** 4h of repair time. Graph on the left shows single values of foci numbers per nucleus for all conducted experiments, graph on the right depicts mean values of percentages of strong positive cells.

The observed reduction of phosphorylation events at T2609 was not caused by decreased protein levels of total DNA-PKcs (Fig. 20A) or Ku70 (Fig. 20B).

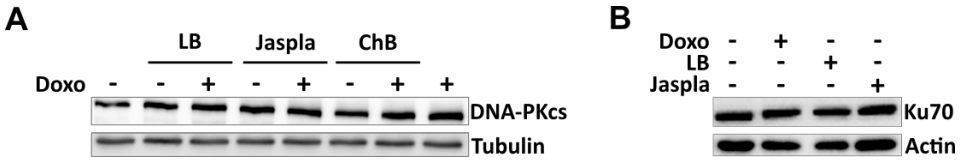

Figure 20: **DNA-PK protein levels. A DNA-PKcs.** HeLa cells were treated with Doxo [1μM] and/or the indicated actin binders (LB [1μM], Jaspla [100nM], ChB [100nM]) for 1h. Cells were harvested and lysed followed by immunoblotting. Tubulin served as loading control. One blot out of three independent experiments is depicted. **B Ku70.** HeLa cells were treated with the indicated substances (Doxo [250nM], LB [500nM], Jaspla [100nM]) and immunoblotting performed for detection of Ku70 and actin. One exemplary blot is shown.

Furthermore, DNA-PKcs was not bound to nuclear actin before or after DNA damage induction, indicated by the lack of positive events in a proximity ligation assay (Duolink®) (Fig. 21B). Functionality of the applied DNA-PKcs antibody was confirmed with control immunocytochemistry (Fig. 21A). Thus, obstructed binding of nuclear actin to DNA-PKcs was considered not to be the cause of reduced DNA-PKcs autophosphorylation at T2609. Autophosphorylation of DNA-PKcs is induced upon binding to DNA-bound Ku [40, 41]. The observed decrease of phosphorylation could therefore also be caused by altered recruitment of Ku to the DNA. Duolink assay revealed that indeed Ku70 seems to be bound to nuclear actin under control conditions (Fig. 21C). This binding was slightly reduced after induction of DNA damage (Fig. 21C1). Hyperpolymerization of actin by overexpression of the actin mutant S14C led to a decreased binding of Ku70 to nuclear actin, whereas depolymerization upon G13R overexpression did not show any effects (Fig. 21C2).

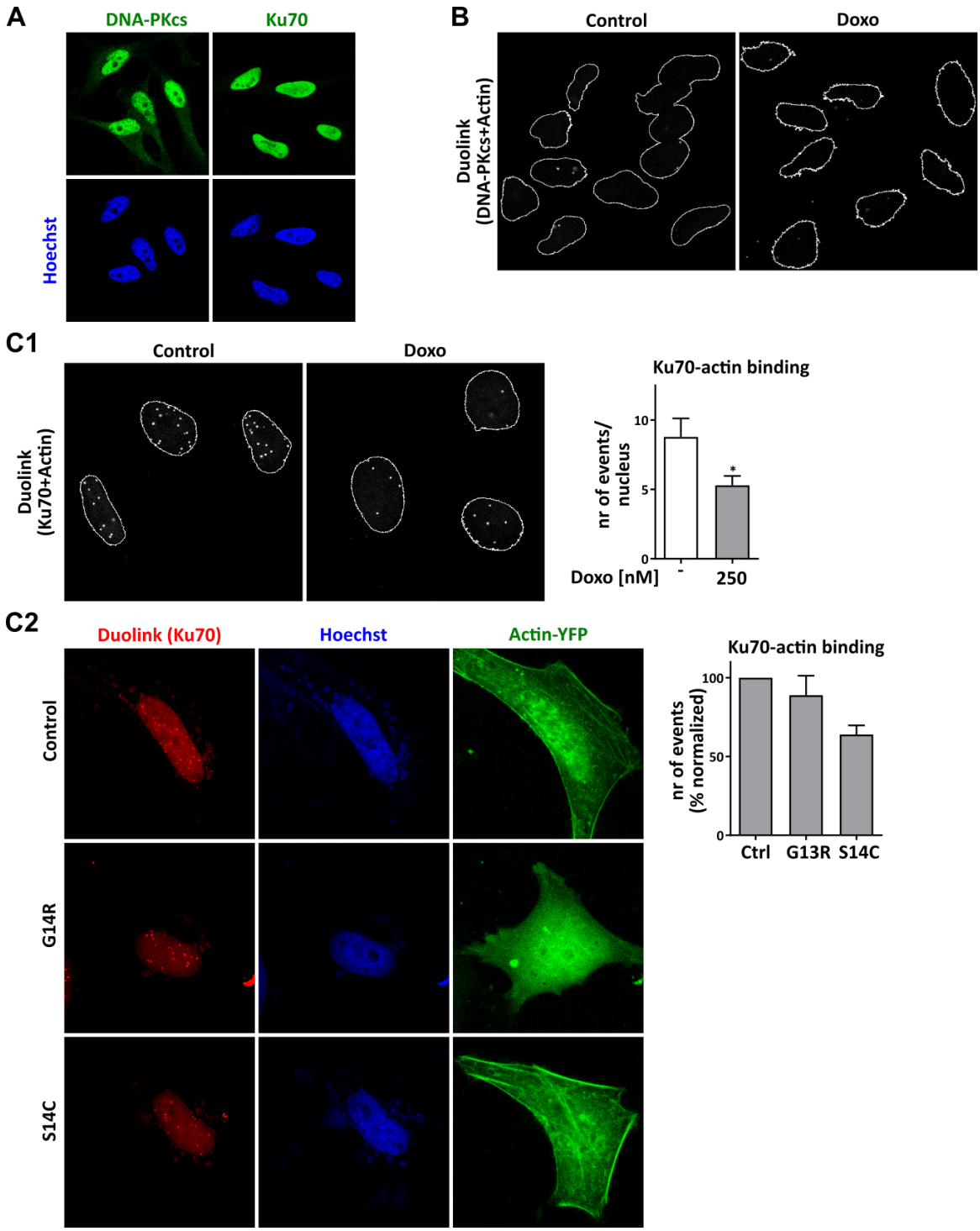

Figure 21: **Interaction of nuclear actin and DNA-PK. A Control staining.** HeLa cells were fixed, permeabilized and stained for DNA-PKcs or Ku70 and Hoechst to ensure functionality of the applied antibodies. **B Binding of nuclear actin to DNA-PKcs.** HeLa cells were treated with Doxo [250nM] for 2h and Duolink assay (Duolink reagents GREEN) performed. Antibodies against actin and DNA-PKcs were used (nuclear area is shown and nuclear outlines highlighted in white). **C Binding of nuclear actin to Ku70.** Antibodies against actin and Ku70 were applied. **C1** HeLa cells were treated with Doxo [250nM] for 2h and Duolink assay (Duolink reagents GREEN) performed. Nuclear events were counted manually. Outlines of nuclei are shown in white. Mean values of four experiments are shown, *p>0.01, unpaired t test, one-tailed. **C2** HeLa cells were transfected with the indicated plasmids and Duolink assay (Duolink reagents RED) performed. Nuclei were stained with Hoechst (blue). Nuclear events were counted manually. Mean values of three independent experiments are shown, values normalized on control.

4.1.8 Nuclear actin is bound to RPA and is involved in its recruitment to the site of damage.

Interestingly, HDR and SSA were affected by actin manipulation, whereas alt-EJ was not. Therefore, key mediators of HDR and/or SSA that specifically play a role in one or both of these pathways but not in alt-EJ can be the cause for differential responses to treatment with actin binders. One key player in HDR and SSA is RPA (Replication Protein A). RPA binds to ssDNA and protects DNA ends from degradation preventing spontaneous annealing between microhomologies (inhibits alt-EJ). Successful recruitment of RPA to the site of damage and its chromatin association is required for both HDR and SSA [127].

Recruitment of RPA-2 to DSBs was diminished upon combination treatment with LB and Jaspla, indicated by a significant decrease in the number of RPA-2 foci in the nuclei (Fig. 22A) and a reduced chromatin association of RPA-2 upon DNA damage induction (Fig. 22B). LB was found to be more efficient than Jaspla in the short term inhibition of RPA-2 recruitment with the tested substance concentrations (Fig. 22B).

To assess whether actin regulates recruitment by direct (or indirect) interaction with RPA-2, proximity ligation assay was performed (Duolink®). Indeed, actin was found to be bound to RPA-2 in the nucleus under control conditions. The number of positive events (i.e. actin molecules that are bound to RPA-2) decreased significantly upon Doxo treatment, suggesting a release of RPA-2 from actin when DNA damage was induced (Fig. 23A). Reduced events were also observed after short term treatment of cells with either LB or Jaspla (Fig. 23A). The suggested interaction of RPA-2 and nuclear actin could be verified by co-immunoprecipitation. Under control conditions, actin was bound to precipitated RPA-2 and the interaction was decreased upon damage induction and actin manipulation by LB (Fig. 23B). Hyperpolymerization of actin by overexpression of mutant actin (S14C) decreased binding of actin to RPA, whereas reduced polymerization of actin (G13R) slightly increased the number of positive events (Fig. 23C). Binding of RPA-2 to nuclear actin might thus depend on the state of actin, and an increase in G-actin monomers might favor the interaction of actin and RPA-2.

Treatment with actin binders and/or Doxo did not alter protein levels of RPA-2 (Fig. 24). The above observed reduction in the detected interaction of actin and RPA-2 was therefore not caused by decreased protein quantities.

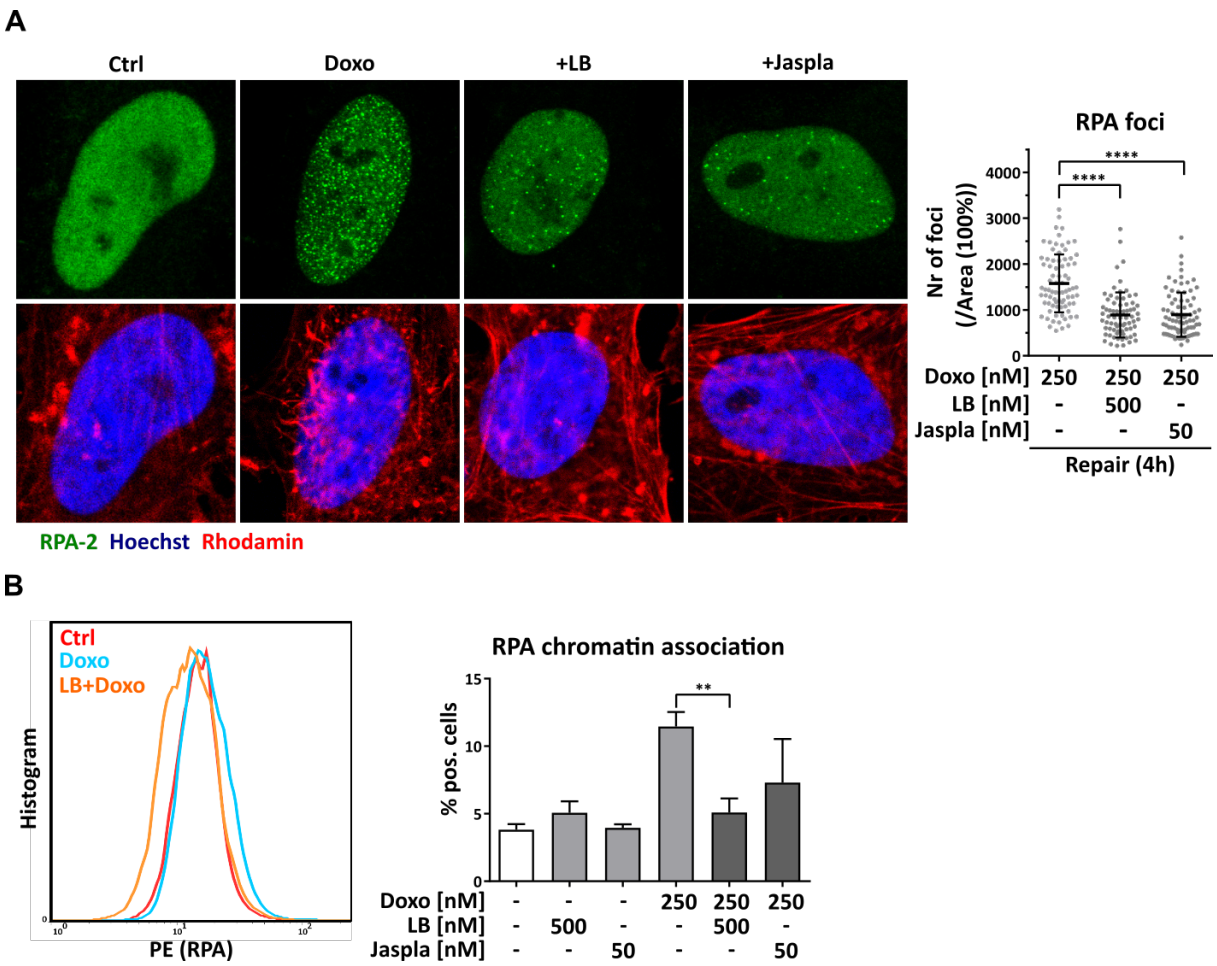

Figure 22: **Recruitment of RPA-2 to the site of DSB. A RPA foci formation.** HeLa cells were treated with Doxo with or without additional actin substance treatment for 2h. Doxo was then removed and cells incubated in DMEM (repair time 4h) +/- actin substances. RPA-2 foci were visualized by antibody staining. Nuclear RPA-2 foci of positive cells were counted with FiJi Plugin FindFOCI GUI. Numbers of foci were normalized on nuclear area to exclude variances due to changing nuclear sizes. At least 25 nuclei were analyzed for each sample and experiment (mean values +/- SD, n=3, unpaired t test, two-tailed, **** $p<0.0001$). **B Chromatin association of RPA-2.** After treatment with Doxo alone or in combination with the indicated actin substances for 2h, cells were harvested. Free RPA was extracted by washing with extraction buffer, cells fixed, stained for RPA-2 and flow cytometry performed. Mean values of three experiments are shown (+/- SEM), unpaired t test one-tailed, ** $p<0.01$.

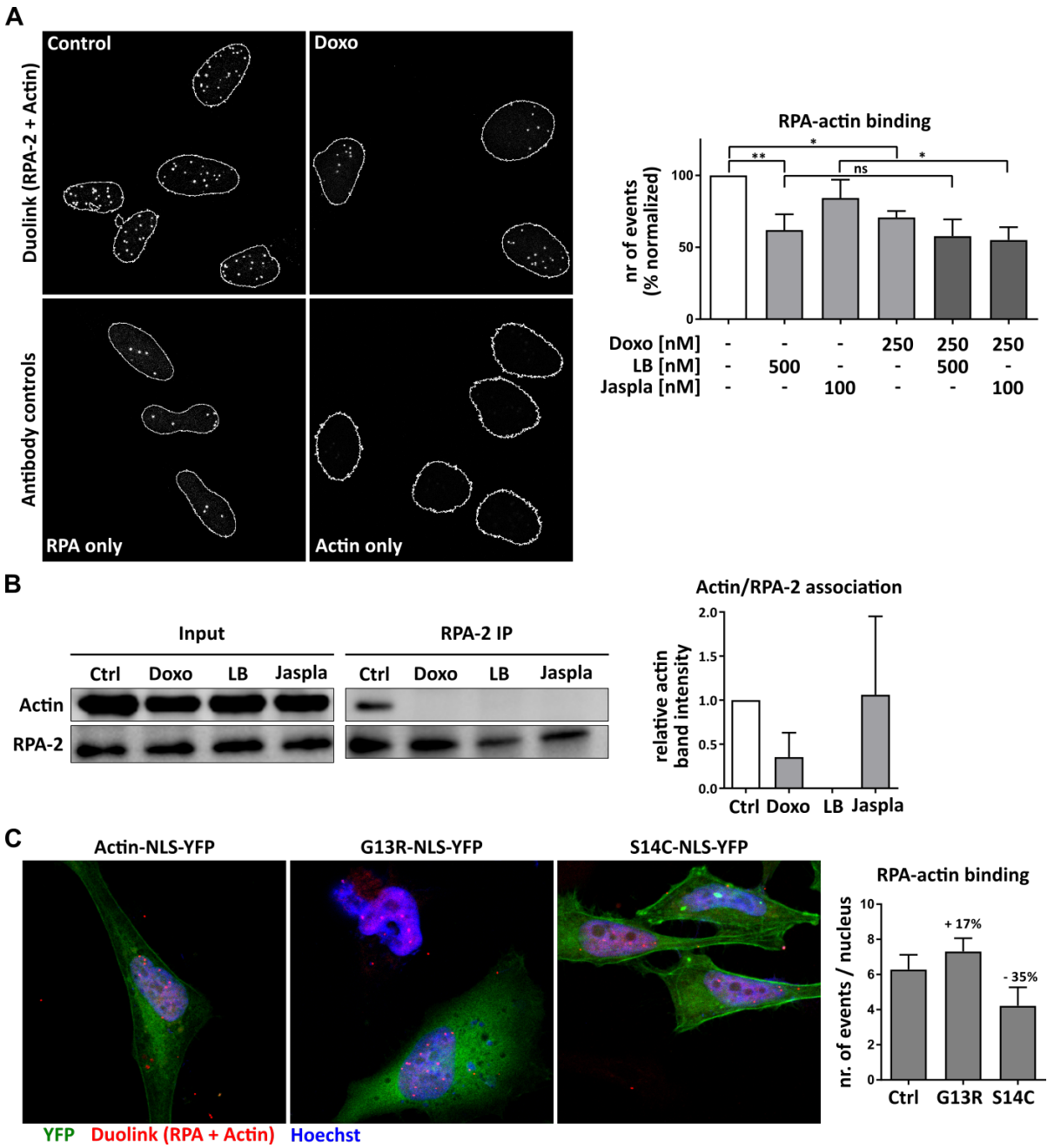

Figure 23: **Binding of RPA-2 to nuclear actin is decreased upon DNA damage induction and actin manipulation. A Duolink® assay.** HeLa cells were treated with Doxo +/- the indicated actin substances and Duolink assay (GREEN) performed with antibodies recognizing RPA-2 and actin, respectively (upper line). To ensure specificity of the applied antibodies, control stainings with only one antibody were performed (lower line). Positive events were normalized on numbers of control cells (mean values +/- SEM). At least 250 cells were analyzed for each treatment condition. Outlines of nuclei are shown in white. One-way ANOVA, Sidaks multiple comparisons test, * $p<0.05$, ** $p<0.01$, ns not significant. **B Co-immunoprecipitation.** HeLa cells were treated with the indicated substances. Protein samples of nuclear extracts were immunoprecipitated with RPA-2 antibody and immunoblotted for actin and RPA-2. 4% of each nuclear lysate was used for preparation of input samples. One exemplary blot is depicted. Band densities were quantified and calculated as a ratio of actin intensity to RPA-2. Graph shows mean values normalized on control. **C Duolink® assay.** HeLa cells were transfected with the indicated actin plasmids and Duolink assay (RED) performed. Positive events were counted in three independent experiments (mean values +/- SEM) with at least 150 cells for each transfection condition.

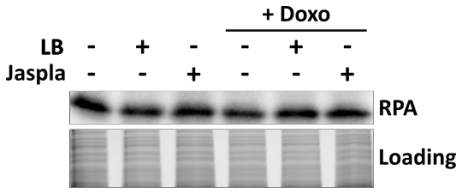

Figure 24: **RPA-2 protein levels.** HeLa cells were treated with Doxo and/or the indicated actin binders for 1h. Cells were harvested and lysed followed by immunoblotting. Stain-Free gel served as loading control. One blot out of three independent experiments is depicted.

Diminished chromatin association of RPA-2 upon DNA damage induction is therefore likely caused by obstructed recruitment resulting from actin manipulation. The finding that RPA-2 is bound to nuclear actin and released upon damage induction indicates a direct involvement of actin in the recruitment process of RPA-2.

4.2 Actin as a potential target for combination chemotherapy

Despite its severe side effects, application of Doxo for chemotherapy is nevertheless still widely used in the clinics as one of the most potent chemotherapeutics [17, 19]. The formulation of combination therapy concepts is considered a promising approach to diminish unwanted side effects during therapy with Doxo while still exploiting its anti-tumoral activities. So far, actin binders have mainly been described as potential substances for single chemotherapy in different experimental setups, both *in vitro* and *in vivo* (as described in 2.2.3). However, since actin manipulation was found to impair nuclear DNA damage repair processes, the combination of actin binders with a DNA damage inducing chemotherapeutic such as Doxo represents a new possibility for combination cancer therapy.

4.2.1 Latrunculin B inhibits cancer cell proliferation in combination with doxorubicin.

The potential application of actin binders for combination treatment with Doxo was tested in two different cancer cell lines. Both metabolic activity (Fig. 25A) and colony formation ability (Fig. 25B) were decreased when Doxo treatment was combined with LB in HeLa and T24 cells, whereas Jaspla treatment could not further inhibit proliferation. Single treatment with actin binders only slightly affected proliferation. The reduction of proliferation by additional application of LB was in both assays synergistic in HeLa cells (Bliss value 1.305 and 1.789 for metabolic activity and colony formation, respectively). This observed blockage of proliferation could be partially attributed to an induction of cell death in HeLa cells (Fig. 25C). In T24 cells a synergistic increase in apoptotic cells was detected (Bliss value 1.746) (Fig. 25D).

In summary, combination treatment of Doxo with LB led to decreased proliferation and increased apoptosis induction in both tested cancer cell lines compared to single Doxo treatment. Low dose Jaspla treatment could not further diminish proliferation when combined with Doxo.

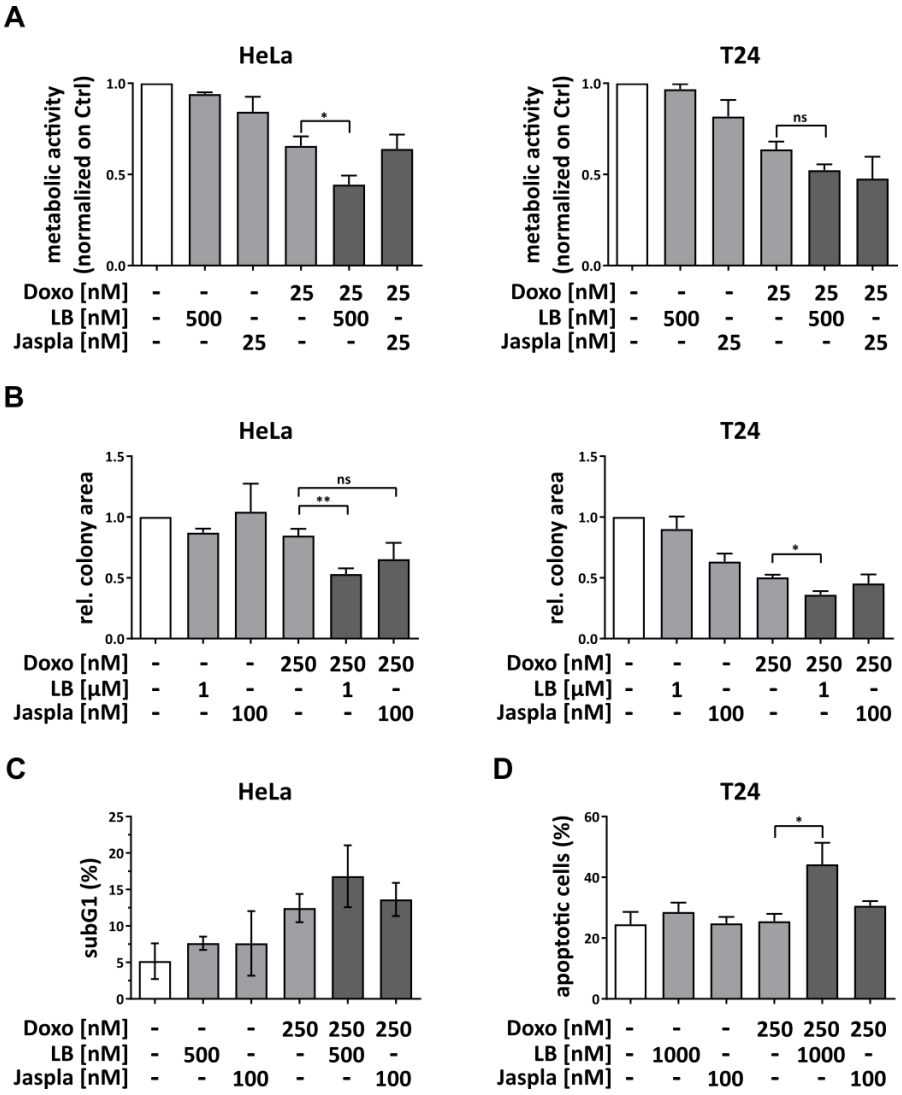

Figure 25: **Effects of combination treatment on cell viability and cell death induction.** HeLa and T24 cells were treated with the indicated actin substances in combination with Doxo. Graphs show mean values (+/- SEM) of three experiments, unpaired t test, one-tailed, * $p<0.05$, ** $p<0.01$, ns not significant. **A Metabolic activity.** Cell titer blue assay was performed after 72h of treatment. **B Colony formation.** HeLa and T24 cells were treated for 2h and then seeded in 6-well plates in new DMEM medium, without any substances. After 6 days of growth, total area was determined using the ImageJ plugin ColonyArea and normalized on control values. **C Cell death induction.** HeLa cells were treated for 48h, then fixed with methanol and stained with 7-AAD. Dead cells were determined by the subG1 gate. **D Apoptosis induction.** T24 cells were treated for 72h hours, followed by YoPro staining without prior fixation and percentage of apoptotic cells was evaluated.

4.2.2 Latrunculin B impairs DNA damage repair in vivo.

As described above, LB was found to inhibit proliferation synergistically *in vitro* when combined with Doxo. To prove if DNA repair inhibition by additional treatment with actin binders can also be achieved *in vivo*, a xenograft tumor model with 4T1 cells (murine breast cancer) was designed.

First *in vitro* tests showed that DNA DSB repair was inhibited after actin manipulation, comparable to the effect observed in HeLa cells (Fig. 26A). Under low dose treatment conditions, the extent of inhibition was higher in LB treated cells compared to Jaspla. Furthermore, LB was tolerated well in mice if injected i.p. and could be combined with i.v. Doxo treatment (Fig. 26B). To assess the effect of LB on DNA damage repair *in vivo*, 4T1-tumors bearing mice were injected i.v. with Doxo alone or in combination with LB (i.p.) for 24h followed by tumor cell isolation. Comet assay was performed to evaluate the extent of damaged DNA in isolated tumor cells. In established tumors, additional application of LB led to a significant increase in damaged DNA compared to single Doxo treatment, whereas LB alone did not induce DNA damage (Fig. 26C).

LB can thus inhibit DNA damage repair in established tumors *in vivo* at tolerable substance concentrations leading to an increase of chemotherapy induced DNA damage.

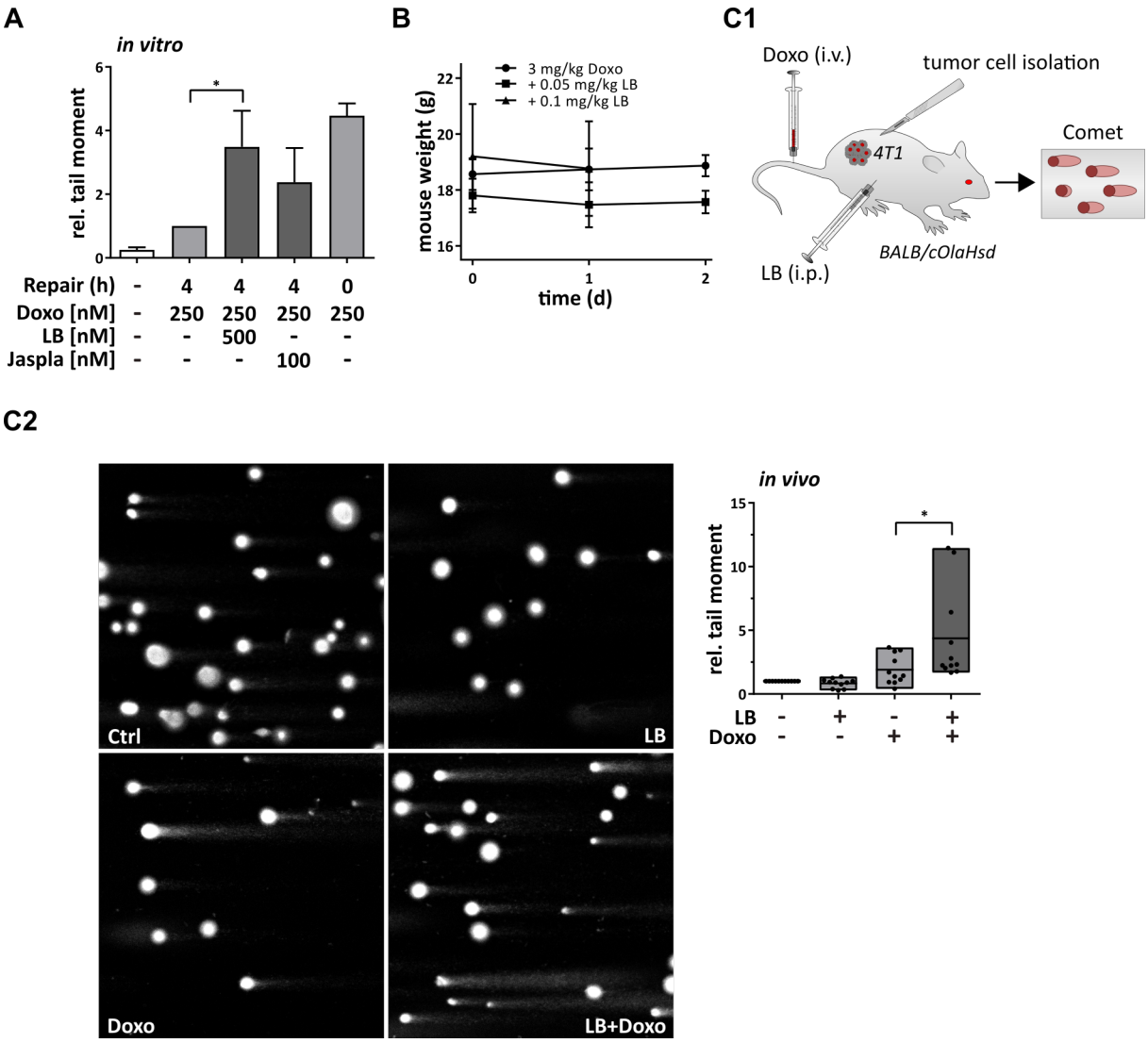

Figure 26: **Effects of latrunculin B on DNA damage repair *in vivo*. A *In vitro* alkaline comet assay.** 4T1 cells were treated with 250nM Doxo for 2h with or without addition of the respective actin substance. Cells were then incubated in DMEM or DMEM + actin substance. Doxo treatment alone without repair time served as positive control. Images were analyzed with OpenComet (ImageJ) and tail moments calculated. Relative tail moment is shown (tail moments normalized on doxo repair samples). Mean values (+/- SEM) of at least three independent experiments are depicted (one-way ANOVA, *p<0.05). **B Toxicity test *in vivo*.** Mice were treated with the indicated substance concentrations and mouse weight observed for up to 48h (n=2). *Performed by Carina Atzberger and Kerstin Loske.* **C *In vivo* alkaline comet assay.** Mice were injected with $1x10^6$ 4T1-luc cells and tumors grown for 7-9 days. Mice were then treated with 3mg/kg doxo (i.v.) with or without additional LB treatment (0.1mg/kg, i.p.) for 24h. Mice treated i.v. with PBS and i.p. with PBS + 5%DMSO + 10%solutol served as negative control. Tumors were harvested, digested enzymatically and single cell suspensions used for alkaline comet assay (**C1**). Tail moments were analyzed with OpenComet. One exemplary picture for each condition is shown on the left. Graph shows relative tail moments (normalized on control samples) and mean values of 11 mice per sample ((one-way ANOVA, *p<0.05) (**C2**). *Tumor cell injection and treatment of mice carried out by Carina Atzberger and Kerstin Loske.*

5 Discussion

5.1 The role of nuclear actin in DNA double strand break repair

In this work, the role of actin in nuclear DNA repair signalling and the influence of actin manipulation on DSB repair pathways were elucidated. Treatment with actin binders led to inhibition of specific processes during different pathways, resulting in inhibition of HDR, SSA and NHEJ, while alt-EJ was not influenced. These results provide new proof that actin is directly involved in nuclear processes during DNA damage repair signalling.

5.1.1 Can actin be polymerized in the nucleus?

In 2006, McDonald et al. provided the first experimental evidence that actin polymers exist in the nucleus [81], and that nuclear functions of actin might thus indeed be controlled by polymerization and depolymerization. Polymerization of nuclear actin has been described to occur upon DNA damage induction and to be required for functioning of DNA repair upon radiation [79, 113]. Visualization of filamental actin, especially in the nucleus, is technically challenging. It is thus difficult to determine the exact state of nuclear actin. All nowadays applied techniques hold pitfalls. Although classical F-actin marker phalloidin shows a very high specificity to filamental actin, it only binds to filaments of at least 7 monomers and specific APBs, such as Cofilin, can compete with phalloidin binding. Phalloidin is therefore not able to visualize all kinds of actin filaments and cannot be used to detect actin oligomers. It can also be applied only in fixed samples. For life cell imaging, fluorophore-tagged actin can be overexpressed to analyze actin dynamics in living cells. But tags, such as GFP, might perturb actin functions due to steric hindrances and changes in physiological actin levels. Nuclear actin can be visualized by overexpression of the nuclear actin-Chromobody (ChromoTek), a nanobody that is directed against actin and harbors a GFP-tag and a NLS sequence. However, overexpression of an actin binding antibody with a NLS might alter nuclear actin levels and stabilize actin structures (reviewed in [123]). Actin binders have been reported in general to induce polymerization in specific cell compartments, especially in the nucleus [128]. This was also true for treatment with the substances applied in this thesis and could, at least partly, be due to induced stress responses upon sensing of changes in overall actin states.

Nevertheless, the observation of actin filaments/agreggates upon damage induction when chromobody was overexpressed (as described in this thesis and in [79]) indicates that reorganization of actin in the nucleus is important for the activation or maintenance of signalling pathways involved in DNA repair. The decrease of free actin measured by FCS and the lack of actin-GFP export from the nucleus strengthen the hypothesis that actin polymerization occurs upon DNA damage induction. Visible actin aggregates could only be detected when damage induction was

performed after transfection of cells with the nuclear actin chromobody, indicating that the overexpression of the NLS-tagged antibody really stabilizes actin structures and thereby exaggerates the observed effect. Most likely, polymerization of actin due to DNA damage induction rather leads to oligomers instead of long filaments or larger aggregates and thus cannot be visualized by standard fluorescence microscopy.

Actin binders have shown different effects on nuclear actin organization. Although LB increased and Jaspla decreased nuclear actin levels, both led to formation of nuclear actin agreggates/filaments. Cofilin-dependent translocation of actin into the nucleus upon LB treatment has been described in rat peritoneal mast cells [84] and might be a general response to actin depolymerization, also in cancer cells. Cofilin is an important nuclear import factor of actin and the formation of nuclear cofilin-actin rods upon stress signals has been described [80, 84, 85]. The observed decrease in nuclear actin levels by Jaspla could arise due to a direct induction of actin export but also through an inhibition of the actin import to the nucleus. Differential changes in the nuclear actin levels upon actin binder treatment could therefore be explained by opposing effects on the active cofilin-dependent import of actin. This explanation seems more likely than effects on the profilin-dependent export [86], as LB did not impede profilin binding (*unpublished data*) and Jaspla binds to filamental actin and is thus not expected to directly obstruct the binding of a G-actin binding partner. Aggregation of actin in the nucleus due to LB treatment could be explained by spontaneous polymerization due to increased actin protein levels if the level of physiological depolymerizers cannot be adjusted fast enough. Again, nuclear actin filament formation was only observed when actin binder treatment was combined with Chromobody overexpression, and might therefore be, at least partially, an experimental artefact. In any case, if nuclear actin is important for DNA repair, deregulation of actin states by treatment with actin binding substances will likely influence actin-dependent DNA damage signalling.

It is still not understood how the polymerization of actin functions in the nucleus and how it is triggered upon stress signals. Actin nucleators from different classes have been found in the nucleus but there is no direct proof so far that they are also able to induce actin nucleation and subsequent formation of nuclear actin filaments (reviewed in [82]). Belonging to the class 1 NPFs (nucleation-promoting factor), N-WASP and its activator NCK1 can for example be localized in the nucleus. Upon UV-induced DNA damage, NCK1 translocates to the nucleus in association with SOCS7 (suppressor of cytokine signalling 7) and G-actin [129]. Another example is JMY, an actin nucleator which activates the Arp2/3 complex and also nucleates actin filaments independently of Arp2/3. DNA damage mediated polymerization of cytoplasmic actin leads to import of JMY to the nucleus, where it is for instance involved in p53 activation [130]. Translocation of actin nucleators to the nucleus upon DNA damage induction might therefore be responsible for actin oligomerization or even polymerization, although this is still only a hypothesis. In addition, the existence of actin binding proteins like profilin, cofilin and gelsolin in the nucleus imply a tight regulation of the state of nuclear actin [131].

5.1.2 Actin manipulation inhibits specific DNA damage repair pathways

The observation that actin manipulation leads to impairment of DSB repair raised the question in which DDR associated processes actin is involved.

Phosphorylation of ATM is an important step in DNA repair as it triggers the activation of many different substrates, such as Chk2 and H2AX, that are involved in DNA repair, cell cycle arrest and apoptosis induction. The activation of the ATM-Chk2 pathway was not impeded by actin manipulation and phosphorylation levels of both members were even slightly increased. Phosphorylation of H2AX is involved in early DSB signalling. However, loss of H2AX only leads to mild phenotypes in mice regarding DNA damage repair capacity [132]. Nevertheless, it is often used as a biomarker for damaged DNA [32, 33]. Latrunculin A has been reported by Leu et. al to inhibit yH2AX foci formation upon irradiation [112], an effect not observed by LB in this work. This might be explained by the high doses that were applied in the study of Leu et. al, which could have induced unspecific inhibition of signalling pathways due to cell death. Although different DSB repair pathways were inhibited by actin binder treatment, yH2AX foci formation was completely unaffected, indicating that yH2AX levels do not necessarily correlate with the functioning of DSB repair pathways. Local relaxation of heterochromatin depends on ATM-mediated phosphorylation of KAP-1 and is required for the recruitment of many repair factors to the DNA break [133]. The local decondensation of chromatin upon UV-induced damage was not impeded by actin manipulation and the global chromatin structure was not significantly changed. Low dose treatment with actin binding substances did not influence overall transcriptional activity. General events, essential for induction of DNA damage repair, were therefore not altered by application of actin binders. The inhibition of DSB repair by actin binding substances seems thus more specific than one might expect.

Actin manipulation inhibited specific nuclear processes involved in DSB repair signalling. The inhibition of HDR and SSA could be attributed to an impaired recruitment of RPA to the site of damage. This also explains why alt-EJ was not influenced, as RPA works against this third pathway. RPA can only be recruited to long stretches of ssDNA which are produced by extensive DNA end resection. The available experimental protocols for the measurement of ssDNA in cells were unfortunately not suitable for the quantification of short term induction of ssDNA upon low dose Doxo treatment. A potential additional involvement of nuclear actin in processes important for the formation of long ssDNA could therefore neither be validated nor negated. Nevertheless, a direct connection between actin and RPA recruitment could be provided. Nuclear actin was bound to RPA-2 under control conditions and released upon induction of DSBs, and the binding was found to be favoured by an increased G-actin pool. Serebryannyy et al. suggested RPA-3 as a potential nuclear actin binding partner, displayed in mass spectrometry analyses following a pulldown assay with purified non-muscle actin of nuclear HeLa extracts [114]. The proposed interaction, however, has not been confirmed by the group. This study provides now the first experimental proof that RPA (in this case subunit RPA-2) can bind to actin in the nucleus.

Actin hyperpolymerization by application of Jaspla or ChB led to inhibition of NHEJ which could be connected to a significantly decreased activation of DNA-PK. LB treatment also led to a slight reduction of DNA-PK phosphorylation. The missing effect of LB on the repair of I-SceI

induced damage in the respective reporter cell line could be due to the experimental setup. The repair efficacy was measured after 72h and LB can only affect the actin cytoskeleton for a couple of hours (as shown in this thesis and in [106]). It can therefore not be concluded that actin depolymerization has no effect on NHEJ signalling. Recruitment of Ku to the DNA is critical for the formation and activation of DNA-PK. Ku70 was demonstrated to bind to actin in a proximity ligation assay. These findings go in line with the published study of Andrin et al., which showed that Ku binds to F-actin and that actin depolymerization leads to perturbed retention of Ku80 at the DNA break [113]. Nuclear actin seems thus to be directly involved in Ku recruitment to damaged DNA. The in this work observed reduction of positive events upon DNA damage induction in the proximity ligation assay might be caused by an association of protein complexes involving Ku and/or actin with chromatin. For a better understanding of the exact mechanism further investigations are necessary.

5.1.3 How do actin binding substances influence repair factor recruitment?

An obstructed binding of nuclear actin to repair factors could on the one hand be explained by a dependence on the state of actin, i.e. G-actin or F-actin, or on the other hand by a direct replacement of actin binding partners by actin binding compounds.

Overexpression of mutant actin inducing nuclear actin hyperpolymerization decreased the binding of RPA to actin, implying that the state of actin does play a role. RPA could be trapped by monomeric actin in the nucleoplasm under physiological conditions and actin oligomerization or polymerization might be necessary to release RPA, followed by recruitment to ssDNA surrounding the break (as depicted in Fig. 27). Such a principle was described in the cytoplasm for the actin binder JMY. In this case, JMY is bound to G-actin under control conditions and released upon actin polymerization followed by a transport to the nucleus, where it enhances the transcriptional activity of p53 [118, 119]. This type of process might thus not only happen in the cytoplasm, but also in the nucleus. The potential actin hyperpolymerization in the nucleus due to treatment with actin binding substances might lead to the release of RPA-2 from actin, and thereby delivers RPA-2 at the wrong time point.

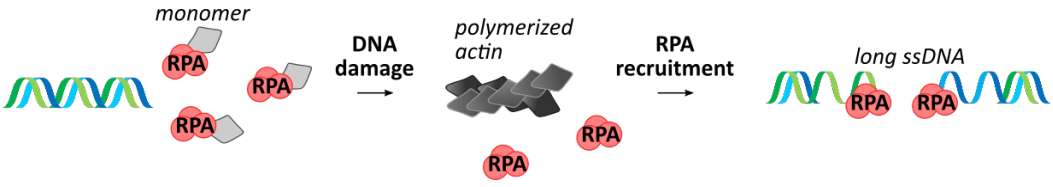

Figure 27: **Model for actin dependent RPA recruitment to ssDNA.** RPA recruitment to the site of DNA damage might depend on the regulation of actin states in the nucleus. Under normal conditions RPA is bound to G-actin in the nucleus. The occurence of DNA damage induces nuclear actin polymerization and thereby releases RPA. Free RPA can then be recruited to ssDNA.

G-actin consists of a smaller and a larger domain which are further divided into subdomains 1 and 2 (smaller domain) and subdomains 3 and 4 (larger domain). The nucleotide binding cleft (NBC) is located between subdomains 1 and 4 where a nucleotide - either ADP or ATP - bound to a divalent cation can be positioned. The NBC is separated from the hydrophobic cleft,

which represents the primary binding site for many ABPs [134]. Binding of ABPs can be favored by different nucleotide states. Cofilin, for example, binds to ADP-bound actin, whereas profilin prefers ATP-bound actin. Nucleotide-dependent conformational changes can occur and different nucleotide-sensitive regions have been described, namely the DNAse binding loop (D-loop), the WH2 binding loop (W-loop) and both the N- and C-terminal end of actin [134]. Binding of the D-loop of one actin subunit to the hydrophobic cleft of a neighboring subunit can be regulated by nucleotide hydrolysis and is thus predicted to be involved in contacts of actin-monomers along the F-actin helix [135]. The W-loop is the prime interaction site for WH2 domain proteins [134] and plays an important role in the binding of e.g. profilin [136] and cofilin [137].

LB binds in the nucleotide binding cleft of actin [138]. As nucleotide sensitive regions, important for the binding of specific ABPs, have been described, NBC obstruction could therefore hinder binding of actin binding partners. LB might thus lead to allosteric inhibition of the binding of specific ABPs. Such an effect might in general rather depend on the exact binding site than on the class of the actin binding compound. In this respect, LB for example does not impair profilin binding to actin whereas Chivosazole A does (*unpublished data*).

Both phalloidin and Jaspla bind in the gap between two F-actin strands, or in other words to the actin-actin contact sites at the interface of three actin subunits [139, 140]. Phalloidin competes for example with nebulin [141] and gelsolin [142], suggesting that also Jaspla might directly or indirectly displace ABPs or prevent them from being added.

Actin binding substances might therefore directly replace DNA repair factors from actin in the nucleus, resulting in a blockage of recruitment to the DNA break. In the case of RPA, LB might directly replace RPA-2 from G-actin (Fig. 28A). On the contrary, the reduction of G-actin abundance by Jaspla treatment might indirectly decrease the interaction of RPA-2 and actin (Fig. 28B). To unravel which DNA repair factors bind to actin and which ABPs could be displaced by actin binding compunds, further extensive research is still needed.

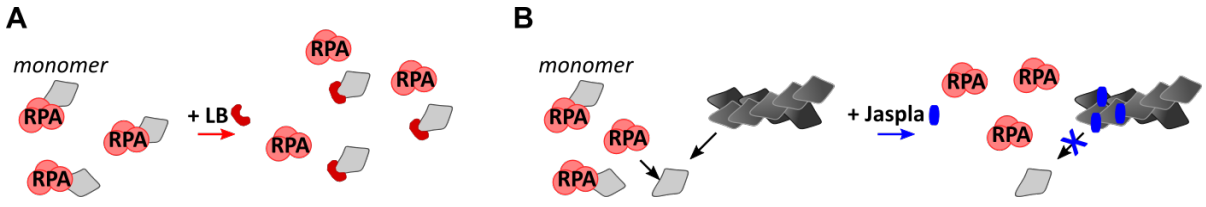

Figure 28: **Model for the displacement of RPA-2 from actin by actin binding compounds. A LB.** Binding of LB to G-actin directly inhibits the interaction of RPA-2 and nuclear actin. **B Jaspla.** Jaspla stabilizes F-actin and thereby indirectly prevents the potential interaction of RPA-2 and G-actin.

5.2 Targeting actin for combination chemotherapy - should we bring actin binding substances back into focus?

DNA damage inducing therapy is successfully used for cancer treatment, as extensive and persistent DNA damage induces cell cycle arrest or cell death [143]. However, several problems arise with this kind of tumor treatment. First, all rapidly proliferating cells will be targeted, thus it is not a tumor tissue specific treatment. Secondly, in addition to killing the wrong cells, it can lead to therapy-induced malignancies, as error-prone DNA repair pathways like NHEJ will result in DNA mutations [22, 144]. As a consequence, classical chemotherapy often causes severe side effects. The decrease of required substance concentrations by improvement of drug delivery represents one approach to prevent unwanted secondary effects. To name one example, pegulated liposomal doxorubicin (PLD) has been the first approved nanomedicine and is nowadays used in breast cancer treatment. Its special formulation was designed to increase both the stability of doxorubicin in the blood circulation and its selective release to the tumor tissue (reviewed in [145]). However, PLD has not replaced free Doxo as a therapeutic option for all indications, as several studies pointed out that PLD could not show higher anti-tumor activities compared to each respective competitor (reviewed in [146]). The above mentioned problems are therefore not (completely) solved yet. Another approach is the administration of combination therapy. Inhibitors of specific factors important for DNA repair signalling have been developed and are currently being tested for their potential application in cancer therapy. The evaluation of combining DNA repair inhibitors with classical chemotherapy, however, represents an underinvestigated approach.

NHEJ is considered to be the main pathway responsible for rapid DSB repair after chemotherapy [147] and represents thus one promising target for combination therapy. As one of the core factors for functional NHEJ, DNA-PKcs can be targeted by different inhibitors that have been developed recently. DNA-PKcs inhibition has been shown to sensitize for radiotherapy or top2 inhibitor treatment *in vitro* and in xenografts [148, 149]. The dual mTOR DNA-PKcs inhibitor CC-115 has even been used for several preclinical phase I trials [23] (and clinicaltrials.gov). CC-122, another DNA-PK inhibitor, has been tested for solid tumors, non-Hodgkin lymphoma and multiple myeloma in a phase I clinical trial (NCT01421524) [150]. The most famous substance is probably olaparib, the first FDA approved DNA repair inhibitor, which is currently being tested in different contexts for combination therapy [21, 151]. Even though HDR is limited to the S and G2 phase of the cell cycle, it is essential for the maintenance of genomic stability as it not only repairs DSBs, but is also involved in the repair of both stalled and collapsed replication forks and interstrand crosslinks. Tumors with defects in HDR functions are described to be highly sensitive to DSB inducing therapies and targeting HDR factors therefore seems to be another attractive option for cancer therapy [23]. Different strategies to inhibit HDR have been suggested, such as inhibition of Rad51 [152] or the interference with the ATM-Chk1/2 pathways (reviewed in [23]). Although beneficial effects have been suggested *in vitro* and in preclinical studies, the simultaneous combination of DNA damaging agents with DNA repair inhibitors is not an established treatment option in the clinics yet.

The inhibition of nuclear DSB repair pathways by application of actin binding substances demonstrated in this work, proposes a new strategy for combination chemotherapy. Manipulation of actin by different actin binding substances revealed inhibition, not only of one specific repair factor, but of distinctive and separate DSB repair pathways. While designing treatment strategies for cancer therapy, the following dilemma has to be faced: broad range therapeutics (i.e. classical chemotherapy like Doxo) are very potent but generally not tumor-specific enough and thus induce strong side effects, whereas highly specific therapeutics often lead to resistances. On a long term basis, only a small subpopulation of cancer patients benefits from such a treatment, due to the very heterogeneous nature of cancer [153]. Actin binding substances that inhibit different DNA repair pathways simultaneously might thus represent a promising tool for cancer therapy, as they specifically inhibit the repair of chemotherapy induced DNA damage targeting several pathways that could otherwise fill in for each other. The effects of actin manipulation on the functioning of DSB repair might, as a result, reduce the required concentration of Doxo. Synergistic effects of LB and Doxo *in vitro* and the increase in DNA damage when Doxo treatment was combined with i.p. application of LB *in vivo*, as observed in this thesis, strongly support this hypothesis. The reduction of Doxo concentrations would as a consequence be considered to decrease the expected cardiotoxic side effects.

In general, the disruption of the cytoskeleton of malignant cells represents an ideal approach for chemotherapeutic treatment, since malignant cells often exhibit a perturbed cytoskeleton and are especially dependent on cytoskeletal functions due to their high proliferation rates [154]. However, all clinically approved cytoskeletal-directed substances inhibit the microtubule system, whereas microfilaments or intermediate filaments are not targeted in the clinics (yet) (reviewed in [155]). The functioning of the actin cytoskeleton is crucial for both proliferation and metastasis formation, processes involved in the development of malignancies. However, severe side effects are feared and actin binding substances have not been introduced to clinical investigations.

Not much has been published about actin binders in preclinical studies so far. Jasplakinolide was soon dropped from consideration for clinical trials as it showed a very narrow therapeutic index in rats and dogs when applied i.v. and lethality was accompanied by edema, hemorrhage and congestion [156]. On the other hand, in mice bearing Lewis lung carcinoma, Jaspla has been successfully applied i.p. and s.c. and led to tumor growth delay and sensitization to radiation therapy [107]. The width of the therapeutic window might thus depend on how the substance is administered. Cytotoxic effects of Jaspla have been described in human induced pluripotent stem cell-derived cardiomyocytes *in vitro*, leading to a dose dependent decrease in viable cell numbers and mitochondrial membrane potential and increase in membrane permeability [157]. The possibility of an even more pronounced cardiotoxicity would therefore have to be excluded experimentally *in vivo*, although decreased substance concentrations in the combination therapy might still lead to beneficial effects. In different *in vitro* proliferation assays performed for this thesis, addition of Jaspla to Doxo treatment only led to slight effects on tumor cell proliferation and colony formation ability. Further experiments are needed to determine the right concentrations for both substances and the correct time points for pretreatment schedules for the best results possible. Nevertheless, it can also be concluded that Jaspla is not a promising

actin binding compound for further preclinical research.

Successful application of chondramide *in vivo* has been reported for i.v. and i.p. injection, showing that chondramide treatment can be tolerated by mice [109, 158]. Additionally, in a 4T1-Luc BALB/c mouse model, premedication with chondramide led to reduced metastasis of tumor cells to the lungs [109]. However, probably due to the negative report regarding Jaspla treatment of rats and dogs, not many publications can be found about *in vivo* investigations with the actin polymerizer chondramide. One important finding has to be mentioned, in which chondramide induced caspase dependent apoptosis in breast cancer cell lines, whereas non-tumor breast epithelial cells were found to be less sensitive to an apoptosis induction by chondramide treatment. This suggests a tumor cell specificity of chondramide induced effects, even though a universal protein such as actin was targeted [110].

Reports about the application of latrunculins are also rare. In this work it could be shown that application of 0.1mg/kg LB i.p. is well tolerated in mice and increases the extent of Doxo induced DNA damage. The additionally observed positive effects in combination with Doxo for inhibition of tumor cell growth *in vitro* in two different cancer cell lines highlight the potential of LB in combination therapy with DNA damaging agents.

In addition to a reduction of the required Doxo concentration, DNA repair inhibition through application of actin binding substances can be achieved by concentrations lower than the ones required for anti-cancer effects by actin binder monotherapy. The above described issue of the narrow therapeutic window of actin binders *in vivo* might then not be a major problem anymore. The improvement of drug delivery to the site of interest could further decrease feared side effects. One possibility could be the application of nanotechnology based carrier systems, which would allow the directed transport of actin binding substances to the tumor (e.g. [159]). Moreover, photoresponsive conjugates of actin binders would allow local activation of the substance only in the tumor (the feasibility of this approach has been published in [160]). Hence, there is still a lot of room for future research to further enhance the efficacy of actin binder treatment in order to reduce or even prevent possible remaining side effects.

The extent of potential positive effects of actin binder treatment in addition to Doxo likely depends as well on the cancer type and its specific characteristics. The increased phosphorylation of both ATM and Chk2 after combination treatment with Doxo and actin binders indicates an increased activation of the ATM-Chk2 pathway which is involved in p53-mediated induction of apoptosis. In this work, HeLa cells were used for most of the experiments, a HPV infected cell line which harbors inactivated p53 [161]. P53 dependent induction of cell death can thus not occur. This suggests a testing of combination treatment with p53 wild type cancer cells, as the synergism might strongly increase. This hypothesis is further supported by the finding that F-actin negatively regulates translocation of p53 to the nucleus upon damage induction [117]. A decrease of polymerized actin in the cytoplasm by treatment with actin depolymerizers like LB might further enhance the synergistic effect of actin manipulation and Doxo treatment. On the other hand, latrunculin A has been reported to reduce JMY-mediated p53 activation upon DNA

damage induced cytoplasmatic actin polymerization [162]. It is therefore difficult to predict the outcome of such a treatment in different cancer cell lines and further experiments would be needed. Hyperactivation of ATM as a feedback to DNA-PKcs inhibition has been published and amplified the p53 response to damage, thereby sensitizing the cells to damage induced senescence [163]. In this work, ATM-Chk2 phosphorylation was shown to be induced which could therefore (at least partially) be due to the decreased autophosphorylation (i.e. inactivation) of DNA-PK upon actin manipulation. This underlines again that p53 wildtype cancer cells might be even more susceptible for Doxo + actin binder combination treatment. Furthermore, highly motile cancers with a high metastatic potential might be more susceptible to an additional targeting of actin, since they strongly depend on cytoskeletal functions. In that case, even low dose treatment with actin binders will still inhibit the actin cytoskeleton to a certain degree.

In summary, the inhibition of DSB repair by application of actin binding substances, such as Jaspla and LB, proposes a new approach for combination chemotherapy. Especially the actin depolymerizer LB showed promising results as it was well tolerated in mice, while increasing DNA damage levels in combination with Doxo *in vivo* and decreaing proliferation when combined with Doxo *in vitro*. Actin binding substances should thus definitely be brought back into focus, as they show a high potential in the development of new cancer treatment strategies.

5.3 Summary and conclusion

In this work, specific roles of nuclear actin in the repair of chemotherapy induced DNA DSBs could be demonstrated (summarized in Fig. 29). Application of the actin binding substances Jaspla and LB inhibited both HDR and SSA by impairing the recruitment of RPA to the site of DNA damage. RPA-2 was demonstrated to be bound to nuclear actin and the impaired RPA recruitment was hypothesized to be caused by an altered interaction of RPA-2 and nuclear actin. Additionally, actin hyperpolymerization led to reduced activation of DNA-PK, resulting in an inhibition of NHEJ. A fourth DSB repair pathway, alt-EJ, was not influenced by actin manipulation. Due to the observed inhibition of DNA repair, actin binding substances were evaluated as potential candidates for combination therapy with the DNA damaging agent Doxo. Addition of LB to Doxo treatment synergistically inhibited proliferation in two different cancer cell lines *in vitro* and increased DNA damage levels in tumor cells *in vivo*.

In conclusion, the successful utilization of actin binding substances in combination therapy could be linked to the inhibition of Doxo induced DSB repair, thus presenting a novel treatment approach for cancer therapy.

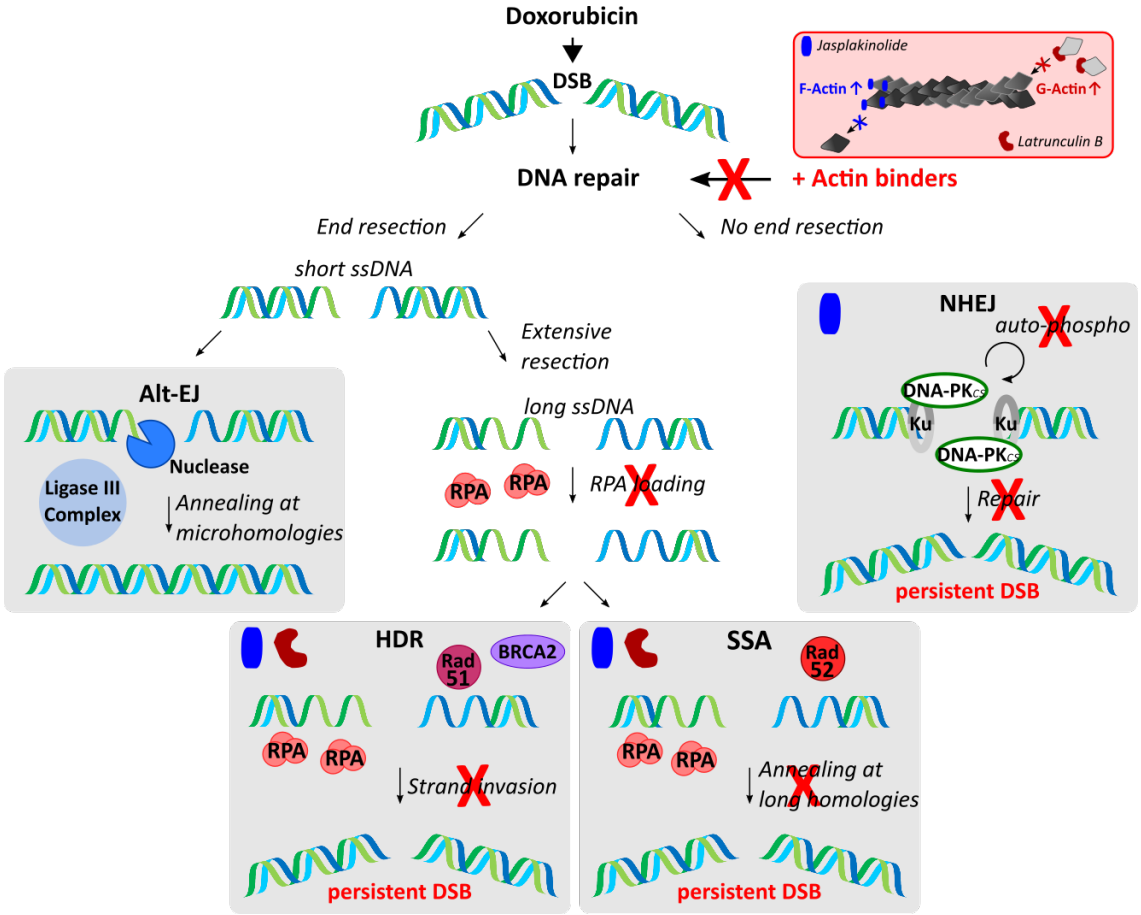

Figure 29: **Effects of actin binders on DSB repair.** During DSB repair, actin manipulation obstructs RPA loading to ssDNA and thereby inhibits HDR and SSA, and decreases auto-phosphorylation of DNA-PK for NHEJ, whereas alt-EJ is not influenced.

6 Bibliography

[1] Ferlay, J. et al. Cancer incidence and mortality worldwide: sources, methods and major patterns in globocan 2012. International journal of cancer **136** (2015).

[2] Stewart, B., Wild, C. P. et al. World cancer report 2014. Health (2017).

[3] Siegel, R. L., Miller, K. D. & Jemal, A. Cancer statistics, 2018. CA: a cancer journal for clinicians **68**, 7–30 (2018).

[4] Hanahan, D. & Weinberg, R. A. The hallmarks of cancer. Cell **100**, 57–70 (2000).

[5] Hanahan, D. & Weinberg, R. A. Hallmarks of cancer: the next generation. Cell **144**, 646–674 (2011).

[6] Skladanowski, A. & Konopa, J. Adriamycin and daunomycin induce programmed cell death (apoptosis) in tumour cells. Biochemical pharmacology **46**, 375–382 (1993).

[7] Spencer, C. M. & Faulds, D. Paclitaxel. Drugs **48**, 794–847 (1994).

[8] Minotti, G., Menna, P., Salvatorelli, E., Cairo, G. & Gianni, L. Anthracyclines: molecular advances and pharmacologic developments in antitumor activity and cardiotoxicity. Pharmacological reviews **56**, 185–229 (2004).

[9] Zhang, J., Yang, P. L. & Gray, N. S. Targeting cancer with small molecule kinase inhibitors. Nature Reviews Cancer **9**, 28 (2009).

[10] Chapman, P. B. Mechanisms of resistance to raf inhibition in melanomas harboring a braf mutation. Am Soc Clin Oncol Educ Book **33**, e80–2 (2013).

[11] Holohan, C., Van Schaeybroeck, S., Longley, D. B. & Johnston, P. G. Cancer drug resistance: an evolving paradigm. Nature Reviews Cancer **13**, 714 (2013).

[12] Arcamone, F. et al. Adriamycin, 14-hydroxydaimomycin, a new antitumor antibiotic from s. peucetius var. caesius. Biotechnology and bioengineering **11**, 1101–1110 (1969).

[13] Burden, D. A. & Osheroff, N. Mechanism of action of eukaryotic topoisomerase ii and drugs targeted to the enzyme. Biochimica et Biophysica Acta (BBA)-Gene Structure and Expression **1400**, 139–154 (1998).

[14] Tewey, K., Rowe, T., Yang, L., Halligan, B. & Liu, L. Adriamycin-induced dna damage mediated by mammalian dna topoisomerase ii. Science **226**, 466–468 (1984).

[15] Tobey, R. A. Effects of cytosine arabinoside, daunomycin, mithramycin, azacytidine, adriamycin, and camptothecin on mammalian cell cycle traverse. Cancer research **32**, 2720–2725 (1972).

[16] Cummings, J. & Smyth, J. Dna topoisomerase i and ii as targets for rational design of new anticancer drugs. Annals of Oncology **4**, 533–543 (1993).

[17] Adriamycin. URL `http://www.medsafe.govt.nz/profs/datasheet/a/adriamycininj.pdf`.

[18] Ibrahim, N. K. et al. Doxorubicin-induced congestive heart failure in elderly patients with metastatic breast cancer, with long-term follow-up: the md anderson experience. Cancer chemotherapy and pharmacology **43**, 471–478 (1999).

[19] Singal, P., Iliskovic, N., Li, T. & Kumar, D. Adriamycin cardiomyopathy: pathophysiology and prevention. The FASEB Journal **11**, 931–936 (1997).

[20] McGowan, J. V. et al. Anthracycline chemotherapy and cardiotoxicity. Cardiovascular drugs and therapy **31**, 63–75 (2017).

[21] Drew, Y. The development of parp inhibitors in ovarian cancer: from bench to bedside. British journal of cancer **113**, S3 (2015).

[22] Khanna, A. Dna damage in cancer therapeutics: a boon or a curse? Cancer research **75**, 2133–2138 (2015).

[23] Curtin, N. J. Dna repair dysregulation from cancer driver to therapeutic target. Nature Reviews Cancer **12**, 801 (2012).

[24] Czornak, K., Chughtai, S. & Chrzanowska, K. H. Mystery of dna repair: the role of the mrn complex and atm kinase in dna damage repair. Journal of applied genetics **49**, 383–396 (2008).

[25] Rupnik, A., Lowndes, N. F. & Grenon, M. Mrn and the race to the break. Chromosoma **119**, 115–135 (2010).

[26] Matsuoka, S. et al. Atm and atr substrate analysis reveals extensive protein networks responsive to dna damage. science **316**, 1160–1166 (2007).

[27] Burma, S., Chen, B. P., Murphy, M., Kurimasa, A. & Chen, D. J. Atm phosphorylates histone h2ax in response to dna double-strand breaks. Journal of Biological Chemistry **276**, 42462–42467 (2001).

[28] Stucki, M. et al. Mdc1 directly binds phosphorylated histone h2ax to regulate cellular responses to dna double-strand breaks. Cell **123**, 1213–1226 (2005).

[29] Scully, R. & Xie, A. Double strand break repair functions of histone h2ax. Mutation Research/Fundamental and Molecular Mechanisms of Mutagenesis **750**, 5–14 (2013).

[30] Chapman, J. R. & Jackson, S. P. Phospho-dependent interactions between nbs1 and mdc1 mediate chromatin retention of the mrn complex at sites of dna damage. EMBO reports **9**, 795–801 (2008).

[31] Lou, Z. et al. Mdc1 maintains genomic stability by participating in the amplification of atm-dependent dna damage signals. Molecular cell **21**, 187–200 (2006).

[32] Löbrich, M. et al. γh2ax foci analysis for monitoring dna double-strand break repair: strengths, limitations and optimization. Cell cycle **9**, 662–669 (2010).

[33] Sharma, A., Singh, K. & Almasan, A. Histone h2ax phosphorylation: a marker for dna damage. In DNA repair protocols, 613–626 (Springer, 2012).

[34] Ceccaldi, R., Rondinelli, B. & DAndrea, A. D. Repair pathway choices and consequences at the double-strand break. Trends in cell biology **26**, 52–64 (2016).

[35] Symington, L. S. & Gautier, J. Double-strand break end resection and repair pathway choice. Annual review of genetics **45**, 247–271 (2011).

[36] Lieber, M. R. The mechanism of human nonhomologous dna end joining. Journal of Biological Chemistry **283**, 1–5 (2008).

[37] Ma, Y. et al. A biochemically defined system for mammalian nonhomologous dna end joining. Molecular cell **16**, 701–713 (2004).

[38] West, R. B., Yaneva, M. & Lieber, M. R. Productive and nonproductive complexes of ku and dna-dependent protein kinase at dna termini. Molecular and cellular biology **18**, 5908–5920 (1998).

[39] Walker, J. R., Corpina, R. A. & Goldberg, J. Structure of the ku heterodimer bound to dna and its implications for double-strand break repair. Nature **412**, 607 (2001).

[40] Lehman, J. A., Hoelz, D. J. & Turchi, J. J. Dna-dependent conformational changes in the ku heterodimer. Biochemistry **47**, 4359–4368 (2008).

[41] Chiruvella, K. K., Liang, Z. & Wilson, T. E. Repair of double-strand breaks by end joining. Cold Spring Harbor perspectives in biology **5**, a012757 (2013).

[42] Goodarzi, A. A. et al. Dna-pk autophosphorylation facilitates artemis endonuclease activity. The EMBO journal **25**, 3880–3889 (2006).

[43] Chang, H. H., Watanabe, G. & Lieber, M. R. Unifying the dna end-processing roles of the artemis nuclease ku-dependent artemis resection at blunt dna ends. Journal of Biological Chemistry **290**, 24036–24050 (2015).

[44] Mimori, T. & Hardin, J. A. Mechanism of interaction between ku protein and dna. Journal of Biological Chemistry **261**, 10375–10379 (1986).

[45] Costantini, S., Woodbine, L., Andreoli, L., Jeggo, P. A. & Vindigni, A. Interaction of the ku heterodimer with the dna ligase iv/xrcc4 complex and its regulation by dna-pk. DNA repair **6**, 712–722 (2007).

[46] Grawunder, U., Zimmer, D., Kulesza, P. & Lieber, M. R. Requirement for an interaction of xrcc4 with dna ligase iv for wild-type v (d) j recombination and dna double-strand break repairin vivo. Journal of Biological Chemistry **273**, 24708–24714 (1998).

[47] Garcia-Diaz, M. et al. Structure–function studies of dna polymerase lambda. DNA repair **4**, 1358–1367 (2005).

[48] Longhese, M. P., Bonetti, D., Manfrini, N. & Clerici, M. Mechanisms and regulation of dna end resection. The EMBO journal **29**, 2864–2874 (2010).

[49] Huertas, P. Dna resection in eukaryotes: deciding how to fix the break. Nature structural and molecular biology **17**, 11 (2010).

[50] Tsubouchi, H. & Ogawa, H. A novel mre11 mutation impairs processing of double-strand breaks of dna during both mitosis and meiosis. Molecular and cellular biology **18**, 260–268 (1998).

[51] Furuse, M. et al. Distinct roles of two separable in vitro activities of yeast mre11 in mitotic and meiotic recombination. The EMBO Journal **17**, 6412–6425 (1998).

[52] Bernstein, K. A. & Rothstein, R. At loose ends: resecting a double-strand break. Cell **137**, 807–810 (2009).

[53] Kim, C., Paulus, B. F. & Wold, M. S. Interactions of human replication protein a with oligonucleotides. Biochemistry **33**, 14197–14206 (1994).

[54] Jensen, R. B., Carreira, A. & Kowalczykowski, S. C. Purified human brca2 stimulates rad51-mediated recombination. Nature **467**, 678 (2010).

[55] New, J. H., Sugiyama, T., Zaitseva, E. & Kowalczykowski, S. C. Rad52 protein stimulates dna strand exchange by rad51 and replication protein a. Nature **391**, 407 (1998).

[56] Kass, E. M. & Jasin, M. Collaboration and competition between dna double-strand break repair pathways. FEBS letters **584**, 3703–3708 (2010).

[57] Iyama, T. & Wilson, D. M. Dna repair mechanisms in dividing and non-dividing cells. DNA repair **12**, 620–636 (2013).

[58] Rothenberg, E., Grimme, J. M., Spies, M. & Ha, T. Human rad52-mediated homology search and annealing occurs by continuous interactions between overlapping nucleoprotein complexes. Proceedings of the National Academy of Sciences **105**, 20274–20279 (2008).

[59] Grimme, J. M. et al. Human rad52 binds and wraps single-stranded dna and mediates annealing via two hrad52–ssdna complexes. Nucleic acids research **38**, 2917–2930 (2010).

[60] Bhargava, R., Onyango, D. O. & Stark, J. M. Regulation of single-strand annealing and its role in genome maintenance. Trends in Genetics **32**, 566–575 (2016).

[61] Fischer, R. S. & Fowler, V. M. Thematic minireview series: the state of the cytoskeleton in 2015. Journal of Biological Chemistry **290**, 17133–17136 (2015).

[62] Borisy, G. G. & Taylor, E. The mechanism of action of colchicine: binding of colchincine-3h to cellular protein. The Journal of cell biology **34**, 525–533 (1967).

[63] Ishikawa, H., Bischoff, R. & Holtzer, H. Mitosis and intermediate-sized filaments in developing skeletal muscle. The Journal of cell biology **38**, 538–555 (1968).

[64] Straub, F. Actin. Stud. Inst. Med. Chem. Univ. Szeged **2**, 3–15 (1942).

[65] Hatano, S. & Oosawa, F. Isolation and characterization of plasmodium actin. Biochimica et Biophysica Acta (BBA)-General Subjects **127**, 488–498 (1966).

[66] Adelman, M. & Taylor, E. W. Isolation of an actomyosin-like protein complex from slime mold plasmodium and the separation of the complex into actin-and myosin-like fractions. Biochemistry **8**, 4964–4975 (1969).

[67] Perrin, B. J. & Ervasti, J. M. The actin gene family: function follows isoform. Cytoskeleton **67**, 630–634 (2010).

[68] Pollard, T. D. & Cooper, J. A. Actin, a central player in cell shape and movement. Science **326**, 1208–1212 (2009).

[69] Bailly, M. & Condeelis, J. Cell motility: insights from the backstage (2002).

[70] Lodish, H. et al. Molecular cell biology 4th edition. National Center for Biotechnology Information, Bookshelf (2000).

[71] Pollard, T. D., Blanchoin, L. & Mullins, R. D. Molecular mechanisms controlling actin filament dynamics in nonmuscle cells. Annual review of biophysics and biomolecular structure **29**, 545–576 (2000).

[72] Korn, E. D. Actin polymerization and its regulation by proteins from nonmuscle cells. Physiological Reviews **62**, 672–737 (1982).

[73] Burtnick, L. D. et al. The crystal structure of plasma gelsolin: implications for actin severing, capping, and nucleation. Cell **90**, 661–670 (1997).

[74] Bernstein, B. W. & Bamburg, J. R. Adf/cofilin: a functional node in cell biology. Trends in cell biology **20**, 187–195 (2010).

[75] Dos Remedios, C. et al. Actin binding proteins: regulation of cytoskeletal microfilaments. Physiological reviews **83**, 433–473 (2003).

[76] Dominguez, R. & Holmes, K. C. Actin structure and function. Annu Rev Biophys. **40**, 169–86 (2011).

[77] Lane, N. J. Intranuclear fibrillar bodies in actinomycin d-treated oocytes. The Journal of cell biology **40**, 286 (1969).

[78] Schoenenberger, C.-A. et al. Conformation-specific antibodies reveal distinct actin structures in the nucleus and the cytoplasm. Journal of structural biology **152**, 157–168 (2005).

[79] Belin, B. J., Lee, T. & Mullins, R. D. Dna damage induces nuclear actin filament assembly by formin-2 and spire-1/2 that promotes efficient dna repair. Elife **4**, e07735 (2015).

[80] Iida, K., Matsumoto, S. & Yahara, I. The kkrkk sequence is involved in heat shock-induced nuclear translocation of the 18-kda actin-binding protein, cofilin. Cell structure and function **17**, 39–46 (1992).

[81] McDonald, D., Carrero, G., Andrin, C., de Vries, G. & Hendzel, M. J. Nucleoplasmic β-actin exists in a dynamic equilibrium between low-mobility polymeric species and rapidly diffusing populations. J Cell Biol **172**, 541–552 (2006).

[82] Weston, L., Coutts, A. S. & La Thangue, N. B. Actin nucleators in the nucleus: an emerging theme. J Cell Sci **125**, 3519–3527 (2012).

[83] Terry, L. J., Shows, E. B. & Wente, S. R. Crossing the nuclear envelope: hierarchical regulation of nucleocytoplasmic transport. Science **318**, 1412–1416 (2007).

[84] Pendleton, A., Pope, B., Weeds, A. & Koffer, A. Latrunculin b or atp depletion induces cofilin-dependent translocation of actin into nuclei of mast cells. Journal of Biological Chemistry **278**, 14394–14400 (2003).

[85] Dopie, J., Skarp, K.-P., Rajakylä, E. K., Tanhuanpää, K. & Vartiainen, M. K. Active maintenance of nuclear actin by importin 9 supports transcription. Proceedings of the National Academy of Sciences **109**, E544–E552 (2012).

[86] Stüven, T., Hartmann, E. & Görlich, D. Exportin 6: a novel nuclear export receptor that is specific for profilin· actin complexes. The EMBO journal **22**, 5928–5940 (2003).

[87] Wada, A., Fukuda, M., Mishima, M. & Nishida, E. Nuclear export of actin: a novel mechanism regulating the subcellular localization of a major cytoskeletal protein. The EMBO Journal **17**, 1635–1641 (1998).

[88] Kiseleva, E. et al. Actin-and protein-4.1-containing filaments link nuclear pore complexes to subnuclear organelles in xenopus oocyte nuclei. Journal of cell science **117**, 2481–2490 (2004).

[89] Falahzadeh, K., Banaei-Esfahani, A. & Shahhoseini, M. The potential roles of actin in the nucleus. Cell Journal (Yakhteh) **17**, 7 (2015).

[90] Castano, E. et al. Actin complexes in the cell nucleus: new stones in an old field. Histochemistry and cell biology **133**, 607–626 (2010).

[91] Scheer, U., Hinssen, H., Franke, W. W. & Jockusch, B. M. Microinjection of actin-binding proteins and actin antibodies demonstrates involvement of nuclear actin in transcription of lampbrush chromosomes. Cell **39**, 111–122 (1984).

[92] Scott, V., Boehme, R. & Matthews, T. New class of antifungal agents: jasplakinolide, a cyclodepsipeptide from the marine sponge, jaspis species. Antimicrobial agents and chemotherapy **32**, 1154–1157 (1988).

[93] Bubb, M. R., Senderowicz, A., Sausville, E. A., Duncan, K. & Korn, E. D. Jasplakinolide, a cytotoxic natural product, induces actin polymerization and competitively inhibits the binding of phalloidin to f-actin. Journal of Biological Chemistry **269**, 14869–14871 (1994).

[94] Kunze, B., JANSEN, R., Sasse, F., HÖFLE, G. & REICHENBACH, H. Chondramides ad, new antifungal and cytostatic depsipeptides from chondromyces crocatus (myxobacteria). The Journal of antibiotics **48**, 1262–1266 (1995).

[95] Sasse, F., Kunze, B., Gronewold, T. M. & Reichenbach, H. The chondramides: cytostatic agents from myxobacteria acting on the actin cytoskeleton. Journal of the National Cancer Institute **90**, 1559–1563 (1998).

[96] Holzinger, A. & Lütz-Meindl, U. Chondramides, novel cyclodepsipeptides from myxobacteria, influence cell development and induce actin filament polymerization in the green alga micrasterias. Cytoskeleton **48**, 87–95 (2001).

[97] Iizuka, T. et al. Miuraenamides a and b, novel antimicrobial cyclic depsipeptides from a new slightly halophilic myxobacterium: taxonomy, production, and biological properties. The Journal of antibiotics **59**, 385 (2006).

[98] Sumiya, E. et al. Cell-morphology profiling of a natural product library identifies bisebromoamide and miuraenamide a as actin filament stabilizers. ACS chemical biology **6**, 425–431 (2011).

[99] Karmann, L., Schultz, K., Herrmann, J., Müller, R. & Kazmaier, U. Total syntheses and biological evaluation of miuraenamides. Angewandte Chemie International Edition **54**, 4502–4507 (2015).

[100] Ojima, D. et al. Total synthesis of miuraenamides a and d. The Journal of organic chemistry **81**, 9886–9894 (2016).

[101] Spector, I., Shochet, N. R., Kashman, Y. & Groweiss, A. Latrunculins: novel marine toxins that disrupt microfilament organization in cultured cells. Science **219**, 493–495 (1983).

[102] Coué, M., Brenner, S. L., Spector, I. & Korn, E. D. Inhibition of actin polymerization by latrunculin a. FEBS letters **213**, 316–318 (1987).

[103] Zibuck, R., Liverton, N. J. & Smith, A. B. Total synthesis of (+)-latrunculin b. Journal of the American Chemical Society **108**, 2451–2453 (1986).

[104] Pradella, S. et al. Characterisation, genome size and genetic manipulation of the myxobacterium sorangium cellulosum so ce56. Archives of microbiology **178**, 484–492 (2002).

[105] Diestel, R. et al. Chivosazoles a and f, cytostatic macrolides from myxobacteria, interfere with actin. ChemBioChem **10**, 2900–2903 (2009).

[106] Spector, I., Shochet, N. R., Blasberger, D. & Kashman, Y. Latrunculinsnovel marine macrolides that disrupt microfilament organization and affect cell growth: I. comparison with cytochalasin d. Cytoskeleton **13**, 127–144 (1989).

[107] Takeuchi, H., Ara, G., Sausville, E. A. & Teicher, B. Jasplakinolide: interaction with radiation and hyperthermia in human prostate carcinoma and lewis lung carcinoma. Cancer chemotherapy and pharmacology **42**, 491–496 (1998).

[108] Senderowicz, A. M. et al. Jasplakinolide's inhibition of the growth of prostate carcinoma cells in vitro with disruption of the actin cytoskeleton. JNCI: Journal of the National Cancer Institute **87**, 46–51 (1995).

[109] Menhofer, M. H. et al. The actin targeting compound chondramide inhibits breast cancer metastasis via reduction of cellular contractility. PloS one **9**, e112542 (2014).

[110] Foerster, F. et al. Targeting the actin cytoskeleton: selective antitumor action via trapping pkc. Cell death & disease **5**, e1398 (2014).

[111] Konishi, H. et al. Latrunculin a has a strong anticancer effect in a peritoneal dissemination model of human gastric cancer in mice. Anticancer research **29**, 2091–2097 (2009).

[112] Leu, J.-D. et al. Enhanced cellular radiosensitivity induced by cofilin-1 over-expression is associated with reduced dna repair capacity. International journal of radiation biology **89**, 433–444 (2013).

[113] Andrin, C. et al. A requirement for polymerized actin in dna double-strand break repair. Nucleus **3**, 384–395 (2012).

[114] Serebryannyy, L. A., Cruz, C. M. & De Lanerolle, P. A role for nuclear actin in hdac 1 and 2 regulation. Scientific reports **6**, 28460 (2016).

[115] Okorokov, A. L., Rubbi, C. P., Metcalfe, S. & Milner, J. The interaction of p53 with the nuclear matrix is mediated by f-actin and modulated by dna damage. Oncogene **21**, 356 (2002).

[116] Metcalfe, S. et al. Wild-type p53 protein shows calcium-dependent binding to f-actin. Oncogene **18**, 2351 (1999).

[117] Wang, L. et al. Actin polymerization negatively regulates p53 function by impairing its nuclear import in response to dna damage. PloS one **8**, e60179 (2013).

[118] Zuchero, J. B., Belin, B. & Mullins, R. D. Actin binding to wh2 domains regulates nuclear import of the multifunctional actin regulator jmy. Molecular biology of the cell **23**, 853–863 (2012).

[119] Lin, Z., Xu, Y.-N., Namgoong, S. & Kim, N.-H. Jmy functions as actin nucleation-promoting factor and mediator for p53-mediated dna damage in porcine oocytes. Plos one **9**, e109385 (2014).

[120] Gunn, A. & Stark, J. M. I-scei-based assays to examine distinct repair outcomes of mammalian chromosomal double strand breaks. DNA Repair Protocols 379–391 (2012).

[121] Richardson, C., Moynahan, M. E. & Jasin, M. Double-strand break repair by interchromosomal recombination: suppression of chromosomal translocations. Genes & development **12**, 3831–3842 (1998).

[122] Forment, J. V. & Jackson, S. P. A flow cytometry-based method to simplify the analysis and quantification of protein association to chromatin in mammalian cells. Nature protocols **10**, 1297–1307 (2015).

[123] Melak, M., Plessner, M. & Grosse, R. Actin visualization at a glance. J Cell Sci **130**, 525–530 (2017).

[124] Waldes, H. & Center, M. S. Adriamycin-induced compaction of isolated chromatin. Biochemical pharmacology **31**, 1057–1061 (1982).

[125] Kruhlak, M. J. et al. Changes in chromatin structure and mobility in living cells at sites of dna double-strand breaks. J Cell Biol **172**, 823–834 (2006).

[126] Cann, K. L. & Dellaire, G. Heterochromatin and the dna damage response: the need to relax. Biochemistry and cell biology **89**, 45–60 (2010).

[127] Maréchal, A. & Zou, L. Rpa-coated single-stranded dna as a platform for post-translational modifications in the dna damage response. Cell research **25**, 9 (2015).

[128] Belin, B. J., Cimini, B. A., Blackburn, E. H. & Mullins, R. D. Visualization of actin filaments and monomers in somatic cell nuclei. Molecular biology of the cell **24**, 982–994 (2013).

[129] Kremer, B. E., Adang, L. A. & Macara, I. G. Septins regulate actin organization and cell-cycle arrest through nuclear accumulation of nck mediated by socs7. Cell **130**, 837–850 (2007).

[130] Zuchero, J. B., Coutts, A. S., Quinlan, M. E., La Thangue, N. B. & Mullins, R. D. p53-cofactor jmy is a multifunctional actin nucleation factor. Nature cell biology **11**, 451 (2009).

[131] Gettemans, J. et al. Nuclear actin-binding proteins as modulators of gene transcription. traffic **6**, 847–857 (2005).

[132] Celeste, A. et al. Genomic instability in mice lacking histone h2ax. Science **296**, 922–927 (2002).

[133] Firsanov, D. V., Solovjeva, L. V. & Svetlova, M. P. H2ax phosphorylation at the sites of dna double-strand breaks in cultivated mammalian cells and tissues. Clinical epigenetics **2**, 283 (2011).

[134] Kudryashov, D. S. & Reisler, E. Atp and adp actin states. Biopolymers **99**, 245–256 (2013).

[135] Dominguez, R. Actin-binding proteins–a unifying hypothesis. Trends in biochemical sciences **29**, 572–578 (2004).

[136] Chik, J. K., Lindberg, U. & Schutt, C. E. The structure of an open state of β-actin at 2.65 å resolution. Journal of molecular biology **263**, 607–623 (1996).

[137] Paavilainen, V. O., Oksanen, E., Goldman, A. & Lappalainen, P. Structure of the actin-depolymerizing factor homology domain in complex with actin. J Cell Biol **182**, 51–59 (2008).

[138] Yarmola, E. G., Somasundaram, T., Boring, T. A., Spector, I. & Bubb, M. R. Actin-latrunculin a structure and function differential modulation of actin-binding protein function by latrunculin a. Journal of Biological Chemistry **275**, 28120–28127 (2000).

[139] Heidecker, M., Yan-Marriott, Y. & Marriott, G. Proximity relationships and structural dynamics of the phalloidin binding site of actin filaments in solution and on single actin filaments on heavy meromyosin. Biochemistry **34**, 11017–11025 (1995).

[140] Usui, T. Actin-and microtubule-targeting bioprobes: their binding sites and inhibitory mechanisms. Bioscience, biotechnology, and biochemistry **71**, 300–308 (2007).

[141] Ao, X. & Lehrer, S. S. Phalloidin unzips nebulin from thin filaments in skeletal myofibrils. Journal of Cell Science **108**, 3397–3403 (1995).

[142] Allen, P. G. & Janmey, P. A. Gelsolin displaces phalloidin from actin filaments. a new fluorescence method shows that both ca2+ and mg2+ affect the rate at which gelsolin severs f-actin. Journal of Biological Chemistry **269**, 32916–32923 (1994).

[143] Jackson, S. P. & Bartek, J. The dna-damage response in human biology and disease. Nature **461**, 1071 (2009).

[144] Nitiss, J. L. Targeting dna topoisomerase ii in cancer chemotherapy. Nature Reviews Cancer **9**, 338 (2009).

[145] Tran, S., DeGiovanni, P.-J., Piel, B. & Rai, P. Cancer nanomedicine: a review of recent success in drug delivery. Clinical and translational medicine **6**, 44 (2017).

[146] Gabizon, A. A., Patil, Y. & La-Beck, N. M. New insights and evolving role of pegylated liposomal doxorubicin in cancer therapy. Drug Resistance Updates **29**, 90–106 (2016).

[147] Mahaney, B. L., Meek, K. & Lees-Miller, S. P. Repair of ionizing radiation-induced dna double-strand breaks by non-homologous end-joining. Biochemical Journal **417**, 639–650 (2009).

[148] Zhao, Y. et al. Preclinical evaluation of a potent novel dna-dependent protein kinase inhibitor nu7441. Cancer research **66**, 5354–5362 (2006).

[149] Munck, J. M. et al. Chemosensitization of cancer cells by ku-0060648, a dual inhibitor of dna-pk and pi-3k. Molecular cancer therapeutics **11**, 1789–1798 (2012).

[150] Goodwin, J. F. & Knudsen, K. E. Beyond dna repair: Dna-pk function in cancer. Cancer discovery **4**, 1126–1139 (2014).

[151] Dréan, A., Lord, C. J. & Ashworth, A. Parp inhibitor combination therapy. Critical reviews in oncology/hematology **108**, 73–85 (2016).

[152] Huang, F. et al. Identification of specific inhibitors of human rad51 recombinase using high-throughput screening. ACS chemical biology **6**, 628–635 (2011).

[153] Bonello, T. T., Stehn, J. R. & Gunning, P. W. New approaches to targeting the actin cytoskeleton for chemotherapy. Future medicinal chemistry **1**, 1311–1331 (2009).

[154] Weinberg, R. The biology of cancer (Garland science, 2013).

[155] Trendowski, M. Exploiting the cytoskeletal filaments of neoplastic cells to potentiate a novel therapeutic approach. Biochimica et Biophysica Acta (BBA)-Reviews on Cancer **1846**, 599–616 (2014).

[156] Schindler-Horvat, J. et al. Toxicity of jasplakinolide (nsc 613009) in rats and dogs. In Proc Am Assoc Cancer Res, vol. 39, 597 (1998).

[157] Schweikart, K. et al. The effects of jaspamide on human cardiomyocyte function and cardiac ion channel activity. Toxicology in Vitro **27**, 745–751 (2013).

[158] Menhofer, M. H. et al. In vitro and in vivo characterization of the actin polymerizing compound chondramide as an angiogenic inhibitor. Cardiovascular research **104**, 303–314 (2014).

[159] Liu, J. et al. ph-sensitive nano-systems for drug delivery in cancer therapy. Biotechnology advances **32**, 693–710 (2014).

[160] Velema, W. A. et al. Ciprofloxacin–photoswitch conjugates: A facile strategy for photopharmacology. Bioconjugate chemistry **26**, 2592–2597 (2015).

[161] Ajay, A. K., Meena, A. S. & Bhat, M. K. Human papillomavirus 18 e6 inhibits phosphorylation of p53 expressed in hela cells. Cell & bioscience **2**, 2 (2012).

[162] Coutts, A. S., Weston, L. & La Thangue, N. B. A transcription co-factor integrates cell adhesion and motility with the p53 response. Proceedings of the National Academy of Sciences **106**, 19872–19877 (2009).

[163] Finzel, A., Grybowski, A., Strasen, J., Cristiano, E. & Loewer, A. Hyperactivation of atm upon dna-pkcs inhibition modulates p53 dynamics and cell fate in response to dna damage. Molecular biology of the cell **27**, 2360–2367 (2016).

7 Appendix

7.1 Abbreviations and units

Table 15

Abbreviation	Meaning
ad.	Fill up to
A	Ampere
ABP	Actin-binding protein
Alt-EJ	Alternative end joining
ANOVA	Analysis of variance between groups
ATM	Ataxia-telangiectasia mutated
ATP/ADP	Adenosine triphosphate/diphosphate
ATR	ATM- and RAD3-related
bp	base pair
BSA	Bovine serum albumine
°C	Degree Celsius
ChB	Chondramide B
Chivo	Chivosazole A
Chk2	Checkpoint kinase 2
CM	Complete media
Co-IP	Co-immunoprecipitation
cs	Catalytical subunit
CtIP	C-terminal binding protein 1 (CtBP1) interacting protein
Da	Dalton
DDR	DNA damage response
DMEM	Dulbeccos Modified Eagle Medium
DMSO	Dimethyl sulfoxide
DNA	Deoxyribonucleic acid
DNA-PK	DNA-dependent protein kinase
Doxo	Doxorubicin
ds	Double stranded
DSB	DNA double strand break
ECL	Enhanced chemical luminescence
EDTA	Ethylenediaminetetraacetic acid
e.g.	For example
EXO1	Exonuclease 1

Table 15: *continued from previous page*

Abbreviation	**Meaning**
et al.	And others
F-actin	Filamental actin
FACS	Fluorescence-activated cell sorting
FCS	Fetal calf serum
FCS	Fluorescence correlation spectroscopy
Fig.	Figure
FSC	Forward scatter
g	Gram
G-actin	Globular actin
GFP	Green fluorescent protein
G-phase	Gap phase
h	Hour
HDR	Homology derived repair
HEPES	4-(2-hydroxyethyl)-1-piperazineethanesulfonic acid
HRP	Horseradish peroxidase
i.e.	*Id est* (that is)
i.p.	Intraperitoneal
i.v.	Intravenous
Jaspla	Jasplakinolide
k	1000 (number)
kg	Kilogram
Ku	Ku70/80 heterodimer
l	Liter(s)
LB	Latrunculin B
m	Milli / meter
M	Molar
min	Minute(s)
Miu	Miuraenamide A
n	Nano
NBC	Nucleotide binding cleft
NHEJ	Non-homologous end joining
p	Phosphorylated
PBS	Phosphate buffered saline
PARP	Poly (ADP-ribose) polymerase
Pen/Strep	Penicillin-Streptomycin
PMSF	Phenylmethanesulfonylfluoride
PVDF	Polyvinylidene difluoride
RNA	Ribonucleic acid
ROS	Reactive oxygen species
rpm	Revolutions per minute

Table 15: *continued from previous page*

Abbreviation	**Meaning**
RPMI	Roswell Park Memorial Institute
RT	Room temperature
s	Second(s)
s.c.	Subcutaneous
Ser	Serine
ss	Single stranded
SSA	Single strand annealing
S-phase	Synthesis phase
SD	Standard deviation
SDS	Sodium dodecylsulfate
SEM	Standard error of the mean
SSC	Sideward scatter
T	Threonine
Tab.	Table
TBS-T	Tris-buffered saline and Tween 20
TE	Trypsin-EDTA
top2	Topoisomerase 2
Tris	Tris(hydroxymethyl)aminomethane
UV	Ultraviolet
V	Volt
w/v	Weight per volume
yH2AX	Phospho-histone H2AX
μ	Micro

7.2 Publications

7.2.1 Original publications

Cyclin-dependent kinase 5 stabilizes hypoxia-inducible factor-1α: a novel approach for inhibiting angiogenesis in hepatocellular carcinoma

Herzog J, Ehrlich SM, Pfitzer L, Liebl J, Fröhlich T, Arnold GJ, Mikulits W, Haider C, Vollmar AM, Zahler S.

Oncotarget. 2016, May 10.

Targeting actin inhibits repair of chemotherapy induced DNA damage: a novel therapeutic approach for combination therapy

Pfitzer L, Moser C, Foerster F, Atzberger C, Zisis T, Kubisch-Dohmen R, Busse J, Smith R, Timinszky G, Kalinina O, Wagner E, Vollmar AM, Zahler S

In preparation.

7.2.2 Poster presentations

Effects of actin manipulation on the recruitment of nuclear DNA damage repair factors

Lisa Pfitzer, Rebecca Smith, Gyula Timinszky, Angelika M. Vollmar, Stefan Zahler

EACR conference series - Radiation Break-through: from DNA damage responses to precision cancer therapy, 12-14th March, 2018, Oxford, UK.

7.3 Acknowledgments

Mein erster Dank geht an Herrn Prof. Zahler. Danke, dass Sie mir die Möglichkeit gegeben haben in Ihrer Arbeitsgruppe in der Pharmazeutischen Biologie an diesem spannenden Projekt zu arbeiten. Die Tür zu ihrem Büro war immer offen und ich konnte jederzeit mit Fragen zu Ihnen kommen. Ich habe während meiner Doktorarbeit viel gelernt und Sie haben mir die Freiheit gegeben mein Projekt selbstständig weiterzuentwickeln. Danke auch für Ihre Unterstützung, um Konferenzen in München, Heidelberg und Oxford zu besuchen.

Mein zweiter Dank geht an Frau Prof. Vollmar. Herzlichen Dank für die Meetings und Diskussionen und für Ihre ansteckende Begeisterung für die Forschung. Sie hatten immer ein offenes Ohr und einen Rat parat. Danke auch für Ihre Bereitschaft in meinem Prüfungskommitee zu sein.

Ich danke außerdem meinen weiteren Prüfern Frau Prof. Spitzweg, Herrn PD Grimm, Herrn PD Michalakis und Herrn Prof. Wahl. Herzlichen Dank, dass Sie sich die Zeit genommen haben meine Arbeit zu bewerten und bei meiner Verteidigung dabei zu sein.

Danken möchte ich auch meinen Kooperationspartnern. Als erstes möchte ich Dr. Gyula Timinszky und Dr. Rebecca Smith danken, die zusammen zu wichtigen Ergebnissen dieser Arbeit beigetragen haben. Vor allem danke an Rebecca, Du hast dir super viel Zeit genommen und mich mit Tipps, Zellen und Plasmiden versorgt und in Experimenten unterstützt. Danke auch an Dr. Olga Kalinina für die Beteiligung am Paper, welches aus dieser Arbeit entstanden ist.

Vielen Dank auch an das gesamte Labor! Ich hätte mir keine besseren Kollegen wünschen können. Vielen Dank für die gute Stimmung, all die gemeinsamen Mittagspausen, die Hilfe und wissenschaftlichen Diskussionen. Ich bin immer gerne in die Arbeit gekommen! Danke auch für das ein oder andere Feierabendbier, Grillaktionen und Filmabende und sonstige Unternehmungen nach der Arbeit - hat super viel Spaß gemacht mit euch!! Ein spezieller Dank geht als erstes an Flo - vielen Dank für all deine Hilfe! Außerdem auch danke an Jana, für deine Einweisung am Anfang und deine Hilfe bei Experimenten. Danke an Kerstin und Simon für die Hilfe am Anfang. Danke an Carina und Kerstin für die Unterstützung bei den *in vivo* Versuchen und noch einmal an Carina für die coole Zeit im D-Zimmer. Danke an Christina für die vielen Diskussionen zum Thema Aktin und Doxo und an dich und Flo für eine echt coole Konferenz in Heidelberg! Danke auch an Melanie und Christina für die gute Zeit im Labor! Danke auch an Themis für die FCS Messungen. Außerdem auch danke an meine Masterstudentin Anja Arner. Es hat mir echt Spaß gemacht mir dir zusammenzuarbeiten und deine Ergebnisse haben mir wirklich weitergeholfen!

Lieber Victor, danke für deine Unterstützung, deine Geduld, deine Aufmunterungen. Danke, dass Du immer für mich da bist.

Mein letzter und wichtigster Dank gilt meiner Familie, allen voran meinen Eltern Ingrid und Gerhard. Danke, dass ihr immer hinter mir steht und ihr mich in allem unterstützt. Ohne euch hätte ich das nie geschafft. Und danke an Jan, den besten kleinen Bruder der Welt.